University of Alberta

Cloning and Characterization of Liver Lipases

by

Bruce David Erickson

©

A thesis submitted to the Faculty of Graduate Studies and Research
in partial fulfillment of the requirements for the degree of

Master of Science

in

Medical Sciences - Pediatrics

Edmonton, Alberta
Fall 2006

Library and
Archives Canada

Published Heritage
Branch

395 Wellington Street
Ottawa ON K1A 0N4
Canada

Bibliothèque et
Archives Canada

Direction du
Patrimoine de l'édition

395, rue Wellington
Ottawa ON K1A 0N4
Canada

Your file Votre référence
ISBN: 978-0-494-22257-7
Our file Notre référence
ISBN: 978-0-494-22257-7

NOTICE:
The author has granted a non-exclusive license allowing Library and Archives Canada to reproduce, publish, archive, preserve, conserve, communicate to the public by telecommunication or on the Internet, loan, distribute and sell theses worldwide, for commercial or non-commercial purposes, in microform, paper, electronic and/or any other formats.

The author retains copyright ownership and moral rights in this thesis. Neither the thesis nor substantial extracts from it may be printed or otherwise reproduced without the author's permission.

AVIS:
L'auteur a accordé une licence non exclusive permettant à la Bibliothèque et Archives Canada de reproduire, publier, archiver, sauvegarder, conserver, transmettre au public par télécommunication ou par l'Internet, prêter, distribuer et vendre des thèses partout dans le monde, à des fins commerciales ou autres, sur support microforme, papier, électronique et/ou autres formats.

L'auteur conserve la propriété du droit d'auteur et des droits moraux qui protège cette thèse. Ni la thèse ni des extraits substantiels de celle-ci ne doivent être imprimés ou autrement reproduits sans son autorisation.

In compliance with the Canadian Privacy Act some supporting forms may have been removed from this thesis.

While these forms may be included in the document page count, their removal does not represent any loss of content from the thesis.

Conformément à la loi canadienne sur la protection de la vie privée, quelques formulaires secondaires ont été enlevés de cette thèse.

Bien que ces formulaires aient inclus dans la pagination, il n'y aura aucun contenu manquant.

Canada

ABSTRACT

Very low density lipoproteins (VLDL) are secreted from the liver in the post-absorptive state and are metabolized in the circulation, generating atherogenic low density lipoproteins. These dense lipoproteins are a major contributor to atherosclerosis, which ultimately leads to myocardial infarction and stroke. Triacylglycerol destined for secretion with VLDL is mobilized by hydrolysis followed by re-esterification. Triacylglycerol hydrolase is known to stimulate VLDL secretion, yet evidence suggests that additional lipases are involved. The objective of this work was to study the potential roles of Hepatic Lipase, Arylacetamide Deacetylase, Esterase-X and Esterase-22 in VLDL secretion from McArdle RH7777 rat hepatoma cells. This work demonstrates that intracellular Hepatic Lipase activity depletes neutral lipid stores and decreases VLDL secretion. Arylacetamide deacetylase also exhibits lipase activity, depletes cellular TG stores and reduces TG secretion. Lastly, evidence is presented that both Esterase-X and Esterase-22 are lipases, but their contribution to VLDL secretion remains to be established.

ACKNOWLEDGEMENTS

Thank you, Richard Lehner, for taking me on as a graduate student in your lab. The project has been challenging, yet rewarding. You have been a great boss and a friend.

It has been wonderful to work with everyone in the Lehner lab. Thanks especially to Dino G. for showing me around, teaching me many things and being a good friend. Your love of science is inspiring.

The Group on the Molecular and Cell Biology of Lipids (MCBL) has been my science family. Thank you to everyone in the group who has helped me along with advice, constructive criticisms and friendship.

I thank Priscilla Gao for all the hundreds of LB plates and media she has prepared, not to even mention the number of GC samples which she has analyzed for me. I also owe thanks to Johanne Lamoureaux for GC extractions. Audric has also been invaluable with computer solutions-thanks buddy. Honey Chan has also been very helpful with confocal imaging and deserves credit for it.

I would like to thank my supervisory and examination committee for the advice, comments and review of this work: Thank you Drs. Richard Lehner, Jason Dyck and Dennis Vance.

DEDICATION

This is for my Mother

Thank you for giving me the strength to persevere

and for being my inspiration to do so.

TABLE OF CONTENTS

Chapter 1: **Introduction** 1

1.1 Diseases Related to Lipid Metabolism 2

1.2 Triacylglycerol and Lipid Droplets 5

1.3 Lipid Synthesis 7

1.4 Lipoproteins 11

1.5 ApoB and VLDL Secretion 14

1.6 Provision of Lipid for VLDL Secretion 16

1.7 Lipolysis and Re-esterification of TG is Required for VLDL Assembly 17

1.8 Triacylglycerol Hydrolase (TGH) and VLDL Assembly 21

1.10 HL and Lipid Metabolism 26

- 1.10.1 HL Substrate Specificity and Localization 26
- 1.10.2 HL Hydrolyzes Lipoproteins and Facilitates Remnant Removal 27
- 1.10.3 HL Mediates Selective Uptake of CE 30
- 1.10.4 HL and Atherosclerosis 31
- 1.10.5 HL Activity in Humans 31
- 1.10.6 Rationale for Studying HL and VLDL Assembly 32

1.11 A Potential Role for AADA in Lipid Metabolism 34

1.12 A Potential Role for Es-X and Es-22 in Lipid Metabolism 35

1.13 The McA Cell Line 37

1.14 Thesis Objectives 40

Chapter 2: **General Methodology** 42

2.1 Chemicals and Materials 43
2.2 Molecular Biology Reagents 43
2.3 Cloning of Native and Chimeric cDNAs 44
2.4 Cell Culture and Generation of McA Stably Expressing Chimeric cDNAs 46
2.5 Lipase Assays 47
    2.5.1 4-MUH Lipase Assay 47
    2.5.2 Resorufin Ester Lipase Assay 48
2.6 Stimulation of TG Synthesis and VLDL Secretion 49
2.7 Pulse/Chase Experiments 49
2.8 Analyses of Radiolabeled Lipids 50
2.9 Lipid Mass Analyses by Gas Chromatograhy (GC) 51
2.10 Preparation of Microsomal Membranes 51
2.11 Protein Electrophoresis and Western Blotting 52
2.12 Protein Concentration Measurements 52

Chapter 3: **Role of Hepatic Lipase in the Mobilization of Intracellular Lipids and VLDL Assembly** 54

3.1 Introduction 55
3.2 Materials and Methods 56
    3.2.1 Chemicals and Materials 56

3.2.2 Screening of Stable McA Cell Lines for Expression of FLAG-tagged HL 56
3.2.3 Precipitation of HL-S from Media 57
3.2.4 Resorufin Ester Lipase Assay 57
3.2.5 Confocal Immunofluorescence Imaging 58
3.2.6 Incorporation of [^{3}H]Oleic Acid into Lipids 60
3.2.7 Pulse/Chase Experiments 60
3.2.8 Radiolabel Pulse/Chase Experiments 60
3.2.9 Secretion of ApoB and Densitometry 60
3.2.10 Measurements of Secreted Fatty Acids and Acid Soluble Products 61
3.2.11 Poloxamer 407 (P-407) Inhibition of HL Activity 62
3.2.12 LDH Activity Assay 62
3.2.13 Radiolabel Pulse/Chase in the Presence of 50 μM P-407 63
3.2.14 Clearance of Exogenous Lipoproteins 63
3.2.15 Total Lipase Activity Secreted 64
3.2.16 Statistical Analyses 65
3.3 Results 66
3.3.1 HL is Active Intracellularly 66
3.3.2 Intracellular HL Depletes Neutral Lipid Storage 70
3.3.3 Intracellular HL Reduces TG Secretion 76
3.3.4 Intracellular HL Reduces ApoB100 Secretion 79

3.3.5 Intracellular HL Does Not Direct Fatty Acids Towards Secretion or Oxidation 81

3.3.6 Extracellular HL Activity is Not Responsible for Reduced Media TG 83

3.3.7 Secreted HL Does Not Expediate Clearance of Secreted Lipoproteins 86

3.3.8 HL-S Overexpression Levels 89

3.4 Discussion 91

Chapter 4: Role of Arylacetamide Deacetylase in the Mobilization of Intracellular Lipids and VLDL Assembly 101

4.1 Introduction 102

4.2 Materials and Methods 103

4.2.1 Chemicals and Materials 103

4.2.2 Screening of Stable McA Cell Lines for Expression of FLAG-tagged AADA 103

4.2.3 Esterase Assay 103

4.2.4 4-MUH Lipase Assay 104

4.2.5 Determination of the AADA Membrane Interaction 104

4.2.6 PNGase Treatments 104

4.2.7 Endo H Treatments 105

4.2.8 Incorportation of [^{3}H]Oleic Acid into Radiolabeled Lipids 105

4.2.9 Pulse/Chase Experiments 106

4.2.10 Radiolabel Pulse/Chase Experiments 106

4.2.11 Secretion of ApoB 106

4.2.12 Protein Electrophoresis and Western Blotting 106

4.2.13 Statistical Analyses 107

4.3 Results 108

4.3.1 AADA has Esterase and Lipase Activity 108

4.3.2 AADA is a Glycosylated Lumenal-facing ER Transmembrane Enzyme 108

4.3.3 AADA Hydrolyzes Cellular TG in McA Cells 113

4.3.4 AADA Does Not Increase VLDL Secretion from McA Cells 118

4.4 Discussion 121

Chapter 5: Role of Esterase-X and Esterase-22 in the Mobilization of Intracellular Lipids and VLDL Assembly 127

5.1 Introduction 128

5.2 Materials and Methods 129

5.2.1 Chemicals and Materials 129

5.2.2 Screening of Stable McA Cell Lines for Expression of FLAG-tagged Es-X and Es-22 129

5.2.3 Protein Electrophoresis and Western Blotting 129

5.2.4 Resorufin Ester Lipase Assay 129

5.2.5 4-MUH Lipase Assay and Inhibition by GSKi 129

5.3 Results 131

5.4 Discussion 134

Chapter 6: General Discussion and Future Directions **136**

6.1 The Generation of New Research Tools 137

6.2 Conclusions from Studies Presented in the Thesis 137

6.3 Future Directions 139

References **146**

LIST OF TABLES

Table 2-1: Primers used for the amplification of native cDNAs and chimeric cDNAs. 45

Tables 3-1: Reduced TG in media from HL cells is due to intracellular HL activity and not extracellular HL activity. 87

Tables 3-2: Reduced TG in media from HL cells is due to intracellular HL activity and not HL-facilitated lipid or lipoprotein uptake. 88

Table 4-1: A13 cells secrete less radiolabeled TG and PC than McA cells. 119

LIST OF FIGURES

Fig. 1-1: The chemical structure of triacylglycerol. 6

Fig. 1-2: The general structure of a lipoprotein. 12

Fig. 1-3: The lipolysis and re-esterification cycle of TG for VLDL secretion. 19

Fig. 1-4: Inhibition of TGH markedly reduces plasma apoB100 ipoproteins. 25

Fig. 1-5: Mouse Es-X and Es-22 share 76% sequence homology with TGH. 36

Fig. 1-6: McArdle RH7777 cells do not express TGH, Es-X or AADA and have low level expression of Es-22 compared to rat hepatocytes. 39

Fig. 3-1: Schematic of beam path and channel assignment used for confocal immunofluorescence of HL-R and pNEO1 cells in Fig. 3-3. 59

Fig. 3-2: Generation of FLAG-tagged HL stably transfected McA cell lines. 67

Fig. 3-3: HL-R is targeted to the ER in stable cell line R12 while HL-S is secreted into the media from S7 cells; both enzymes have intracellular lipase activity. 68

Fig. 3-4: Confocal immunofluorescence imaging of HL-R and PDI. 69

Fig. 3-5: Incorporation of [^{3}H]oleic acid into cellular CE, TG and PC in pNEO1, R12 and S7 cells as a function of time. 71

Fig. 3-6: HL depletes R12 and S7 cells of neutral lipid stores. 73

Fig. 3-7: HL depletes R12 and S7 cells of radiolabeled neutral lipid stores. 74

Fig. 3-8: HL depletes R5 and S1 cells of neutral lipid stores. 75

Fig. 3-9: HL cells secrete less TG into the media than control cells. 77

Fig. 3-10: HL cells secrete less radiolabeled TG into the media than control cells. 78

Fig. 3-11: HL cells secrete less apoB100 into media upon removal of oleate. 80

Fig. 3-12: HL cells do not secrete more fatty acids or produce more ^{3}H-acid soluble products (ASP) than control cells. 82

Fig. 3-13: 50 µM P-407 completely inhibits secreted HL activity. 84

Fig. 3-14: 50 µM P-407 is not toxic to cells during a 16 h incubation. 85

Fig. 3-15: HL activity secreted from S7 cells is only 25% greater than that secreted from primary mouse hepatocytes. 90

Fig. 4-1: AADA has both esterase and lipase activity. 109

Fig. 4-2: AADA is a integral microsomal membrane protein. 110

Fig. 4-3: AADA is a glycosylated enzyme which localizes to the ER. 112

Fig. 4-4: Incorporation of [^{3}H]oleic acid into cellular CE, TG and PC in pNEO1 and A13 cells as a function of time. 114

Fig. 4-5: (Pulse) AADA depletes cells of TG. 115

Fig. 4-6: (Chase) AADA depletes cells of TG. 116

Fig. 4-7: AADA does not alter secretion of apoB100 from McA cells. 120

Fig. 4-8: AADA's proposed role in lipid remodeling. 123

Fig. 5-1: FLAG-tagged Es-X and Es-22 are expressed in McA cells and have lipase activity. 132

Fig. 5-2: GSKi also inhibits Es-X and Es-22. 133

LIST OF ABBREVIATIONS

4-MU	4-methylumbelliferone
4-MUH	4-methylumbelliferylheptanoate
11β-HSD	11β-hydroxysteroid dehydrogenase
AADA	arylacetamide deacetylase
ABC	ATP-binding cassette
ACAT	acylCoA:cholesterol acyltransferase
ACS	acyl Coenzyme A synthetases
acylCoA	acyl Coenzyme A
AGPAT	1-acylglycerol-3-phosphate acyltransferase
apo	apolipoprotein
ASP	acid soluble products
ATGL	adipose TG lipase
Atgl	ATGL gene
ATP	adenosine triphosphate
BMI	body mass index
BSA	bovine serum albumin (fatty acid free)
C-terminus	carboxy terminus
Cab-o-sil	fumed silica
cDNA	complementary deoxyribonucleic acid
CDP-choline	cytidine diphosphocholine
CE	cholesteryl ester
C/EBPα	CCAAT enhancer binding protein alpha
Ces1	carboxylesterase 1

CETP	cholesteryl ester transfer protein
CHAPS	(3-[(3-Cholamidopropyl)dimethylammonio]-1-propane-sulfonate) detergent
CHO	Chinese Hamster Ovary
Ci	curies
ciHL	catalyticallly inactive HL
CNX	calnexin
COS	CV-1 origin, SV40 transformed monkey kidney cell line
CPT	CDP-choline:1,2-diacylglycerol choline phosphotransferase
CT	CTP:phosphocholine cytidylyltransferase
CTP	cytidine triphosphate
dpm	disintegrations per minute
DG	diacylglycerol
DGAT	acylCoA:diacylglycerol acyltransferase
DGTA	diacylglycerol transacylase
DMEM	Dulbecco's Modified Eagle's Medium
E600	diethyl-*p*-nitrophenyl phosphate (general serine esterase inhibitor)
EDTA	ethylenediaminetetraacetic acid
EL	endothelial lipase
Endo H	endoglycosidase H
ER	endoplasmic reticulum
Es-22	esterase-22 (also Egasyn)

Es-X	esterase-X (also Ces1)
FBS	fetal bovine serum
FFA	free fatty acid
FLAG epitope	amino acid sequence: DYKDDDDK
Fld	fatty liver dystrophy
g	grams
g	relative centrifugal force
G-418	geneticin antibiotic
GC	gas chromatography
GFP	green fluorescent protein
GLUT4	glucose transporter 4
GPAT	glycerol-3-phosphate acyltransferase
GSKi	GlaxoSmithKline “TGH-specific” inhibitor (GR148672X)
h	hours
HDL	high density lipoprotein
HepG2	human hepatoma cell line
HF/HC	high fat and high cholesterol
HL	hepatic lipase
HL-R	HL-retained (FLAG and HVEL)
HL-S	HL-secreted (FLAG, but no HVEL)
HMG CoA	3-hydroxy-3-methylglutaryl-CoA
HRP	horseradish peroxidase
HS	horse serum

HSL	hormone sensitive lipase
HSPG	heparin sulphate proteoglycans
hTGH	human TGH
HVEL	mammalian ER retrieval signal
IDL	intermediate density lipoprotein
L	litre
LCAT	lecithin:cholesterol acyltransferase
LDH	lactate dehydrogenase
LDL	low density lipoprotein
LIPC	HL gene
LpL	lipoprotein lipase
LTS	lumenal targeting signal
M	moles/L
McA	McArdle RH7777 rat hepatoma
MG	monoacylglycerol
MGAT	acylCoA:monoacylglycerol acyltransferase
min	minutes
mRNA	messenger ribonucleic acid
MTP	microsomal triglyceride transfer protein
N-terminus	amino terminus
NADH	reduced nicotinamide adenine dinucleotide
P-407	poloxamer 407 (also Lutrol F127 NF Prill Surfactant)
PA	phosphatidic acid

PAGE	polyacrylamide gel electrophoresis
PAPH	phosphatidic acid phosphohydrolase
PBS	phosphate buffered saline
PC	phosphatidylcholine
PCR	polymerase chain reaction
PDI	protein disulphide isomerase
PE	phosphatidylethanolamine
PEMT	phosphatidylethanolamine-*N*-methyltransferase
PKC	protein kinase C
PL	phospholipids
PL-C	phospholipase C
PLTP	phospholipid transfer protein
pNEO1	empty vector pCI-neo stably transfected McA cell line (control)
PNGase	glycopeptidase F
pNp-acetate	*p*-nitrophenylacetate
pNp-OH	*p*-nitrophenol
PPARγ	peroxisome proliferator activated receptor gamma
RCT	reverse cholesterol transport
rpm	revolutions per minute
SCP2/SCPx	sterol carrier protein 2 / sterol carrier protein X
SDS	sodium dodecyl sulphate
SDS-PAGE	sodium dodecyl sulphate polyacrylamide gel electrophoresis

sec	seconds
sn	stereospecific number
SNP	single nucleotide polymorphism
SR-BI	scavenger receptor class B type 1
TBS	tris-buffered saline
TCA	trichloroacetic acid
TG	triacylglycerol
TGH	triacylglycerol hydrolase
THL	tetrahydrolipstatin (lipase inhibitor)
TLC	thin layer chromatography
T-TBS	TBS containing 0.1% Tween 20
UC	unesterified cholesterol
VLDL	very low density lipoprotein
v/v	volume per volume

Chapter 1:

Introduction

1.1 Diseases Related to Lipid Metabolism

The prevalence of obesity is rising at an alarming rate in industrialized countries. Obesity is closely linked to insulin resistance and Type II diabetes as well as hyperlipidemia and the progression of atherosclerosis, cardiovascular disease and stroke (Pi-Sunyer, 1998). With the exception of genetic abnormalities, obesity is the product of excess caloric intake coupled with insufficient exercise. In western civilizations, high fat diets (such as "fast food") and sedentary lifestyles (such as sitting in front of computers all day) are partly to blame. On the other hand, individuals' lifestyle choices ultimately determine their physical health (such as eating vegetables instead of McDonalds, using stairs rather than the elevator, etcetera). Obesity is loosely defined as increased adiposity to the extent of it producing adverse metabolic consequences. A non-invasive measurement of obesity is predicted by one's body mass index (BMI) (Pi-Sunyer, 1998), which is calculated by dividing body weight (in kilograms) by the square of ones height (in meters). A BMI of 25-29.9 kg/m^2 is considered overweight and a BMI over 30 kg/m^2 is considered obese. I happen to have a BMI of 25 kg/m^2, but I take comfort in the fact that the BMI index is not accurate for athletes.

While obesity gives rise to a plethora of disease states, normal amounts of adipose tissue are critical for an individual's health. This is evidenced by the fatty liver dystrophic (*fld*) (Reue et al., 2000) and A-ZIP/F1 (Kim et al., 2000) mouse models which lack adipose tissue. Like obese mice, these skinny mice are also insulin resistant and exhibit hepatic steatosis (Kim et al., 2000; Reue et al., 2000). This underscores the importance of storing fatty acids as triacylglycerol (TG) in the adipose tissue-an organ adapted for TG storage. Accumulation of fatty acids and TG in non-adipose tissues, such as the pancreas, skeletal muscle or liver, is associated with insulin resistance (Farese, 2001; Shulman, 2000). Hepatic insulin resistance results in dysregulation of glucose storage and production (Lam et al., 2003; Michael et al., 2000). Muscle and adipose insulin resistance is the major cause of impaired insulin-stimulated glucose utilization, largely due to defective trafficking of the insulin-sensitive glucose transporter (GLUT4) to the plasma membrane (Boden and Shulman, 2002; Farese, 2001; Shulman, 2000). Additionally, substandard insulin signaling results in increased hormone-sensitive lipase (HSL) mediated fatty acid release from adipose tissue. Elevated plasma fatty acid concentrations perpetuate insulin resistance by promoting fatty acid uptake and TG storage by tissues maladapted for TG storage; thus, insulin resistance is a cyclic phenomenom.

Atherosclerosis is the underlying reason for coronary heart disease and stroke, which accounts for nearly half the mortality in western nations annually (Lusis, 2000; Ross, 1999). It is a progressive disease that begins at the onset of life and is characterized by gradual hardening of the arteries. Throughout one's life, unesterified cholesterol (UC) and neutral lipids accumulate within the arterial wall and give rise to atheromatous plaques. Atherosclerosis is an inflammatory disease as much as it is a lipid related disorder (Ross, 1999). The accumulation of arterial lipids promotes migration of monocytes into the subendothelial space, their differentiation into cytokine- and chemokine-releasing macrophages, resulting in smooth muscle cell proliferation and further infiltration of immune cells. Macrophages and smooth muscle cells become enriched in neutral lipids and are termed foam cells-a hallmark of the atherosclerotic plaque. Arteries enriched in cholesterol lose their elasticity (harden) and the lesion protrudes into the lumen of the vessel, restricting blood flow. The ultimate cause of heart attack or stroke is often a result of plaque rupture (Lusis, 2000). As lipid-laden foam cells die and release their contents, plaques become unstable and sometimes release their contents into the circulation. The resultant emboli may trigger thrombosis or completely occlude blood flow in an artery. Cutting off oxygen delivery to distal tissues may result in the loss of limbs or life itself.

The progression of atherosclerosis begins in adolescence; fatty streaks are even apparent in the arteries of teenagers. Still, most individuals do not suffer adverse affects from atherosclerosis at this age unless they are homozygous carriers of recessive alleles causing diseases such as familial hypercholesterolemia (Brugger et al., 1996) or Tangier disease (Oram, 2000). For the general population, atherosclerosis does not produce maladies until the latter half of life (Lusis, 2000). However, its progression may be significantly enhanced by several factors including (but not limited to): smoking cigarettes, elevated blood pressure, stress, hyperlipidemia, bacterial or viral infections, etcetera (Ross, 1999). Endothelial damage increases the permeability of the artery wall and the expression of adhesion molecules facilitates infiltration of immune cells and atherogenic lipoproteins.

The correlation between elevated plasma lipids and the progression of atherosclerosis has been recognized for decades (Brown and Goldstein, 1983). Furthermore, high plasma apolipoprotein B (apoB) concentrations and low apolipoprotein AI (apoAI) concentrations are also risk factors for atherosclerotic disease (Sniderman et al., 2004). Regression of coronary artery disease has been demonstrated in men treated with lipid-lowering drugs that produce a concomitant reduction in plasma apoB concentrations (Brown et al., 1990). The purpose of the research embodied by this thesis was to identify enzymes which may contribute to very low density lipoprotein (VLDL) production. Any enzymes which enhance TG and apoB secretion might prove to be an effective target for the development of selective therapies to curb or reverse the adverse effects of atherosclerotic disease.

1.2 Triacylglycerol and Lipid Droplets

TG is composed of three fatty acyl chains esterified to a glycerol backbone via carboxylester bonds (Fig. 1-1). TG are the most energy dense biomolecules available for adenosine triphosphate (ATP) generation: they are less oxidized than carbohydrates or proteins and yield significantly more energy per unit mass on complete oxidation (Voet, 1999). TG is stored in the anhydrous form, unlike glycogen which binds twice its weight in water. For this reason, the long journey of a migrating bird is powered almost exclusively by TG oxidation; the mass of carbohydrate or protein required to power this voyage would prevent a bird from ever leaving the ground (Gibbons et al., 2000).

Nearly all tissues have the ability to synthesize and store small quantities of TG. The heart and skeletal muscle, for example, store small amounts of TG as an energy reservoir to power contraction. Only a few organs, however, are adapted to synthesize and store large amounts of bulk TG. The intestine is responsible for the absorption of dietary lipids and is extremely efficient in

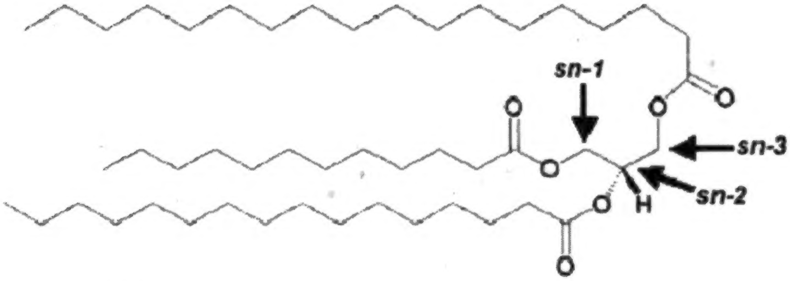

Fig. 1-1: The chemical structure of triacylglycerol. Three acyl chains are covalently linked to glycerol via ester bonds. Arrows indicate the stereospecific numbering (*sn*) of the glycerol carbon atoms. Acyl chains vary in their length and saturation. Triacylglycerol is extremely hydrophobic and therefore must be packaged with amphipathic lipids and proteins in lipid droplets for storage and in lipoproteins for transport within the circulation.

generating TG, but this organ packages TG into chylomicron particles for secretion into the lymph rather than long-term cytoplasmic storage. The adipose tissue is the primary storage organ for TG in mammals. In addition to its function as an energy reservoir, adipose TG also acts as a thermal insulator and is a benign storage form for fatty acids. The liver also has a remarkable capacity for TG storage, second only to the adipose tissue. It too is thought to play an important role in removal of free fatty acids from the circulation. Storing TG (or fatty acids) in appropriate tissues is of paramount importance.

Neutral lipids-TG and cholesteryl esters (CE)-are stored in cytoplasmic lipid droplets (Murphy and Vance, 1999). The neutral lipids are surrounded by a monolayer of phospholipids (PL), cholesterol, and a number of coat proteins which sequester the hydrophobic lipids away from the aqueous cytosol. Whereas lipid droplets have traditionally been regarded as an inert energy storage pool, they are now recognized as an important metabolic compartment. The turnover of lipid droplets is regulated by their coat proteins, associated enzymes and intracellular trafficking (Wolins et al., 2005). Lipid droplets are not only an inert storage pool for metabolic energy, but also provide fatty acids for PL biosynthesis (Unger et al., 1999) and moderate the amount of cholesterol in cellular membranes by storing excess cholesterol as CE. In this regard, lipid droplets are also critical for maintaining the fluidity of cell membranes and the activities of membrane associated enzymes.

1.3 Lipid Synthesis

The origin of fatty acids for TG synthesis varies between tissues (Lehner and Kuksis, 1996). The acyl groups for nearly all lipid biosynthetic reactions are provided by acyl coenzyme A (acylCoAs); these activated fatty acids are generated by a variety of fatty acylCoA synthetases (ACS) (Coleman et al., 2002; Lewin et al., 2001). Enterocytes absorb fatty acids and 2-monoacylglycerols (MG), the catabolic products of dietary TG, and re-synthesize TG for chylomicron production. The first step is the acylation of MG by acylCoA:monoacylglycerol acyltransferase (MGAT) to produce diacylglycerol (DG). The formation of TG from DG is catalyzed by either acylCoA:diacylglycerol acyltransferase (DGAT) or diacylglycerol transacylase (DGTA). Both MGAT and DGAT utilize acylCoA substrates for DG and TG synthesis, respectively, whereas DGTA produces TG in an acylCoA-independent reaction (Lehner and Kuksis, 1993). Two DGAT isoforms exist: DGAT1 (Cases et al., 1998) is ubiquitously expressed and DGAT2 (Cases et al., 2001) is primarily expressed in liver and adipose. All of these enzyme activities are localized to the endoplasmic reticulum (ER) membranes.

Nearly every other cell type produces TG through the glycerol-3-phosphate pathway (recently reviewed in (Coleman and Lee, 2004)). The first step in this pathway is catalyzed by glycerol-3-phosphate acyltransferases (GPAT), which is the first committed step in glycerolipid synthesis, generating 1-acylglycerol-3-phosphate. This molecule is acylated by 1-acylglycerol-3-phosphate acyltransferases (AGPAT) producing phosphatidic acid (PA). Both GPAT and AGPAT activities are associated with ER and mitochondrial membranes. A cytoplasmic PA phosphohydrolase (PAPH) activity liberates DG, the key metabolite for both TG and phosphatidylcholine (PC) synthesis. The gene encoding PAPH has been recently identified to be identical to lipin (Han et al., 2006).

The murine gene *Lpin1* was reported to be defective in *fld* mice (Peterfy et al., 2001). Ectopic expression of wild-type *Lpin1* in *fld* mouse embryonic fibroblasts was sufficient for TG accumulation (Phan et al., 2004). Lipin was found to stimulate an early stage of adipogenesis: Lipin1 expression even preceeded that of C/EBPα and PPARγ (Phan et al., 2004). Its nuclear localization sequence and early expression hinted that it might be a transcription factor. A lipin homolog was discovered in *Saccharomyces cerevisiae* based on sequence homology to mammalian lipin and both were shown to have PAPH activity (Han et al., 2006). Two closely related genes, Lpin2 and Lpin3, are present in mice and humans. This progress has pinpointed at least three potential genes which might be responsible for lipodystrophy in humans. Lipin is also at a key point in the TG and PL biosynthetic pathways and might be an attractive target for the development of drugs to curb obesity.

PC is synthesized in every nucleated cell through the cytidine diphosphocholine (CDP-choline) pathway, commonly known as the Kennedy pathway (Kennedy, 1956). It is the most abundant PL in cell membranes and all classes of mammalian lipoproteins (Vance and Vance, 1985). The Kennedy pathway begins with the cellular uptake of choline, followed by its immediate phosphorylation by choline kinase (Uchida and Yamashita, 1992). The resultant phosphocholine is linked to cytidine triphosphate (CTP) forming the high energy compound CDP-choline by CTP:phosphocholine cytidylyltransferase (CT); this is the rate limiting reaction in PC biosynthesis (Vance, 1990). Finally, this high energy molecule is combined with DG in a reaction catalyzed by CDP-choline:1,2-diacylglycerol choline phosphotransferase (CPT) to form PC (Vance, 1990)).

Hepatic PC synthesis is so important that mammals evolved a second pathway for its production. PC can also be generated from phosphatidylethanolamine (PE) by three consecutive methylation reactions all catalyzed by the liver-specific enzyme phosphatidylethanolamine-*N*-methyltransferase (PEMT) (Vance and Ridgway, 1988). The methyl donors for this reaction are S-adenosylmethionine and the reaction products are S-adenosylhomocysteine. This product is rapidly hydrolyzed to homocysteine, which is an independent risk factor for coronary heart disease (Refsum et al., 1998). The PEMT pathway accounts for approximately 30% of hepatic PC synthesis. PEMT is especially important for PC synthesis in times of choline deficiency, such as starvation and pregnancy (Walkey et al., 1998).

There is a high demand for PC in the liver. The maintenance of the plasma membrane-the permeability barrier of the cell-requires constant PC synthesis for cellular survival (Li et al., 2006). PC is also necessary for lipoprotein production and secretion (Jacobs et al., 2004; Noga and Vance, 2003; Yao and Vance, 1988); it encompasses the surface monolayer of lipoproteins as well as the vesicles of the secretory pathway through which they travel. Secretion of PC into bile is very taxing on the hepatic PC pool (Li et al., 2006), but it is absolutely required for intestinal absorption of dietary lipids.

Cholesterol synthesis occurs in all mammalian cells and involves many enzymes. Cholesterol modulates the fluidity of cellular membranes and is a precursor of steroids and bile acids. The rate limiting step in cholesterol synthesis is catalyzed by the enzyme 3-hydroxy-3-methylglutaryl-CoA (HMG-CoA) reductase. The activity of this enzyme is regulated by cellular cholesterol concentration. HMG-CoA reductase is the target of the 'statin' family of pharmaceutical drugs, which have been very successful in treating patients with hypercholesterolemia (Ganesh et al., 2003). Excess cholesterol is toxic to cells because it increases the rigidity of membranes and it can crystallize at very high concentrations. Mammalian somatic cells are unable to catabolize cholesterol. Instead, cholesterol must be effluxed from cells and returned to the liver for excretion in bile; it is converted into bile acids and dissolved in the bile. Alternately, cholesterol can be esterified to a fatty acid by the activity of acylCoA:cholesterol acyltransferases (ACAT). Two ACAT isoforms are encoded by separate genes (Buhman et al., 2000a; Rudel et al., 2001). Both ACAT1 and ACAT2 are ER transmembrane proteins.

1.4 Lipoproteins

Since neutral lipids are insoluble in an aqueous environment, they must be packaged into lipoprotein particles for transport in the circulation (Fig. 1-2). Lipoproteins share many characteristics with intracellular lipid droplets. TG and CE form the inner hydrophobic core, which is surrounded by a monolayer of cholesterol, PL and proteins. The amphipathic nature of the surface lipids and apolipoproteins allows transport of lipoproteins in the blood. Lipoproteins are

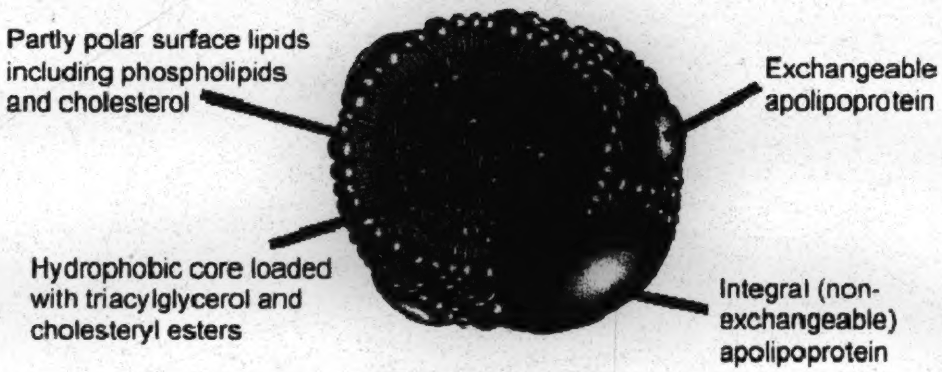
Partly polar surface lipids including phospholipids and cholesterol
Exchangeable apolipoprotein
Hydrophobic core loaded with triacylglycerol and cholesteryl esters
Integral (non-exchangeable) apolipoprotein

Fig. 1-2: The general structure of a lipoprotein. Integral and exchangeable apolipoproteins as well as free cholesterol and phospholipids surround the periphery of the lipoprotein particle; their amphipathic nature allows for the transport of neutral lipids in aqueous blood. The neutral lipids are sequestered into the hydrophobic core of the lipoprotein. The composition of both lipids and apolipoproteins defines the class of the lipoprotein and its metabolism. This figure is adapted from (Grundy, 1990).

classified by many characteristics: size, density, lipid content, apolipoprotein composition, electrophoretic mobility, etcetera.

TG-rich lipoproteins each have one molecule of apoB (Mahley et al., 1984). Chylomicrons are the largest, least dense and most TG-rich lipoproteins. They are secreted from the small intestine in the post-prandial state and function to deliver dietary lipids and lipid-soluble vitamins to the peripheral tissues. VLDL are the second largest TG-rich lipoproteins. These lipoproteins are secreted by the liver in the post-absorptive state (Gibbons et al., 2000). Similar to chylomicrons, VLDL transport TG to provide peripheral tissues with a source of metabolic energy (the fatty acids which are released by lipolysis). As VLDL are metabolized in the circulation, they give rise to intermediate density lipoproteins (IDL) and low density lipoproteins (LDL). IDL and LDL are, in a sense, VLDL remnant lipoproteins which are relatively depleted of TG and enriched in total cholesterol compared to their precursors. The apoB lipoproteins enter cells through receptor mediated endocytosis (Goldstein et al., 1983).

The transport of total cholesterol away from the peripheral tissues and back to the liver for excretion in bile is termed the reverse cholesterol transport (RCT) pathway (Fredenrich and Bayer, 2003). RCT is mediated by high density lipoproteins (HDL), which are the smallest of the lipoproteins. Each HDL contains at least one molecule of apoAI among other apolipoproteins (Mahley et al., 1984). Lipid-poor apoAI stimulates cholesterol and PL efflux from the peripheral tissues by interacting with ATP-binding cassette (ABC) transporter A1, facilitating the formation of the HDL particle; the lipidated HDL particle then acts as a cholesterol and PL acceptor by interacting with ABCG1 (Kennedy et al., 2005). The neutral lipid core of HDL particles consists of mainly CE. Both lecithin:cholesterol acyltransferase (LCAT) and phospholipid transfer protein (PLTP) activities in the blood facilitate the conversion of cholesterol on the surface of HDL to CE which partitions into the core of the HDL particle (Fielding and Fielding, 2001). These processes are thought to assist RCT by maintaining the concentration gradient of cholesterol between the plasma membrane (high cholesterol concentration) and the HDL surface (low cholesterol concentration).

HDL interacts with hepatic scavenger receptor class B type 1 (SR-B1) to return CE to the liver (Fredenrich and Bayer, 2003). SR-B1 stimulates selective uptake of CE from HDL; that is, CE is taken up by hepatocytes without holoparticle endocytosis. A less obvious pathway of RCT is mediated by cholesteryl ester transfer protein (CETP), which exchanges CE from HDL for TG from the apoB lipoproteins (Curtiss et al., 2006). The CE may then be cleared via receptor mediated endocytosis of apoB lipoproteins.

1.5 ApoB and VLDL Secretion

Both the liver and the intestine actively synthesize and secrete TG-rich lipoproteins. In humans, the intestine secretes neutral lipids with apoB48 in chylomicrons and the liver secretes neutral lipids with apoB100 in VLDL. A single gene encodes apoB, but it is found in two forms as a result of messenger RNA editing: apoB100 and apoB48 (Chen et al., 1987). Full-length apoB100 is one of the larger mammalian proteins, comprised of 4536 amino acids. ApoB48 is the N-terminal 48% of apoB100 (apoB100 represents 100% of the apoB gene product). It is generated by deamination of cytidine at codon 2153 which produces a premature stop codon in apoB mRNA (Chen et al., 1987). ApoB100 is the sole form of apoB secreted by human liver whereas both apoB100 and apoB48 are secreted by murine liver and the McArdle RH7777 (McA) rat hepatoma cell line used in my studies.

Hepatic apoB is translated continuously on ribosomes associated with the rough ER. Its secretion is not limited by transcriptional or translational mechanisms (Pullinger et al., 1989), but by the availability of lipids. In the presence of adequate lipid supply, apoB is correctly folded and packaged into a secretion-competent lipoprotein; conversely, when lipids are limiting, apoB becomes misfolded, stalls in the translocon and is targeted for degradation (Fisher and Ginsberg, 2002). Both proteases and the proteosome play an active role in apoB degradation (Cardozo et al., 2002; Fisher et al., 2001). It is generally accepted that apoB is lipidated in a two step process (Fisher and Ginsberg, 2002; Rustaeus et al., 1999). First, the nascent apoB polypeptide is cotranslationally lipidated with small quantities of TG, cholesterol and PL as it enters the ER lumen, forming a lipid-poor apoB particle which associates with the membrane in a peripheral fashion. Next, the poorly-lipidated particle receives a bulk transfer of neutral lipid to form true VLDL. The precise location where bulk lipidation occurs still remains a matter of controversy. One camp suggests that bulk lipidation occurs in the ER (Rusinol et al., 1993; Yamaguchi et al., 2003) while the other claims that it occurs in the Golgi apparatus (Bamberger and Lane, 1990; Gusarova et al., 2003; Tran et al., 2002). There is experimental evidence to support both hypotheses.

1.6 Provision of Lipid for VLDL Secretion

TG and CE make up the bulk of the VLDL neutral lipid core, which is surrounded by PL, cholesterol and apolipoproteins (Fig. 1-2). Many studies agree that active hepatic TG synthesis enhances the rate of both TG and apoB secretion (Yao and McLeod, 1994). Incubating primary murine hepatocytes or McA rat hepatoma cells in the presence of exogenous oleic acid stimulates VLDL secretion (Lehner and Vance, 1999; Tran et al., 2002). Furthermore, the synthesis of PC, CE and cholesterol also influence apoB and VLDL secretion.

Liver-specific CTα and PEMT knockout mice have provided conclusive evidence that both the Kennedy pathway and the PEMT pathway contribute PC for lipoprotein secretion (Jacobs et al., 2004; Noga and Vance, 2003). On a chow diet alone, liver CTα deficient mice have lower plasma total cholesterol and TG after an overnight fast, corresponding to decreased plasma apoAI and apoB100 levels compared to control mice; this resulted in hepatic steatosis, especially in female mice (Jacobs et al., 2004). When challenged with a high fat and high cholesterol (HF/HC) diet, both female and male PEMT knockout mice have reduced plasma PC and total cholesterol compared to controls; female mice also showed this phenotype on a chow diet (Noga and Vance, 2003). On the HF/HC diet, male PEMT knockout mice had plasma apoB100 and TG levels half those of wild-type mice after an overnight fast, resulting in hepatic steatosis. Plasma apoAI levels were similar between the two groups (Noga and Vance, 2003). These studies highlight the necessity of PC synthesis for VLDL secretion.

Deletion of the ACAT1 or ACAT2 genes in mice failed to demonstrate that CE synthesis was essential for lipoprotein secretion (Buhman et al., 2000b;

Meiner et al., 1996), although ACAT deficiency did reduce the size of the lipoproteins (Buhman et al., 2000b). Yet, CE synthesis has been implicated in regulating VLDL secretion in other studies. Overexpression of either ACAT1 or ACAT2 in McA cells increased CE synthesis as well as apoB100 secretion and the proportion of CE associated with this apolipoprotein (Liang et al., 2004). Adenoviral mediated gene transfer of human ACAT1 into murine liver also had similar effects: hepatic secretion of CE, TG, apoB48 and apoB100 in the VLDL density range was increased over twofold by targeted expression of ACAT1 in low density lipoprotein receptor deficient mice (Spady et al., 2000). In hamster hepatocytes, the secretion of apoB100 correlated well with cellular CE mass and active cholesterol synthesis; incubation with statin drugs markedly reduced both CE synthesis and apoB100 secretion (Zhang et al., 1999). Depletion of CE stores by incubating hepatocytes with exogenous apoAI has also been shown to decrease apoB and TG secretion (Sahoo et al., 2004). The results of these studies all agree that CE availability is a regulator of apoB100 secretion from hepatocytes, regardless of whether they are of murine, hamster or hepatoma origin.

1.7 Lipolysis and Re-esterification of TG is Required for VLDL Assembly

Fatty acids taken up by hepatocytes are not secreted directly as VLDL-TG; they must first enter a cytoplasmic storage pool (Wiggins and Gibbons, 1992). It is estimated that around 70% of TG secreted by primary hepatocytes originates from stored TG rather than from de novo lipogenesis. The transfer of neutral lipid from cytoplasmic lipid droplets into the ER lumen requires microsomal triglyceride transfer protein (MTP). The existence of an ER lumenal lipid droplet was first documented three decades ago (Alexander et al., 1976). MTP facilitates the formation of the ER lumenal, apoB-free lipid droplet. This has been demonstrated via liver-specific ablation of MTP (Raabe et al., 1999) and with MTP-specific inhibitors in primary hepatocytes (Kulinski et al., 2002). The absolute necessity of MTP for apoB secretion is highlighted by the condition abetalipoproteinemia (Wetterau et al., 1992), in which patients are devoid of MTP activity and have virtually absent circulating apoB. While MTP activity is a prerequisite of apoB bulk lipidation by forming the lumenal lipid droplet, it may not be directly involved in the fusion of the primordial particle with bulk lipid (Rustaeus et al., 1998).

Cytosolic TG is not added to apoB en bloc; instead, 60-70% of the TG secreted with VLDL first undergoes lipolysis and re-esterification (Gibbons et al., 2000). The concept entails TG hydrolysis enhancing the proportion of acylglycerols within the ER membrane which are substrates for DGAT activity. The re-synthesis of TG proximal to the nascent apoB polypeptide chain would protect apoB from presecretory degradation by facilitating apoB folding (the first step of VLDL assembly). As a result, more primordial lipoprotein particles would be available for further lipidation (the second step of VLDL assembly), ultimately increasing apoB and TG secretion. Some lipolysis products would also return to storage droplets in a futile cycle (Fig. 1-3).

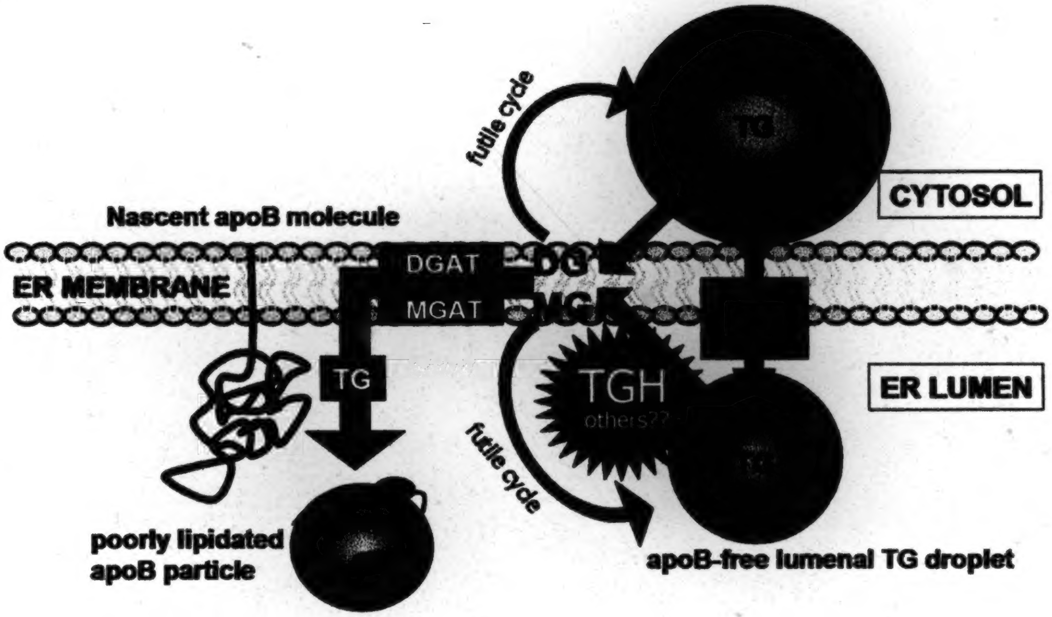
futile cycle
TG
CYTOSOL
Nascent apoB molecule
ER MEMBRANE
DGAT
DG
MGAT
MG
TG
TGH
others??
ER LUMEN
futile cycle
poorly lipidated
apoB particle
apoB-free lumenal TG droplet

Fig. 1-3: The lipolysis and re-esterification cycle of TG for VLDL secretion. Cytosolic TG is transferred into the lumen by microsomal triacylglycerol transfer protein (MTP). Triacylglycerol hydrolase (TGH)-and possibly other lumenal lipases-hydrolyze the lumenal lipid droplet. This increases the proportion of diacylglycerol (DG) and monoacylglycerol (MG) which is available for re-acylation by the acyltransferases (MGAT and DGAT) to form triacylglycerol (TG). Newly formed TG may associate with the nascent apoB polypeptide to form a poorly lipidated apoB particle which is available for bulk lipidation. Alternately, TG may be returned to cytosolic or lumenal lipid droplets in a futile cycle.

Fatty acids secreted in VLDL-TG are not directly from *de novo* TG lipogenesis, but arise from lipolysis of stored TG followed by its re-synthesis. First, Wiggins and Gibbons (1992) labeled TG stores in rat hepatocytes simultaneously with [^{14}C]glycerol and [^{3}H]oleic acid and measured the specific activity of the resultant TG stores and that of VLDL-TG secreted over a 24 h period in the absence of label. They found that the 70% of the VLDL-TG was diluted with unlabeled glycerol relative to stored TG, indicating that TG lipolysis and re-esterification had to have occurred prior to its secretion (Wiggins and Gibbons, 1992). The cellular turnover of TG exceeded the rate necessary to maintain VLDL secretion (Wiggins and Gibbons, 1992). Secondly, Lankester et al. (1998) prelabeled TG stores in rat hepatocytes overnight with [^{3}H]oleic acid, followed by a 3 h incubation with [^{14}C]oleic acid, and measured the contribution of each to VLDL-TG. Less than 20% of the acyl groups in VLDL-TG were derived from exogenous [^{14}C]oleic acid, indicating that preformed TG provides the majority of the acyl groups (Lankester et al., 1998). They also noted that TG was not hydrolyzed fully to fatty acids and glycerol, but only to acylglycerols and fatty acids (Lankester et al., 1998). Thirdly, Yang et al. used chiral and reversed phase high pressure liquid chromatography to study the positional distribution of acyl chains associated with stored TG and VLDL-TG. They concluded that at least 60% of the secreted TG resulted from lipolysis and resynthesis of stored TG (Yang et al., 1995). Finally, these authors followed up their study with radiolabeling experiments showing that a maximum of 40% of the glycerol and fatty acids in VLDL are not products of TG stored in the liver (Yang et al., 1996).

Inhibition of hepatic lipolysis depresses the secretion of both TG and apoB from primary rat hepatocytes (Gibbons et al., 1992; Gilham et al., 2003). The full complement of lipases involved in the lipolysis and re-esterification cycle for provision of TG for VLDL secretion remains obscure. Lysosomal acid lipase is not involved in this cycle since inhibition with chloroquine does not retard VLDL secretion (Gibbons et al., 1992; Wiggins and Gibbons, 1992). The well-characterized HSL is not expressed in the liver and therefore does not contribute to this process either. Interestingly, ectopic expression of HSL in HepG2 human hepatoma cells did not stimulate VLDL secretion (Pease et al., 1999). On the contrary, this cytosolic enzyme directed liberated fatty acids towards β-oxidation (Pease et al., 1999). This suggests that the subcellular localization of lipases plays a paramount role in determining the fate of their lipolysis products. It has been proposed that the lipases which promote TG secretion would most likely be targeted to the ER, since this is the site of VLDL production (Dolinsky et al., 2004b; Gibbons et al., 2000).

In this regard, the apoB-free lumenal lipid droplet is an attractive TG pool for lipolysis because its hydrolysis products would intercalate into the lumenal leaflet of the ER membrane (Fig. 1-3). Re-esterification of TG on this aspect is conceptually ideal for stabilizing the nascent apoB polypeptide.

1.8 Triacylglycerol Hydrolase (TGH) and VLDL Assembly

TGH is a 60 kilodalton carboxylesterase originally purified from porcine liver microsomes (Lehner and Verger, 1997). Subsequently the cDNAs for human, mouse and rat TGH have been cloned and the protein has been isolated from mouse and human microsomes (Alam et al., 2002a; Dolinsky et al., 2001; Lehner and Vance, 1999). Synthesis of TGH is directed to ER ribosomes by its 18 amino acid N-terminal signal peptide, which is cleaved in the ER by signal peptidase (Lehner and Vance, 1999; Lehner and Verger, 1997). The enzyme is retained in the ER by an unusual C-terminal mammalian ER retention motif –HIEL or –HVEL, which is similar to the well-known –KDEL ER retention motif (Gilham et al., 2005). TGH is susceptible to irreversible inhibition by the general serine esterase inhibitor diethyl-*p*-nitrophenyl phosphate (E600) as well as the lipase inhibitor tetrahydrolipstatin (THL) (Lehner et al., 1999; Lehner and Vance, 1999). Consistent with its inhibition profile, TGH contains the amino acid sequence GXSXG at its active site, which is a hallmark of lipases. The active site catalytic triad consists of serine (GXSXG), glutamate and histidine, and is highly conserved between species (Alam et al., 2002b). TGH hydrolyzes long, medium and short chain TG substrates in the sn-1 and sn-3 positions (Fig. 1-1).

Humans express TGH primarily in the liver, adipose and small intestine; in rodents, TGH expression is mainly in the liver and adipose tissue, but is also detected in the small intestine, heart and kidney (Dolinsky et al., 2001). In rodent liver, TGH localizes to adult hepatocytes around the capillary vessels leading to the central vein (Lehner et al., 1999). It is noteworthy that TGH is also expressed in the intestine, which readily secretes apoB48 containing chylomicrons, and in the heart and kidney, which exhibit limited secretion of apoB lipoproteins (Dolinsky et al., 2001). The roles of TGH in these tissues, however, have not been determined.

Both the histological localization of TGH to hepatocytes surrounding the central vein and its ER subcellular localization support the role of TGH in VLDL secretion. The proposed role for TGH in TG mobilization for VLDL secretion is presented in Fig. 1-3. Lipolysis of TG to acylglycerols mediates their incorporation into the lumenal aspect of the ER membrane where they may be re-esterified into TG available for apoB assembly. Of course, this does not produce a vectorial transfer of TG into VLDL, but increases the proportion of TG available for apoB assembly. TG not added to nascent apoB may be returned to either cytosolic or lumenal storage droplets in a futile cycle (Fig. 1-3).

There is a lot of evidence supporting the relationship between TGH and VLDL assembly. Stable transfection of a rat TGH cDNA into McA rat hepatoma cells-a cell line devoid of TGH expression-enhanced their ability to mobilize intracellular TG stores twofold and increased TG secretion by 25% when stimulated with exogenous oleic acid (Lehner and Vance, 1999). Importantly, TGH increased the proportion of apoB lipoproteins secreted in the VLDL density range, but did not alter PL secretion (Lehner and Vance, 1999). This study demonstrates that microsomal TGH activity mobilizes TG stores and promotes the secretion of TG with lipoproteins, rather than directing lipolysis products into the oxidative pathway like cytosolic HSL does (Pease et al., 1999). This affirms the importance of subcellular compartmentation of lipases and the utilization of lipolysis products.

In collaboration with our laboratory, the pharmaceutical company GlaxoSmithKline created a TGH-specific inhibitor, GR148672X, which will hereafter be called GSKi. GSKi does not inhibit pancreatic lipase, HSL, lipoprotein lipase (LpL) or acetylcholine esterase, yet abolishes >95% of TGH activity when assayed with purified TGH enzyme (Borg-Capra et al., personal communication). To investigate the potential of inhibiting TGH as a selective treatment for reducing plasma VLDL concentrations, GlaxoSmithKline treated hamsters with or without GSKi for three days and measured their plasma profiles after a 4 h fast by high performance liquid chromatography. The results were striking: GSKi treatment reduced fasting plasma TG by over 50% and apoB100 by 35% compared to control mice, without altering HDL levels (Fig. 1-4). These studies demonstrate that TGH significantly contributes to VLDL secretion in vivo.

Gilham et al. (2003) complemented these studies by quantifying apoB and lipid secretion from primary rat hepatocytes in the presence of inhibitors. Both the general esterase inhibitor E600 and the GSKi abolish TGH activity in vitro with the purified enzyme. Additionally, E600 and GSKi are both cell permeable and enter the microsomal lumen to inhibit TGH. The results of these studies show that both inhibitors reduced the secretion of TG and apoB from primary hepatocytes, but the general esterase inhibitor E600 was far more potent than GSKi in attenuating secretion (Gilham et al., 2003). E600 inhibition reduced secretion of apoB100 by 90%, apoB48 by 40% and TG by 66% compared to control hepatocytes, whereas GSKi inhibition lowered secretion of apoB100 by 42%, apoB48 by 20% and TG by 46% compared to control hepatocytes (Gilham et al., 2003). This suggests that TGH is responsible for the majority of the lipolysis-stimulated VLDL secretion in rat hepatocytes, but not all of it. Therefore, there must be other lipases in the microsomal fraction of rat hepatocytes which

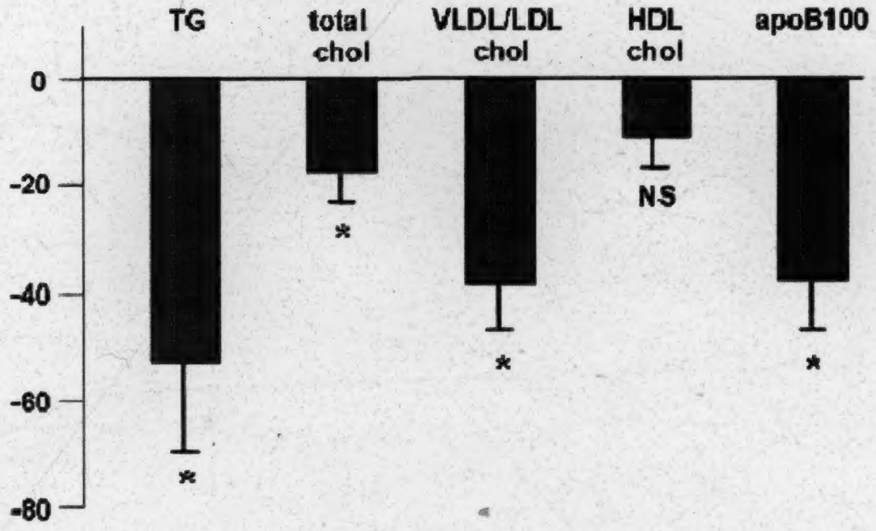

Fig. 1-4: Inhibition of TGH markedly reduces plasma apoB100 lipoproteins. Hamsters fed *ad libitum* were treated with 25 mg GSKi/kg body weight or solvent alone for 3 days. After the last administration, hamsters were sacrificed and their plasma lipids, lipoprotein profile and apoB concentrations were analyzed. These experiments were conducted by Borg-Capra et al. at GlaxoSmithKline.

contribute to VLDL synthesis and secretion; herein lies the rationale for my project: to identify other hepatic lipases involved in VLDL assembly.

1.9 Other Potential Hepatic TG Lipases Contributing to VLDL Assembly

While there has been much progress in elucidating the lipases involved in adipose TG mobilization, the full complement of liver lipases remains ambiguous. The enzyme hepatic lipase (HL) was discovered over two decades ago and has been the focus of intense investigation ever since. It was another decade until TGH was shown to be an intracellular hepatic TG lipase (Lehner and Verger, 1997). The hepatic role of lysosomal acid lipase in lysosomal degradation of endocytosed lipoproteins has been well documented, but this enzyme does not contribute to the lipolysis and re-esterification of TG for VLDL assembly (Wiggins and Gibbons, 1992). This begs the question: which enzymes are liver-specific and could be TG lipases capable of mobilizing TG for VLDL synthesis? As previously discussed, the best candidate enzymes would localize to the ER lumenal space of hepatocytes. The four contenders which fit this profile and I have been charged with investigating are: HL, arylacetamide deacetylase (AADA), esterase-X (Es-X) and esterase-22 (Es-22).

1.10 HL and Lipid Metabolism

1.10.1 HL Substrate Specificity and Localization

HL is a member of the lipase superfamily which also includes LpL, pancreatic lipase and, more recently, endothelial lipase (EL) (Choi et al., 2002; Hide et al., 1992; Wong and Schotz, 2002). These lipases are thought to have evolved from a common ancestral gene by duplication and subsequent divergence. LpL, HL and EL metabolize lipoprotein-associated lipids in the circulatory system whereas pancreatic lipase facilitates the catabolism and absoption of dietary TG in the intestine. Whereas LpL specifically hydrolyzes TG associated with bouyant apoB lipoproteins (Bensadoun, 1991) and EL hydrolyzes PL on the surface of HDL (Choi et al., 2002), HL has both TG hydrolase and phospholipase A1 activities and is capable of hydrolyzing lipids in all classes of lipoproteins (Zambon et al., 2003).

HL is predominantly expressed in hepatocytes of most mammals (hence its name). Rat HL is localized to heparin sulphate proteoglycans (HSPG) mainly on the cell surface of parenchymal cells concentrated at the surfaces of hepatic sinusoids (Breedveld et al., 1997). Rabbits transgenic for human HL also exhibit a similar localization (Sanan et al., 1997). Its distribution is consistent with the role of HL in lipoprotein metabolism. Both rat and human HL bind HSPG with high affinity and are only found in plasma treated with heparin. Mouse HL has a much weaker avidity for HSPG and is found in the circulation without heparin treatment (Peterson et al., 1986). This discrepancy is attributed to differences in the C-termini between human and mouse HL (Brown et al., 2003). It has recently been demonstrated that HL is also expressed in human and mouse macrophages (Gonzalez-Navarro et al., 2002).

1.10.2 HL Hydrolyzes Lipoproteins and Facilitates Remnant Removal

Many in vivo studies agree that HL plays a central role in the catabolism of TG-rich lipoprotein remnants and HDL. LpL specifically hydrolyzes TG in chylomicrons and buoyant VLDL whereas HL hydrolyzes both TG and PL on VLDL remnants and IDL, forming LDL. This is evident in 2 studies of human patients with HL deficiency. Both studies revealed an elevated IDL pool size resulting from a reduced fractional catabolic rate of these lipoproteins in HL deficient patients compared to control subjects (Ruel et al., 2005; Tilly-Kiesi et al., 2004). Additionally, rabbits have very little HL activity and are characterized by a predominance of IDL, buoyant LDL and HDL. Introduction of a human HL transgene into rabbits enhanced conversion of IDL to LDL and HDL2 to HDL3 (Fan et al., 1994). HL knockout mice also show a marked elevation in plasma HDL-C and apoB remnant lipoproteins versus their wild-type controls (Homanics et al., 1995; Qiu et al., 1998).

The HL mediated hydrolysis of lipids associated with remnant lipoproteins and HDL expediates hepatic uptake of these particles. Rabbits fed a cholesterol-rich diet accumulate chylomicron remnants and it has been suggested that this is due to low HL activity associated with the livers of these animals (Chang and Borensztajn, 1993). Exogenous treatment of chylomicron remnants with HL greatly enhanced hepatic endocytosis of β-VLDL in rabbits, demonstrating the role of HL hydrolysis in the clearance of chylomicron remnants (Chang and Borensztajn, 1993). Conversely, perfusion of rat liver with anti-HL antibodies reduced HL activity and impaired the clearance of chylomicron remnants (Shafi et al., 1994). TG-enriched HDL are also cleared more rapidly from rabbits infected with human HL adenovirus relative to those infected with lacZ adenovirus (Rashid et al., 2003), establishing that HL hydrolyzes TG in HDL and facilitates HDL removal.

The facilitated clearance of chylomicron remnants and HDL by HL cannot *be attributed solely to* the lipolytic activity of HL, however. Several studies show that HL also aids the uptake of lipoproteins by its ability to bind to and bridge lipoproteins with HSPG and lipoprotein receptors. Dichek et al. created human HL transgenic mice and catalytically inactive human HL (ciHL) transgenic mice, both on an apoE deficient background, and evaluated their plasma lipid profiles (Dichek et al., 1998). They found that both HL and ciHL reduced fasting TG and cholesterol levels (Dichek et al., 1998). Surprisingly, the ciHL was nearly as efficient at lowering plasma apoB lipoproteins as the catalytically active HL was, highlighting the importance of the bridging function in remnant removal. This study also demonstrates that HL enhances lipoprotein endocytosis independently of apoE (Dichek et al., 1998).

Further, expressing human HL in McA cells enhanced binding and clearance of chylomicron remnants compared to that in wild-type McA cells (Ji et al., 1994). Importantly, heparinase treatment abolished greater than 90% of the HL-mediated remnant binding, showing that the interaction between HL and HSPG is obligatory for stimulating remnant binding to McA (Ji et al., 1994). Increased HL activity in the media was not responsible for augmented remnant binding since the effect still occured at 4°C and HL possesses less than 5% of its lipolytic activity at this temperature (Ji et al., 1994). The presence or absence of apoE in chylomicron remnants did not affect the enhanced binding capacity of McA cells expressing HL (Ji et al., 1994), again showing that the effect is independent of apoE.

1.10.3 HL Mediates Selective Uptake of CE

The ability of HL to bind lipoproteins also assists selective uptake of CE into the liver and steroidogenic tissues. Selective uptake is the cellular internalization of CE directly from a lipoprotein without holoparticle endocytosis of the lipoprotein. SR-B1 is a scavenger receptor which mediates selective uptake of CE into the liver and steroidogenic tissues (Acton et al., 1996) by a mechanism distinct from the classic LDL receptor pathway (Goldstein et al., 1983). It binds HDL with high affinity and is a key player involved in RCT (Fredenrich and Bayer, 2003). HL facilitates the selective uptake of CE from HDL (Lambert et al., 2000; Lambert et al., 1999) and from apoB remnant lipoproteins (Amar et al., 1998) in vivo. Thus HL plays a critical role in RCT by bridging lipoproteins proximal to SR-B1 and allowing the liver to internalize CE.

HL most likely has the same role in steroidogenic tissues. Although HL is not expressed by the adrenal gland, HL protein and activity is abundant (Doolittle et al., 1987). HL originating in the liver is thought to be transported to the adrenal gland via the circulation, probably associated with HDL. HDL is the predominant source of CE for steroidogenesis in the adrenals (Gwynne and Strauss, 1982) and it is known to be able to displace HL from cell surface proteoglycans (Ramsamy et al., 2003). Consistent with HL's proposed role in facilitating selective uptake of CE into the adrenal gland, SR-BI is upregulated in the adrenals of HL knockout female mice (Wang et al., 1996). Furthermore, adrenal cholesterol stores are reduced in these mice, suggesting that HL is necessary for optimal SR-BI mediated HDL-CE selective uptake (Wang et al., 1996).

1.10.4 HL and Atherosclerosis

Given HL's broad range of physiological functions as a multifunctional protein, it is no wonder that there is debate as to whether HL is a pro- or anti-atherogenic factor (reviewed in (Jansen et al., 2002)). The relationship between HL and atherosclerosis often differs depending on the model in which the relationship is studied. HL may be considered proatherogenic since it reduces plasma HDL-C, a factor inversely related with risk of coronary heart disease (Castelli et al., 1986). High HL activity is also correlated with production of small dense LDL (Zambon et al., 1993), which is the most atherogenic subclass of apoB lipoproteins (Krauss, 1995). On the other hand, HL has many anti-atherogenic properties. It expediates clearance of the TG-rich apoB lipoproteins, thereby reducing both plasma TG and plasma apoB concentrations-two factors associated with atherogenesis (Sniderman et al., 2004). HL also stimulates RCT by facilitating selective uptake of CE by the liver, allowing for its disposal in bile (Lambert et al., 2000; Lambert et al., 1999). Additionally, intravascular lipolysis of chylomicrons and VLDL generates excess surface PL which may act as lipid donors for the generation of new HDL from lipid poor apoAI (Havel et al., 1973). The delipidation of HDL2 to HDL3 and pre-β HDL is also an important part of the RCT pathway since the latter stimulate cholesterol efflux from cells efficiently (Fielding and Fielding, 2001).

1.10.5 HL Activity in Humans

Postheparin plasma HL activity varies widely in the general population (~8 fold) and is usually twofold higher in men than women (Deeb et al., 2003). Statin drugs and estrogen both reduce HL activity while visceral obesity, insulin resistance and androgens increase HL activity (Zambon et al., 2003). Genetic variation accounts for nearly 50% the variation in HL activity (Deeb et al., 2003). The most common genetic determinant of HL activity is associated with single nucleotide polymorphisms (SNPs) in the *LIPC* (HL gene) promoter. Four SNPs have been identified (A-763G, T-710C, C-514T and G-250A) which are responsible for decreased HL activity and are inversely related to HDL-C levels (Andersen et al., 2003; Isaacs et al., 2004). Less common are mutations within the coding region of *LIPC* which completely abolish HL activity. Heritable HL deficiency has been described in human patients and is often the result of compound heterozygous mutations (Hegele et al., 1993; Hegele et al., 1991; Ruel et al., 2003; Tilly-Kiesi et al., 2004). HL deficiency is associated with TG enrichment of lipoprotein fractions, abnormal postprandial lipid clearance and premature atherosclerosis (Hegele et al., 1993).

1.10.6 Rationale for Studying HL and VLDL Assembly

While the role of HL in lipoprotein metabolism and lipid clearance is extensively documented, no studies have directly assessed the potential of HL for intracellular lipid metabolism and apoB secretion. One study showed that intracellular human HL protein in Chinese Hamster Ovary (CHO) cells only possessed 2% of the TG hydrolase activity relative to secreted HL (Ben-Zeev and Doolittle, 2004); they concluded that intracellular HL was tightly associated with the ER chaperone calnexin (CNX) and did not gain lipolytic competence until after glycosylation and secretion. Contrary to this study, others had previously reported that HL isolated from rat hepatocytes acquired its TG lipase activity somewhere along the secretory pathway and prior to secretion (Verhoeven et al., 1999). The same authors later reported that the specific activity of HL increased 250% in the Golgi compartment compared to HL in the ER (Verhoeven et al., 2000). These studies indicate that HL could theoretically hydrolyze cellular lipids or lipids associated with lipoproteins destined for secretion. It is also conceivable that HL might contribute to the lipolysis and re-esterification cycle necessary for VLDL secretion.

The concept of a secreted enzyme playing an intracellular role in lipid metabolism may seem improbable, yet PLTP has recently been implicated in the provision of lipids for VLDL intracellularly (Jiang et al., 2001). The role of PLTP in exchanging lipids between lipoproteins in the circulation has been established (Jiang et al., 1999) but its intracellular effects on VLDL secretion were surprising. PLTP deficiency in apoE knockout or human apoB transgenic mice reduced secretion of both apoB and apoB-associated lipids dramatically, resulting in a concomitant reduction in atherosclerotic lesion areas of these mice (fed a Western diet) compared to their respective controls (Jiang et al., 2001). Adenoviral expression of PLTP in knockout hepatocytes enhanced secretion of apoB as well (Jiang et al., 2001). This study established that PLTP isolated from hepatocytes was capable of lipid transfer before its secretion (Jiang et al., 2001). For this reason, we cannot exclude the possibility that HL is capable of intracellular lipolysis based solely on its transient localization in the secretory pathway.

1.11 A Potential Role for AADA in Lipid Metabolism

The second candidate lipase is the 45 kilodalton enzyme AADA. It is proposed to be a lipase which may supplement the role of TGH in the lipolysis and re-esterification process (Gibbons et al., 2002; Gibbons et al., 2000; Gibbons et al., 2004; Trickett et al., 2001). The mouse enzyme is highly expressed in the liver and intestine and to a lesser extent in the pancreas and the adrenal gland (Trickett et al., 2001). AADA possesses esterase activity (Preuss and Svensson, 1996; Probst et al., 1994), shares sequence homology with the active site residues of HSL and is subject to inhibition by the lipase inhibitor THL, suggesting that it too might hydrolyze TG (Trickett et al., 2001). AADA is supposedly targeted to the ER membrane by an uncleaved N-terminal signal peptide sequence which forms a single transmembrane pass (Gibbons et al., 2000; Preuss and Svensson, 1996). It has been shown that fusion of the transmembrane domain of rabbit AADA to green fluorescent protein (GFP) was sufficient to target GFP to the ER membrane and induce a Type II conformation with the bulk of the protein facing the ER lumen (Mziaut et al., 1999).

In a similar fashion to TGH, AADA might mobilize TG for VLDL secretion. Trickett et al. have shown that hepatic AADA mRNA levels follow a diurnal rhythm with an identical pattern to hepatic VLDL secretion in mice (Trickett et al., 2001). Additionally, Gibbons et al. reported that transfection of a human AADA cDNA into HepG2 cells-a human hepatoma cell line deficient in both AADA and

TGH expression (Lehner and Vance, 1999)-caused a threefold increase in TG and fatty acid secretion (Gibbons et al., 2000). Furthermore, perinatal rat hepatocytes are capable of TG secretion although TGH expression is only apparent after the suckling period (Coleman et al., 1988; Lehner et al., 1999). AADA expression in rat liver does not differ between the perinatal, suckling and adult stages of life, suggesting that AADA might contribute to perinatal (and adult) hepatic TG secretion (Trickett et al., 2001).

1.12 A Potential Role for Es-X and Es-22 in Lipid Metabolism

The genes for Es-X, Es-22 and TGH are grouped in a carboxylesterase gene cluster on mouse chromosome 8 and human chromosome 16 (Becker-Follmann et al., 1997; Dolinsky et al., 2004b). Mouse Es-X and Es-22 are potential lipases since both proteins share 76% amino acid identity to mouse TGH (Fig. 1-5; (Dolinsky et al., 2004b)). The residues comprising the active site catalytic triad of TGH are conserved in Es-X and Es-22, as are the glycosylation site, the oxyanion hole, the ER-retrieval sequence and the secondary structures of these proteins (Fig. 1-5). The putative neutral lipid binding domains also show significant conservation, whereas the lid domains of Es-X and Es-22 are varied. (Fig. 1-5). The divergence of the lid domains may confer a different substrate specificity to these enzymes, as the lid domain has been implicated in regulating access of substrates to esterases and lipases (Wong and Schotz, 2002). No lipolytic activity has been demonstrated for Es-X or Es-22 to date, however.

Around 10-20% of murine Es-22 binds to β-glucuronidase in the ER and prevents its translocation to lysosomes (Medda and Swank, 1985). Free Es-22

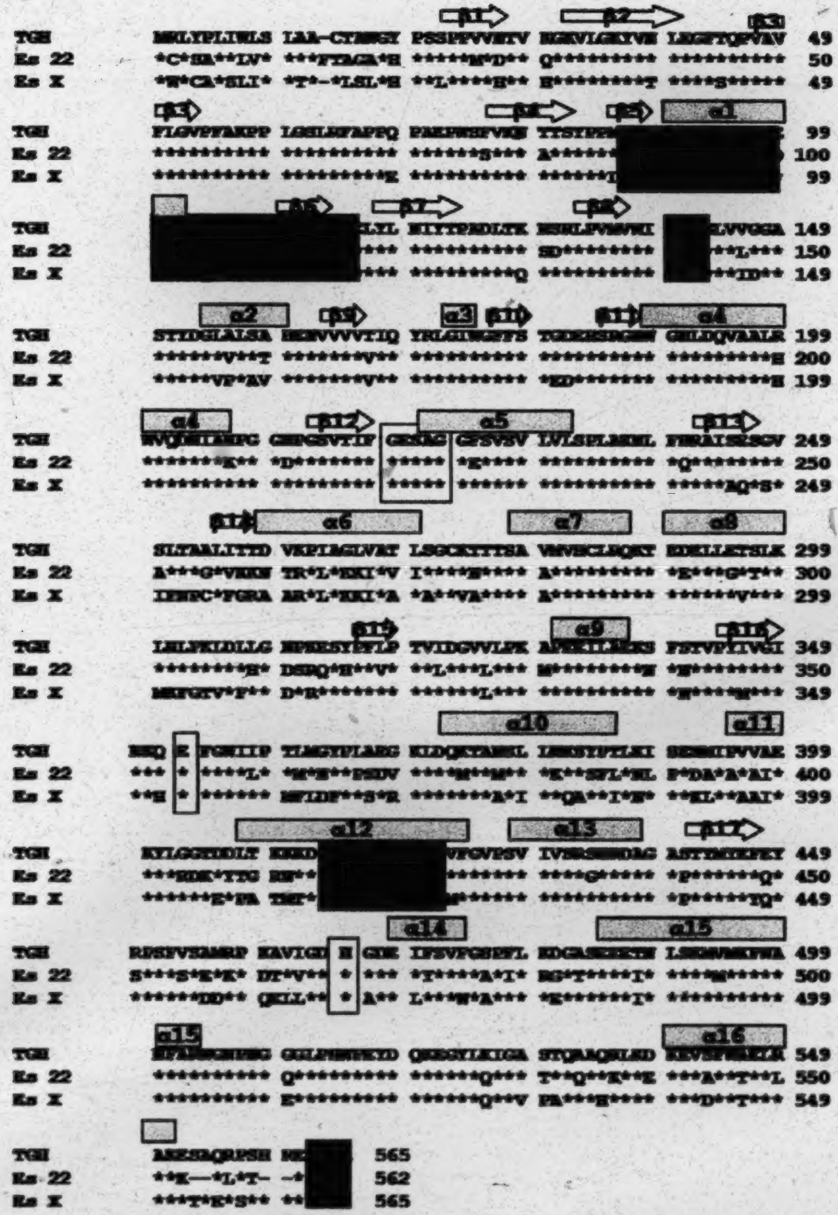
TGH
Es 22
Es X
β1
β2
β3
β4
β5
α1
β6
β7
β8
α2
β9
α3
β10
β11
α4
β12
α5
β13
β14
α6
α7
α8
β15
α9
β16
α10
α11
α12
α13
β17
α14
α15
α16
49
50
99
100
149
150
199
200
249
250
299
300
349
350
399
400
449
450
499
500
549
550
565
562

Fig. 1-5: Mouse Es-X and Es-22 share 76% sequence homology with TGH. The amino acid sequence for TGH is given in single letter code. Amino acid identity is indicated with an asterix and non-aligned amino acids are indicated. Yellow arrows are beta sheets and blue rectangles are alpha helices in the mouse TGH protein. The red box contains the lid domain, the grey box distinguishes the oxanion hole, the green box encompasses the neutral lipid binding domain and the purple box highlights the ER retrieval sequence. The open boxes surround the serine, glutamic acid and histidine residues which comprise the catalytic triad.

has carboxylesterase activity, which is readily inhibited by bis-*p*-nitrophenylphosphate (Medda and Swank, 1985). Murine Es-22 is expressed in the liver, kidney, lung and submandibular gland (Ovnic et al., 1991). Human Es-22 has been crystallized and is known to metabolize cocaine, heroin and statin drugs (Bencharit et al., 2003; Fleming et al., 2005).

Relatively little is known about Es-X (also called mouse carboxylesterase-1 (CES-1)) except that it is predominantly expressed in the liver, with lower expression in the lung and kidney (Ellinghaus et al., 1998). Es-X expression was greatly suppressed in sterol carrier protein 2 / sterol carrier protein X (SCP2/SCPx) double knockout mice compared to wild-type mice (Ellinghaus et al., 1998). Feeding these mice diets containing cholestyramine or sodium cholate increased Es-X expression (Ellinghaus et al., 1998). SCP2/SCPx knockout mice had impaired bile salt and cholesterol secretion into bile (Fuchs et al., 2001). On a lithogenic diet, these mice had 40% reduced plasma VLDL-C levels compared to wild-type mice (Fuchs et al., 2001). The contribution of Es-X to this phenotype is unknown, but its high homology to TGH suggests that the lower VLDL-C levels might result from decreased VLDL secretion in the absence of Es-X.

As Es-X and Es-22 are very similar in structure to TGH and are targeted to the ER lumen in the liver, these are potential lipases which may participate in the TG lipolysis and re-esterification cycle for VLDL secretion.

1.13 The McA Cell Line

McA cells are a rat hepatoma-derived cell line used extensively to study apoB secretion (Lehner and Vance, 1999; Tran et al., 2002; Yamaguchi et al., 2003). They retain many similarities to primary rat hepatocytes, such as their ability to secrete apoB, albumin, apoAI and apoE (Ji et al., 1994). McA cells also efflux cholesterol to apoAI (Sahoo et al., 2004). Yet McA cells, like HepG2 cells, are impaired in the mobilization of stored TG for VLDL assembly and secretion (Gibbons et al., 1994; Lehner and Vance, 1999; Wu et al., 1996). McA cells also exhibit other differences from primary hepatocytes. They no longer express TGH, Es-X or AADA and have only limited expression of Es-22 compared to rat hepatocytes (Fig. 1-6). This may be the reason why McA cells have a slower TG turnover and secretion rate than primary hepatocytes (Lehner and Vance, 1999). Therefore introducing the cDNAs encoding these proteins might partially restore the phenotypic properties of primary hepatocytes. McA cells also differ from primary hepatocytes in that they rapidly divide in culture and are easily transfected, making them an invaluable tool for the study of hepatic metabolism. They are also superior to HepG2 cells (a human hepatoma cell line often used to study apoB secretion) because they form a monolayer in culture and do not pile. More importantly, McA cells are capable of secreting apoB100 in the VLDL density range when stimulated with exogenous oleic acid, whereas HepG2 cells mainly secrete apoB lipoproteins of higher density (Boren et al., 1994; Tran et al., 2002). Unlike primary hepatocytes which continue to secrete lipids at a normal rate after the removal of exogenous oleic acid, lipid secretion is markedly depressed in McA cells without oleic acid (Lehner and Vance, 1999).

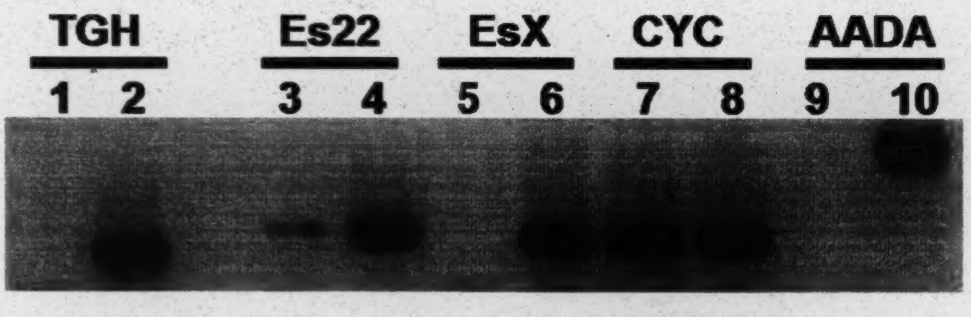

Fig. 1-6: McArdle RH7777 cells do not express TGH, Es-X or AADA and have low level expression of Es-22 compared to rat hepatocytes. Reverse transcriptase PCR of RNA isolated from McArdle RH7777 cells (odd numbers) and from primary rat hepatocytes (even numbers) with specific primers (40 cycles). CYC is cyclophilin. These data are courtesy of Dr. Vern Dolinsky.

1.14 Thesis Objectives

The objective of this project was to clone the cDNAs for mouse HL, AADA, Es-X and Es-22 and generate chimeric cDNAs with sequence encoding the FLAG epitope. The FLAG epitope (DYKDDDDK) allows for protein detection with commercial antibodies (Chubet and Brizzard, 1996). Generation of McA rat hepatoma cells stably expressing either FLAG-tagged mouse AADA, Es-X, Es-22, HL or a mutagenic HL which is targeted to the ER, would provide model systems to study VLDL secretion. Expression of a TGH cDNA in McA cells was sufficient to enhance VLDL secretion (Lehner and Vance, 1999), so the expression of another lipase involved in VLDL secretion is expected to do the same. The hypothesis is that ER lumenal lipases other than TGH contribute to VLDL secretion by preferentially directing lipolysis products into the secretory route. Identification of novel lipases which contribute to the TG lipolysis and re-esterification cycle of VLDL assembly would reveal potential drug targets to reduce plasma apoB and TG concentrations. Treatments resulting in reduced atherogenic lipoprotein secretion might alleviate or reverse the progression of atherosclerosis and coronary heart disease.

The following chapters describe the cloning and characterization of these enzymes: **Chapter 2** presents the general methodology used for cloning, production of stable cell lines, cell maintainence and experimental procedures used throughout this work; **Chapter 3** entails the role of HL in intracellular lipid metabolism and VLDL secretion; **Chapter 4** characterizes AADA with regard to lipase activity, intracellular lipid metabolism and VLDL secretion; **Chapter 5** investigates whether Es-X and Es-22 are lipases; and in **Chapter 6** the summary, conclusions and future directions of this work are discussed.

Chapter 2:

General Methodology

2.1 Chemicals and Materials

All organic solvents were obtained from Fisher Scientific (Ottawa, ON). 4-methylumbelliferylheptanoate (4-MUH), 4-methylumbelliferone sodium salt (4-MU), lipid standards, phospholipase C (PL-C), anhydrous Na_2SO_4 and essentially fatty acid-free bovine serum albumin (BSA) were from Sigma-Aldrich (Oakville, ON). 1,2-dilauryl-rac-glycero-3-glutaric acid resorufin ester (resorufin ester) and free resorufin were from Boehringer-Mannheim (Meylan, France). 40% Acrylamide solution, nitrocellulose membranes and prestained molecular weight markers were from BioRad Laboratories (Mississauga, ON). Secondary antibodies conjugated to horseradish peroxidase (HRP) were from Pierce Biotechnology (Rockford, IL). Lipofectamine2000, penicillin, streptomycin, horse serum (HS), fetal bovine serum (FBS), geneticin (G-418) and Dulbecco's Modified Eagle's Medium (DMEM) were from Invitrogen (Burlington, ON). Culture dishes were from Corning (New York, NY). PE SIL G Flexible Plates for TLC were from Whatman (Florham Park, NJ). CytoScint scintillation fluid was from ICN Biomedicals (Irving, CA). Sylon BFT was from Supelco (Bellefonte, PA). M2 anti-FLAG primary antibodies were from Stratagene (La Jolla, CA). Black and clear Microtest 96-well assay plates were from BD Falcon (Franklin Lakes, NJ). Triton X-100 was from VWR International (Edmonton, AB). Western Blotting Detection Reagents were from Amersham Biosciences (Oakville, ON). BioMax MR film was from Eastman Kodak Company (New Haven, CT).

2.2 Molecular Biology Reagents

Molecular biology techniques were performed as described (Sambrook, 1989). Oligonucleotide primers were synthesized by the Institute for Biomolecular Design at the University of Alberta and DNA sequencing was performed by the Molecular Biology Services Unit at the University of Alberta. DNA was amplified using Pwo polymerase from Roche Applied Science (Indianapolis, IN) or Taq polymerase from Invitrogen. All polymerase chain reactions (PCR) reactions utilized a PTC-200 Peltier Thermal Cycler from MJ Research, Inc. (Scarborough, ON). Restriction endonucleases, deoxynucleotide triphosphates (dNTPs) and T4 DNA ligase were from both Invitrogen and New England Biolabs (Mississauga, ON). The plasmid pBluescript II SK- and QuikChange Site-Directed Mutagenesis Kits were purchased from Stratagene. pCR4 TOPO-TA cloning kits were also from Invitrogen. The mammalian expression vector pCI-neo was from Promega Corporation (Madison, WI). Plasmids were isolated from E. coli using Plasmid QIAprep Spin Miniprep Kits from Qiagen (Mississauga, ON). PCR products and digested plasmids were purified from agarose gels using QIAEX II Gel Extraction Kits, also from Qiagen.

2.3 Cloning of Native and Chimeric cDNAs

Oligonucleotides were designed to amplify the native mouse cDNAs of HL, AADA, Es-X and Es-22 from a mouse liver λgt11 cDNA library (Dolinsky et al., 2001). The forward primers contain sequence from the 5' coding region of the cDNAs and the reverse primers correspond to sequence from the 3' end of the complimentary strands (Table 2-1). Amplification was performed at 93°C 1 min, 60°C 1 min, 72°C 2 min for 30 cycles using Pwo polymerase. PCR products

Table 2-1: Primers used for the amplification of native cDNAs and chimeric cDNAs

Primer Name	Sequence*
HL-f †	5'-C CTA CTC GAG GGT AAG ACG AGA GAC ATG GGA AAT CCC CT-3'
HL-r	5'-A CGT TCT AGA GAA TAG ACT TCT TTA TTT TTT TGC ATG GG-3'
M.(HL-R)-f	5'-T CAT TCT AGA TCA CAG TTC AAC ATG **CTT ATC GTC GTC ATC CTT GTA ATC** TTT TTT TGC ATG GGT CTC TTG ACT CAT CTG C-3'
M.(HL-S)-r	5'-CT AGT CTA GAC TAG TCA **CTT ATC GTC GTC ATC CTT GTA ATC** TTT TTT TGC ATG GGT CTC TTG ACT CAT CTG C-3'
AADA-f	5'-ATG GGG AAA ACC ATT TCT CTT CTC-3'
AADA-r	5'-TTA CAG ATT TTT GAT AAG CCA ACT CAA-3'
M.AADA-f	5'-GCAG CTC GAG ATG GGG AAA ACC ATT TCT CTT CTC ATC C-3'
M.AADA-r	5'-T CAT TCT AGA TCA **CTT ATC GTC GTC ATC CTT GTA ATC** CAG ATT TTT GAT AAG CCA ACT CAA GTA CTG-3'
Es22-f	5'-TG TAG CCT CCT ACC ATG TGC CTC TCT GC-3'
Es22-r	5'- GGC AGA TCA CAG CTC AGT GTG TTC TGT CGG CAG TTG CTT CTT AGC C-3'
M.Es22-f	5'-GCAG CTC GAG ATG TGC CTC TCT GCT CTG ATC CTG G-3'
M.Es22-r	5'-T CAT TCT AGA TCA CAG CTC AGT GTG **CTT ATC GTC GTC ATC CTT GTA ATC** TTC TGT CGG CAG TTG CTT CTT AGC CAG-3'
EsX-f	5'-C TAT TCT TCC ATG ATG TGG CTC TGT G-3'
EsX-r	5'-TCAT TCT AGA TCA CAG TTC AAC ATG TTC CCT ATG GGA TGA CCT CTC TGC-3'
M.EsX-f	5'-GCAG CTC GAG ATG TGG CTC TGT GCT TTG AGT CTG ATC TC-3'
M.EsX-r	5'-TCAT TCT AGA TCA CAG TTC AAC ATG **CTT ATC GTC GTC ATC CTT GTA ATC** TTC CCT ATG GGA TGA CCT CTC TGC TG-3'

*note: CTC GAG is XhoI restriction sequence; TCT AGA is XbaI restriction sequence; **ATC GTC GTC ATC CTT GTA ATC** encodes the FLAG epitope; f=forward, r=reverse; M.=mutagenic/chimeric

†note: HL-f was used to amplify the mutagenic/chimeric cDNA and the native cDNA

were blunt-end ligated into the EcoRV site of pBluescript II SK- plasmid and the entire cDNAs were sequenced. These plasmids were used as templates to generate chimeric cDNAs which incorporate sequence encoding the FLAG epitope (DYKDDDK; (Chubet and Brizzard, 1996)) into each of the native cDNAs as well as sequence encoding the mammalian ER retrieval signal (HVEL; (Gilham et al., 2005)) into the HL cDNA. The mutagenic primers are also listed in Table 2-1. The chimeric cDNAs were amplified from the native cDNAs, as described above, except with Taq polymerase; this facilitated cloning into the pCR4-TOPO plasmid. The chimeric cDNAs were sequenced to ensure fidelity, excised from pCR4-TOPO using XhoI and SpeI restriction endonucleases and ligated into XhoI and XbaI digested pCI-neo mammalian expression vector. Transcription of chimeric cDNAs is driven by the cytomegalovirus enhancer/promoter in pCI-neo.

2.4 Cell Culture and Generation of McA Stably Expressing Chimeric cDNAs

McA and Cos-7 cells were obtained from American Type Culture Collection (Manassas, Virginia). McA were cultured in DMEM containing 50 U/mL penicillin/streptomycin, 10% HS and 10% FBS at 37ºC in humidified air containing 5% CO_2. Cos-7 cells were cultured similarly, except without HS. Cells were maintained to subconfluence and were divided 2-3 times weekly.

To ensure that each chimeric cDNA would yield protein, Cos-7 cells were transiently transfected and cell lysates were analyzed for protein expression by immunoblotting. A 60 mm culture dish of 80% confluent Cos-7 cells was incubated overnight (16 h) with 3 µg of pCI-neo/chimeric cDNA complexed to 10 μL Lipofectamine2000 in 2 mL serum-free DMEM. Cells were grown for an additional 24 h, were harvested in phosphate buffered saline (PBS; 137 mM NaCl, 2.7 mM KCl, 10 mM Na_2HPO_4 and 2 mM KH_2PO_4) and analyzed for FLAG-tagged protein by immunoblotting.

Once it was established that pCI-neo/chimeric cDNA constructs produced protein in mammalian cells, stable cell lines were generated. 60 mm culture dishes of 80% confluent wild-type McA were transfected with 6 μg of pCI-neo/chimeric cDNA complexed to 20 μL Lipofectamine2000 in 2 mL serum-free DMEM overnight. The following day, cells were passaged 1:5 into 100 mm culture dishes and were cultured in the presence of 1.6 mg/mL G-418 for one week to select for neomycin resistance (this media was replaced every 2 days to remove dead cells). Individual clones were isolated and analyzed for FLAG-tagged protein by immunoblotting. Stable cell lines were thereafter maintained in 60 mm culture dishes with 2.5 mL media containing 0.4 mg/mL G-418, while wild-type McA cells were cultured in the absence of G-418.

2.5 Lipase Assays

2.5.1 4-MUH Lipase Assay

Lipase activity was measured using the water-insoluble fluorogenic substrate 4-MUH, as described (Gilham and Lehner, 2005). Hydrolysis of 4-MUH liberates the fluorescent product 4-MU, whose emission is measured at 460 nm. A 100 mM stock of 4-MUH in tetrahydrofuran is diluted to 1 mM 4-MUH in assay buffer B (20 mM Tris buffer, pH 8.0, 1 mM EDTA and 300 μM taurodeoxycholate) immediately before starting the reaction. Samples to be analyzed were brought to a final volume of 180 µL with buffer B in a 96-well black microtiter plate. The reaction was initiated by the injection of 20 µL of 1 mM 4-MUH into each well containing samples, followed by brief shaking and kinetic measurements of fluorescence every 20 s for 5 min. Substrate injection, mixing and measurements were performed with a Fluoroskan Ascent FL Type 374 with the filter pair 355 nm/460 nm and data were collected with Ascent software (Thermo Labsystems, Waltham, MA). Moles of 4-MUH hydrolyzed were calculated from a standard curve generated with 4-MU.

2.5.2 Resorufin Ester Lipase Assay

Lipase activity was measured using the water-insoluble fluorogenic substrate resorufin ester, as described (Gilham and Lehner, 2005). Resorufin ester hydrolysis liberates the fluorescent resorufin molecule, whose emission is measured at 590 nm. A 2 mg/mL stock of resorufin ester in dioxane was diluted to 0.3 mg/mL in assay buffer B immediately before starting the reaction. Samples to be analyzed were brought to a final volume of 180 µL with buffer B in a 96-well black microtiter plate. The reaction was initiated by the injection of 20 µL of 0.3 mg/mL resorufin ester into each well containing samples, followed by brief shaking and kinetic measurements of fluorescence every 4 min for 60 min. Substrate injection, mixing and measurements were performed with a Fluoroskan Ascent FL Type 374 with the filter pair 544 nm/590 nm and data were collected with Ascent software. Moles of resorufin ester hydrolyzed were calculated from a standard curve generated with free resorufin.

2.6 Stimulation of TG Synthesis and VLDL Secretion

To stimulate TG synthesis in McA cells and enhance VLDL secretion, cells were incubated in the presence of 0.4 mM oleic acid complexed to 0.5% BSA for 4 h (Lehner and Vance, 1999). A 20X oleic acid/BSA stock was prepared as follows: 5 g of essentially fatty acid-free BSA was dissolved in 50 mL of serum-free DMEM at 56°C and 0.106 g of oleic acid was warmed to 56°C for 1 min; the DMEM / BSA solution was added to the oleic acid and the mixture was stirred rapidly with a Teflon coated stir bar at 56°C until the solution clarified (indicating that oleic acid was complexed to the BSA). The 20X oleic acid/BSA solution was sterilized by passage through a 0.22 µm filter. This concentrated stock solution was diluted 20 fold to give a final concentration of 0.4 mM oleic acid/0.5% BSA for augmenting TG stores and VLDL secretion from McA cells.

2.7 Pulse/Chase Experiments

Six 60 mm culture dishes of control (McA or the empty pCI-neo stable cell line, pNEO1) and stably transfected cell lines were grown to 70% confluency. The pulse represents a 4 h incubation with 2 mL serum-free DMEM containing 0.4 mM oleic acid complexed to 0.5% BSA to stimulate neutral lipid synthesis. After 4 h, three culture dishes and media were collected for analyses. The remaining three dishes had their pulse media aspirated, were washed three times for 10 min with serum-free DMEM containing 0.5% fatty acid-free BSA and were incubated for an additional 12 or 16 h with 2 mL of serum-free DMEM; this incubation is referred to as the chase. After 12 or 16 h, chase cells and media were collected for analyses. Media were centrifuged at 500 *g* for 10 min to remove cellular debris. Cells from pulse/chase experiments were washed with ice-cold PBS, harvested in the same buffer, and disrupted by sonication. Cell protein concentrations were determined as described in Section 2.12. Lipids from cell lysates and media were isolated and measured by gas chromatography (GC) as described in Section 2.9.

2.8 Analyses of Radiolabeled Lipids

After radiolabeled experiments (described in Chapter 3, Sections 3.2.6 and 3.2.8, and in Chapter 4, Sections 4.2.8 and 4.2.10), lipids were extracted from cell lysates and media with 2:1 (v/v) chloroform:methanol (Folch et al., 1957) in the presence of unlabeled lipid carriers. 4 mL of chloroform/methanol containing 100 µg each of PC, oleic acid, trioleoylglycerol and cholesteryl oleate was used per 1 mL of cell lysate or media. Samples were vortexed rigorously for 15 s followed by 10 min centrifugation at 500 *g* to separate the aqueous phase from the chloroform phase. The chloroform phase was isolated, dried under nitrogen at 37ºC and lipids were resuspended in a small volume of chloroform. Lipid samples were spotted on PE SIL G flexible TLC plates and were resolved in a 2 solvent system. The TLC plates were developed to 1/3 their height with 25:15:4:2 (v/v) chloroform:methanol:acetic acid:water to resolve the glycerophospholipids, allowed to dry, and then were developed to the top with 15:10:1 (v/v) heptane:isopropyl ether:acetic acid to resolve the neutral lipids (Lehner and Vance, 1999). TLC plates were allowed to dry and lipids were visualized by exposure to iodine. Lipids were identified by comigration with lipid standards. Lipid bands were cut from the TLC plates and placed in scintillation vials, to which 5 mL of CytoScint scintillation fluid was added. Vials were rocked overnight, followed by a rigorous 30 s shaking to ensure that lipids were dissolved in the scintillant. Radioactivity associated with each sample was quantified by scintillation counting using a Beckman LS 5000TA counter (Beckman Coultier Canada Inc., Mississauga, ON).

2.9 Lipid Mass Analyses by GC

Lipid masses were measured as previously described (Sahoo et al., 2004). Phospholipids present in 1 mL cell lysate or 1.8 mL cell-free media from pulse/chase experiments were digested with PL-C (from Clostridium welchii) for 2 h at 30°C. Lipids were extracted in 4 mL of 2:1 chloroform:methanol (Folch et al., 1957) per mL of sample in the presence of tridecanoin (internal standard). The chloroform phase was isolated, passed through anhydrous Na_2SO_4 columns and dried under nitrogen at 37°C. Free hydroxyl groups were derivitized with 100 µL Sylon BFT for 1 h at room temperature. Samples were dried under nitrogen and resuspended in 100 µL hexane. Samples were injected into a Zebron ZB-5 (Phenomenex, Inc., Torrance, CA) capillary GC column and lipids were quantified using an Agilent 6890 Series Gas Chromatograpy System equipped with a flame ionization detector (Agilent Technologies, Palo Alto, CA). Data analyses were performed using GC Chemstation software (Agilent Technologies).

2.10 Preparation of Microsomal Membranes

Cells from three 150 mm culture dishes grown to 70% confluency were harvested into 10 mL of 50 mM Tris, pH 7.4, containing 250 mM sucrose and 5 mM EDTA. Cells were disrupted by sonication and microsomal membranes were isolated by ultracentrifugation for 1 h at 106,000 *g* from a post-mitochondrial supernatant (Gilham et al., 2003). Microsomal membranes were resuspended by homogenization in tris-buffered saline (TBS; 20 mM Tris, pH 7.4, 137 mM NaCl).

2.11 Protein Electrophoresis and Western Blotting

Proteins were denatured by boiling for 5 min in 1X denaturing sample treatment buffer, resolved by sodium dodecyl sulfate polyacrylamide gel electrophoresis (SDS-PAGE), transferred to nitrocellulose and immunoblotted. All membranes were blocked with 4% skim milk powder in TBS containing 0.1% Tween 20 (T-TBS) for 1 h prior to antibody incubations and all antibody incubations were carried out in this solution. Membranes were washed three times for 10 minutes with fresh T-TBS after each incubation with antibodies.

Cell lysate and microsomal proteins were separated in 10% polyacrylamide SDS gels. FLAG-tagged proteins were detected by incubating membranes with 1:8,000 mouse anti-FLAG primary antibodies followed by 1:8,000 HRP-conjugated goat anti-mouse secondary antibodies. Blots were exposed to BioMax MR film after using ECL Western Blotting Detection Reagents, unless otherwise specified.

2.12 Protein Concentration Measurements

Protein concentrations were determined with a spectrophotometer using Protein Assay Reagent according to BioRad instructions and using BSA as a standard.

Chapter 3:

Role of Hepatic Lipase in the Mobilization of Intracellular Lipids and VLDL Assembly

3.1 Introduction

HL plays a complex role in the metabolism of circulating lipoproteins. It is capable of hydrolyzing TG and PL associated with all classes of lipoproteins (Zambon et al., 2003). Additionally, HL binds lipoproteins and facilitates remnant removal independent of its catalytic activity (Dichek et al., 1998; Ji et al., 1994). The bridging function of HL also mediates selective uptake of lipoprotein CE via SR-BI (Amar et al., 1998; Lambert et al., 1999). Therefore HL has a central role in extracellular lipid metabolism and the RCT pathway.

Although studies have concluded that HL gains its lipase activity along the secretory pathway (Verhoeven and Jansen, 1991; Verhoeven et al., 2000), no research has evaluated the contribution of HL to intracellular lipid metabolism or VLDL secretion. Its transient localization to the ER suggests that HL could mobilize TG for VLDL secretion in a manner similar to TGH. To investigate these possibilities, cDNAs encoding a FLAG-tagged mouse HL and a FLAG-tagged mouse HL targeted to the ER were stably expressed in McA cells. The intracellularly retained HL was targeted to the ER with the same C-terminal ER retrieval sequence found in mouse TGH (-HVEL; (Gilham et al., 2005)). Previously, McA cells stably expressing a TGH cDNA were shown to enhance VLDL-TG secretion (Lehner and Vance, 1999). Using similar pulse/chase experiments, McA cells stably expressing chimeric mouse HL enzymes were analyzed for cellular lipid turnover as well as apoB and TG secretion.

3.2 Materials and Methods

3.2.1 Chemicals and Materials

Reduced nicotinamide adenine dinucleotide (NADH), sodium pyruvate, trichloroacetic acid (TCA), paraformaldehyde, fumed silica, t-butyl hydroperoxide and Infinity Triglyceride Reagent were from Sigma-Aldrich. Coverslips and slides were from Fisher Scientific. Polyclonal rabbit anti-protein disulfide isomerase (PDI) antibodies were from Stressgen Biotechnologies (Victoria, BC). Alexa488 conjugated goat anti-mouse antibodies and Prolong Antifade Kit were from Molecular Probes (Eugene, Oregon). TexasRed conjugated donkey anti-rabbit antibodies were from Jackson ImmunoResearch (West Grove, PA). Goat anti-apoB antibodies were from Chemicon International (Temecula, CA). A BioCoat Cell Environment collagen-coated culture dish was from BD Biosciences (San Jose, CA). Lutrol F127 NF Prill Surfactant (Poloxamer 407) was from BASF Corporation (Florham Park, NJ). 4-15% Tris-HCl Ready Gels were from BioRad. SuperSignal West Dura Extended Detection Substrate was from Pierce Biotechnology. Amicon Ultra 10,000 MW spin concentrators were from Millipore (Mississauga, ON). [9,10(n)-^{3}H]oleic acid was from Amersham Biosciences. Hionic-Fluor scintillation cocktail was from Packard Instrument Co. (Meriden, CT, USA).

3.2.2 Screening of Stable McA Cell Lines for Expression of FLAG-tagged HL

Generation of McA cells stably expressing FLAG-tagged HL proteins was described in Chapter 2, Sections 2.2, 2.3 and 2.4. HL-R clones were grown to

70% confluency, harvested in ice-cold PBS and 50 µg of cell lysate protein were analyzed for FLAG-tagged protein. HL-S clones were each grown to 70% confluency, washed with PBS and incubated for an additional 16 h in serum-free DMEM. Proteins were precipitated from the media using TCA and were analyzed for FLAG-tagged protein. Proteins were separated by SDS-PAGE and visualized by Western blotting as described in Chapter 2, Section 2.11.

3.2.3 Precipitation of HL-S from Media

200 µL of 72% TCA was added to 1.8 mL of cell-free media. Samples were vortexed and incubated on ice for 30 min, followed by centrifugation at 14,000 rpm for 5 min to pellet precipitated proteins. Supernatants were aspirated and pellets were washed twice with 500 µL of acetone and allowed to dry. Pellets were resuspended in 200 µL of TBS by homogenization and 50 µL were separated by SDS-PAGE and visualized by Western blotting as described in Chapter 2, Section 2.11.

3.2.4 Resorufin Ester Lipase Assay

Lipolytic activities of cell lysates, media and microsomes from stable cell lines were analyzed using resorufin ester (Gilham and Lehner, 2005) for two reasons: 1) it is a TG analogue and 2) detection of resorufin ester hydrolysis by HL was more sensitive than 4-MUH hydrolysis by HL (personal observation). 100 µg of microsomal membranes were prepared as described in Chapter 2, Section 2.10, and were assayed for lipolytic activity as described in Chapter 2, Section 2.5.2. The activity of cell and media samples were determined after a 4 h pulse in DMEM + 0.4 mM oleic acid/0.5% BSA by harvesting the cells in the same volume of PBS as the volume of media (2 mL) and assaying equal volumes (100 µL); values were then correlated to cell protein concentration.

3.2.5 Confocal Immunofluorescence Imaging

pNEO1 and R12 cells were grown sparsely on sterile coverslips overnight in 6-well culture dishes and were incubated with serum-free DMEM for 1 h prior to fixation and staining. Cells were fixed to coverslips with 4% paraformaldehyde in PBS for 5 min and were permeablized with 0.2% Triton X-100 in PBS. Coverslips were incubated with 1:1000 mouse anti-FLAG and 1:1000 rabbit anti-PDI primary antibodies. They were subsequently incubated with 1:1000 goat anti-mouse and 1:1000 donkey anti-rabbit secondary antibodies conjugated to Alexa488 and Texas Red fluorophores, respectively. Both antibody incubations were in PBS containing 3% BSA for 1 h at 37°C. Cells were rinsed gently 3 times with 2 mL PBS after each incubation. Coverslips were mounted on microscope slides with Prolong Antifade and images were obtained using a Zeiss LSM510 confocal microscope (Carl Zeiss Canada Ltd, Toronto, ON). An argon laser producing a wavelength of 488 nm and a HeNe laser producing a wavelength of 543 nm were used to excite Alexa488 and Texas Red fluorophores, respectively. Fluorescence from each fluorophore was measured on separate channels (Fig. 3-1). Images were visualized using Zeiss LSM510 Image Browser software (Carl Zeiss). As controls, pNEO1 and R12 cells were treated with primary or secondary antibodies only; no fluorescence was detected using identical microscope settings.

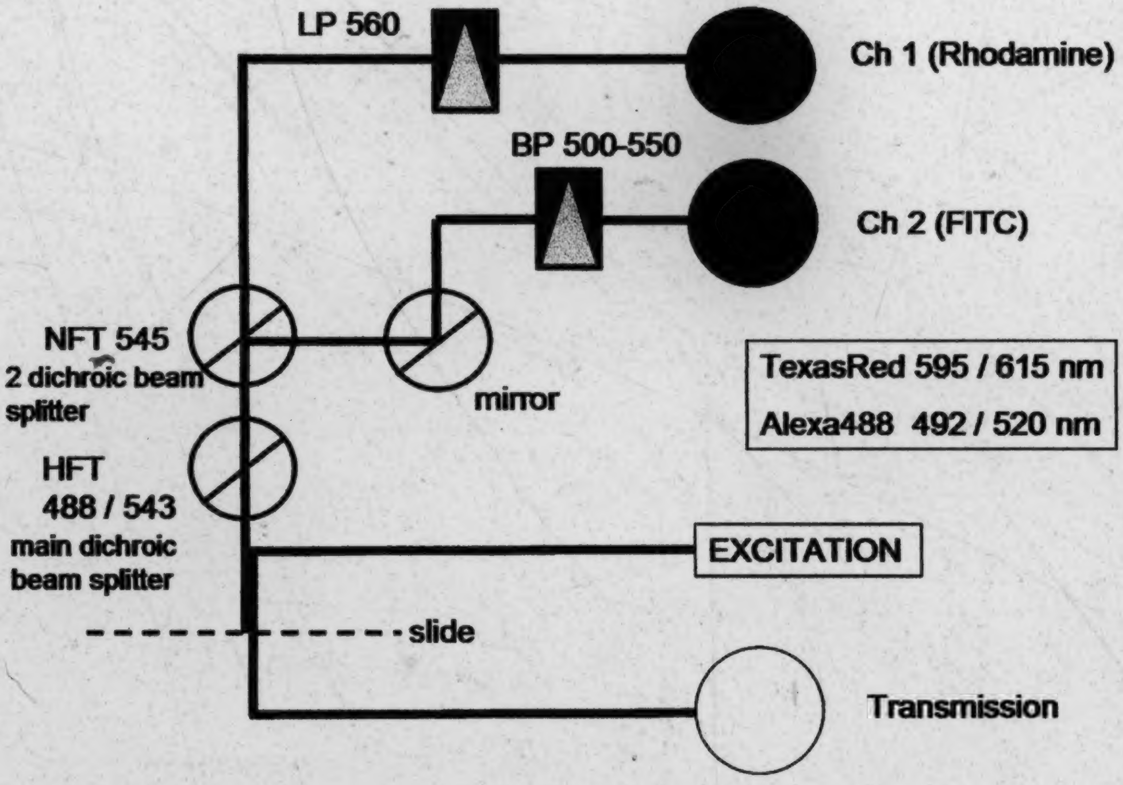
LP 560
Ch 1 (Rhodamine)
BP 500-550
Ch 2 (FITC)
NFT 545
2 dichroic beam splitter
mirror
TexasRed 595 / 615 nm
Alexa488 492 / 520 nm
HFT
488 / 543
main dichroic beam splitter
EXCITATION
slide
Transmission

Fig. 3-1: Schematic of beam path and channel assignment used for confocal immunofluorescence of HL-R and pNEO1 cells in Fig. 3-3.

3.2.6 Incorporation of [^{3}H]Oleic Acid into Lipids

Nine 60 mm culture dishes of 50% confluent pNEO1, R12 and S7 cells were incubated with 2 mL of 0.4 mM oleic acid/0.5% BSA containing 5 µCi [^{3}H]oleic acid. Three dishes of each were collected at 1 h, three more at 2 h and the final three at 4 h. Cells were washed with ice-cold PBS and harvested in this same buffer. Radiolabel incorporation into lipids was quantified as described in Chapter 2, Section 2.8.

3.2.7 Pulse/Chase Experiments

Experiments were performed using pNEO1, R12 and S7 cell lines or McA, R5 and S1 cell lines with a 4 h pulse and 16 h chase, as described in Chapter 2, Section 2.7. Untreated samples are cells grown to 70% confluency, washed with ice-cold PBS and harvested in this same buffer. Lipid masses were quantified by GC as described in Chapter 2, Section 2.9.

3.2.8 Radiolabel Pulse/Chase Experiments

Experiments were performed using pNEO1, R12 and S7 cell lines with a 4 h pulse and 16 h chase, as described in Chapter 2, Section 2.7, except with the addition of 5 µCi [^{3}H]oleic acid per dish in the pulse. Radiolabel incorporation into lipids was quantified as described in Chapter 2, Section 2.8.

3.2.9 Secretion of ApoB and Densitometry

Media were collected from each dish at the end of the pulse and chase (exactly as described in Chapter 2, Section 2.7, except cells were washed 3 times with DMEM *without* BSA after the pulse). 1.5 mL of cell-free media from each dish was transferred to an eppendorf tube, to which 50 µL of 50 mg/mL Cab-o-sil (fumed silica) in water was added (Vance et al., 1984). Tubes were rotated for 2 h at 4°C, then Cab-o-sil was pelleted by centrifugation for 10 min at 1,300 *g*. Supernatants were aspirated and the pellets containing apoB were resuspended in 60 µL 1X denaturing sample treatment buffer by vortexing and boiling for 5 min. Cab-o-sil was pelleted again at 1,300 *g* and the supernatants were resolved in 4-15% Tris-HCl Ready Gels (BioRad). Membranes were blotted with 1:3,000 goat anti-apoB antibody and 1:5,000 anti-albumin affinity-purified rabbit polyclonal antibody (prepared in our laboratory); HRP-mouse anti-goat and HRP-goat anti-rabbit secondary antibodies were used at a 1:5,000 dilution. SuperSignal West Dura Extended Detection Substrate was used for chemilumenescence. ApoB and albumin band intensity was analyzed using Quantity One software (BioRad).

3.2.10 Measurements of Secreted Fatty Acids and Acid Soluble Products

During a radiolabeled pulse/chase experiment, the amount of diluted hydrochloric acid required to drop the pH of the aqueous phase of lipid extractions to pH 3 was determined. Since oleic acid has a pKa of 9.85 (Kanicky and Shah, 2002), I rationalized that at pH 3 all [^{3}H]oleic acid would be protonated and should partition into the chloroform phase while all acid soluble metabolites should partition to the aqueous phase. In hepatocytes, acid-soluble metabolites routinely account for over 90% of total oxidation products (Muoio et al., 1999). Lipid extractions were acidified and radiolabeled lipids, including

$[^3H]$oleic acid in the chase media, were analyzed as described in Chapter 2, Section 2.8. The aqueous phase was isolated and determined to be 2.3 mL for cell extractions and 3.9 mL for media extractions; 400 µL of aqueous sample was added to 5 mL of Hionic-Fluor scintillation cocktail and assayed for radioactive acid soluble metabolites by scintillation counting using a Beckman LS 5000TA counter.

3.2.11 Poloxamer 407 (P-407) Inhibition of HL Activity

Three 60 mm culture dishes of S7 cells grown to 70% confluence were incubated with 2 mL DMEM in the absence of P-407 or in the presence of 10 or 50 µM P-407 for 16 h. As a control, one 60 mm culture dish of pNEO1 cells grown to 70% confluence was treated exactly as P-407 untreated (0 µM) S7 cells. Media were collected and centrifuged at 500 *g* to remove cell debris. Cells were washed with and harvested into 2 mL ice-cold PBS and were disrupted by sonication. Two experiments were performed with these samples: i) a lipase assay to determine if P-407 inhibits HL activity and ii) a lactate dehydrogenase (LDH) activity assay to measure cell damage induced by P-407. HL hydrolysis of resorufin ester was measured in triplicate as described in Chapter 2, Section 2.5.2, using equal volumes of cell lysate and media (80 µL of 2 mL). Final concentrations of 10 or 50 µM P-407 were maintained by addition of P-407 to the assay buffer.

3.2.12 LDH Activity Assay

Equal volumes of cell lysate and media (15 µL of 2 mL) from S7 cells incubated in the presence or absence of P-407, as described above, were assayed in triplicate. The LDH assay has been described previously (Gilham et al., 2003). The assay was initiated by adding 200 µL of 100 mM phosphate buffer, pH 7.4, 1.4 mM sodium pyruvate and 0.2 mM NADH. Absorbance at 340 nm was measured every minute in a clear 96-well microtiter plate with a spectrophotometer. LDH activity was detected in the media after treating cells with 400 µM tertiary butyl-hydroperoxide, indicating that the assay works.

3.2.13 Radiolabel Pulse/Chase in the Presence of 50 µM P-407

This experiment was performed exactly as described above in Section 3.2.8 in the presence or absence of 50 µM P-407 in both the pulse and chase media. Radiolabel incorporation into lipids was quantified as described in Chapter 2, Section 2.8.

3.2.14 Clearance of Exogenous Lipoproteins

One 100 mm culture dish of 80% confluent wild-type McA cells was incubated for 2 h with 5 mL DMEM containing 100 µCi [^{3}H]oleic acid and 0.1 mM oleic acid/0.625% BSA to radiolabel lipid stores and promote lipoprotein secretion. Cells were subsequently washed 3 times for 10 min at 37ºC with DMEM containing 1% fatty acid-free BSA. These cells were then incubated with 5 mL DMEM containing 0.1 mM oleic acid/0.625% BSA for 4 h and medium containing secreted labeled lipoproteins was collected. 5 mL of the radiolabeled medium was diluted with 22 mL of DMEM and mixed by inversion. Three 60 mm culture dishes each of pNEO1, R12 and S7 stable cell lines grown to 70% confluency received 2 mL of the diluted media containing radiolabeled lipoproteins. Two 2 mL aliquots were kept as untreated controls and two 2 mL aliquots were incubated with 2 μL of Infinity Triglyceride Reagent (containing LpL from Chromobacterium viscosum) as a positive control for lipolysis of radiolabeled lipids in the secreted lipoproteins (it should be noted that the bacterial LpL hydrolyzes both CE and TG). All groups were incubated at 37°C for 16 h. Media were collected, centrifuged at 500 *g* to pellet cell debris, and cell protein concentrations were determined as described in Chapter 2, Section 2.12. Radiolabeled lipids in cell and media fractions were analyzed as described in Chapter 2, Section 2-6.

3.2.15 Total Lipase Activity Secreted

Primary hepatocytes were obtained from a 5 month old male C57Bl mouse by collagenase perfusion of the liver (isolation performed by MCBL Group Technician Piscilla Gao) as previously described (Yao and Vance, 1988). 1.5 x 10^6 hepatocytes were cultured in a 60 mm BioCoat Cell Environment collagen-coated culture dish with DMEM + 15% FBS for 3 h to allow hepatocytes to adhere. Hepatocytes were washed with DMEM and were incubated for 4 h in 2 mL DMEM. pNEO1 and S7 cells at 80% confluency in 60 mm culture dishes were washed with DMEM and incubated for 4 h in 2 mL DMEM. After 4 h, media from primary hepatocytes, pNEO1 and S7 cells were collected and centrifuged at 500 *g* for 10 min to pellet cell debris. Cells were washed with ice-cold PBS, harvested in 2 mL of the same buffer, disrupted by sonication and cell protein concentrations were determined as described in Chapter 2, Section 2.12.

50 µL (of the 2 mL) of media were assayed for lipolytic activity in triplicate. Resorufin ester hydrolysis was correlated to the amount of protein in 50 µL (of 2 mL) cell lysate.

3.2.16 Statistical Analyses

Statistical analyses were calculated by one-way ANOVA with a Newman-Keuls post test using Prism software (GraphPad Sofware Inc., San Diego, CA). $P<0.05$ were considered statistically significant.

3.3 Results

3.3.1 HL is Active Intracellularly

To study the potential role of HL on intracellular lipid metabolism, we produced two cDNA constructs by PCR. The first construct, HL-secreted (HL-S), encodes the full length murine HL cDNA plus sequence encoding the FLAG epitope immediately before the stop codon. The second construct, HL-retained (HL-R), is the same as HL-S except with additional sequence encoding the mammalian ER retrieval signal immediately before the stop codon. These cDNAs were ligated into the mammalian expression vector pCI-neo, which confers neomycin resistance. The resultant plasmids were used to generate McA cells stably expressing the FLAG-tagged proteins HL-S and HL-R (Fig. 3-2A). Further experiments were conducted with the stable cell lines R12 and S7 which demonstrated high expression of HL-R and HL-S, respectively (Fig. 3-2B).

Several lines of evidence show that HL-R is retained within the ER of McA cells whereas HL-S follows the normal secretory route. First, HL-S protein could be detected in cell lysate from S7 cells but the vast majority was secreted into the media (Fig. 3-3A); this was expected since mouse HL is a secreted protein with low affinity for cell surface HSPG compared to its orthologous human counterpart (Brown et al., 2003). Conversely, the addition of the ER retrieval signal to the extreme C-terminus resulted in retention of HL within the ER. This is substantiated by the accumulation of HL-R within cell lysates and its virtual absence from media concentrated 10-fold following a 16 h incubation (Fig. 3-3A). Furthermore, confocal immunofluorescence (Fig. 3-4) demonstrates that HL-R stains in a reticular manner similar to the ER resident chaperone PDI.

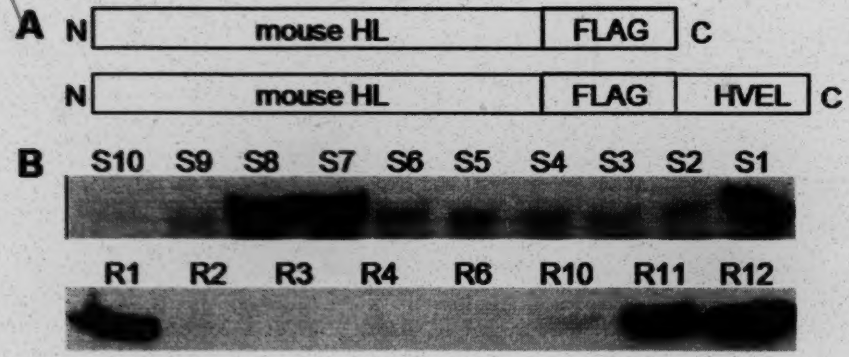
A
N
mouse HL
FLAG
C
N
mouse HL
FLAG
HVEL
C
B
S10
S9
S8
S7
S6
S5
S4
S3
S2
S1
R1
R2
R3
R4
R6
R10
R11
R12

Fig. 3-2: Generation of FLAG-tagged HL stably transfected McA cell lines. (A) Schematic depiction of FLAG-tagged HL-S (top) and HL-R (bottom). (B) Western blots of HL-S (S; top) in media and HL-R (R; bottom) in cell lysates from stable clones.

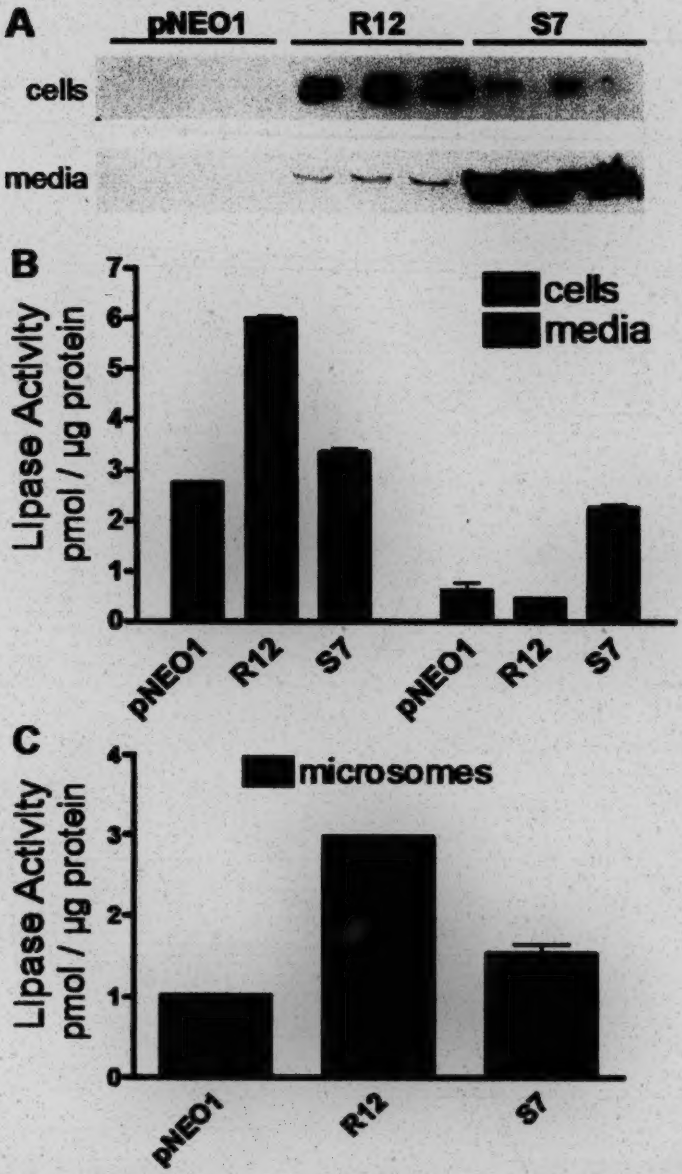

Fig. 3-3: HL-R is targeted to the ER in stable cell line R12 while HL-S is secreted into the media from S7 cells; both enzymes have intracellular lipase activity. (A) Western blots of FLAG-tagged HL from 30 µg cell lysate and 10X concentrated media from stable cell lines incubated in DMEM for 16 h. 2 mL of media from three ~70% confluent dishes were pooled and concentrated using Amicon Ultra 10,000 MW spin concentrators; 50 µL was loaded in triplicate. (B + C) Lipase assays. Resorufin ester hydrolysis by (B) cell lysates and media or (C) microsomes from stable cell lines. Values are mean ± SD of triplicate samples from (B) 40 min or (C) 20 min time points which were within the linear range of the lipase assay.

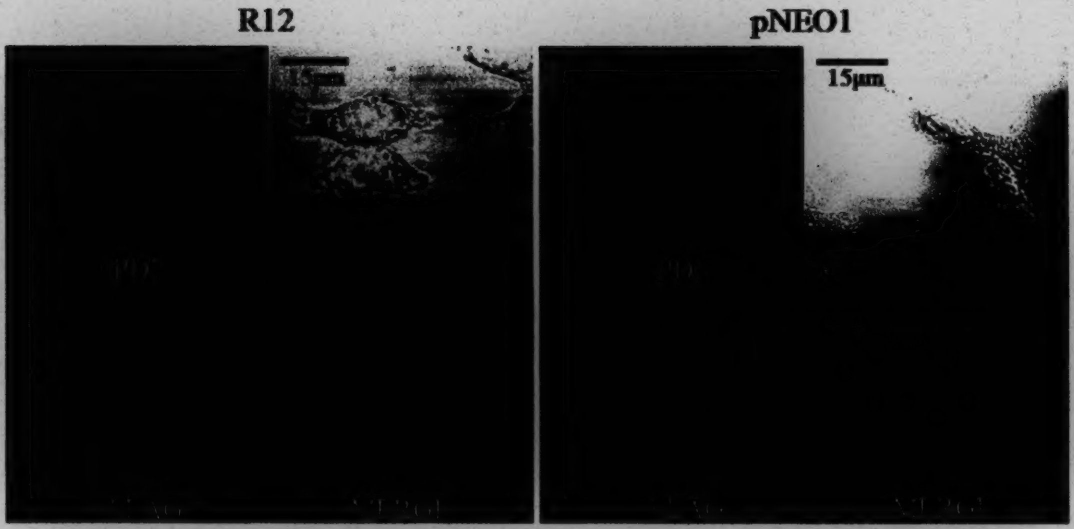

Fig. 3-4: Confocal immunofluorescence imaging of HL-R and PDI. HL-R stains in a reticular manner similar to the ER resident marker PDI (left), indicating that the addition of –HVEL to the extreme C-terminus of HL successfully retains this enzyme in the ER. Control cells exhibit minimal background staining with the anti-FLAG antibody (right).

Lipase assays also confirm the HL localization results and, more importantly, demonstrate that HL which is retained intracellularly (HL-R) is catalytically active (Fig. 3-3B,C). Whereas the lipolytic activity of S7 cell lysate was elevated ~20% compared to that of pNEO1 (McA stably transfected with empty pCI-neo), R12 lipase activity was increased twofold in cell lysates and threefold in microsomes, indicating an enrichment of the lipase in this subcellular fraction (Fig. 3-3B,C). Media from S7 cells had a fourfold increase in lipolytic activity compared to media from either R12 or pNEO1 cells after a 4 h incubation (Fig. 3-3B). Further, microsomes from S7 cells showed a 50% increase in lipolytic activity compared to pNEO1 microsomes, suggesting that intracellularly localized HL destined for secretion is catalytically active prior to secretion (Fig. 3-3C).

3.3.2 Intracellular HL Depletes Neutral Lipid Storage

Since intracellular HL is active, we postulated that it may hydrolyze its native substrates-TG and glycerophospholipids-along the secretory route. If this were the case, it might be capable of mobilizing TG during the assembly of VLDL. We measured the incorporation of [^{3}H]oleic acid into cellular lipids over a time course of 4 h (Fig. 3-5). While the radioactivity associated with ^{3}H-PC was similar between pNEO1 and S7 cells, it remained somewhat lower in R12 cells at every time point. Both R12 and S7 cells had less than half the ^{3}H-TG of pNEO1 cells at every time point. R12 cells also accumulated ^{3}H-CE around half as fast as pNEO1 cells; ^{3}H-CE in S7 cells was intermediate between the levels

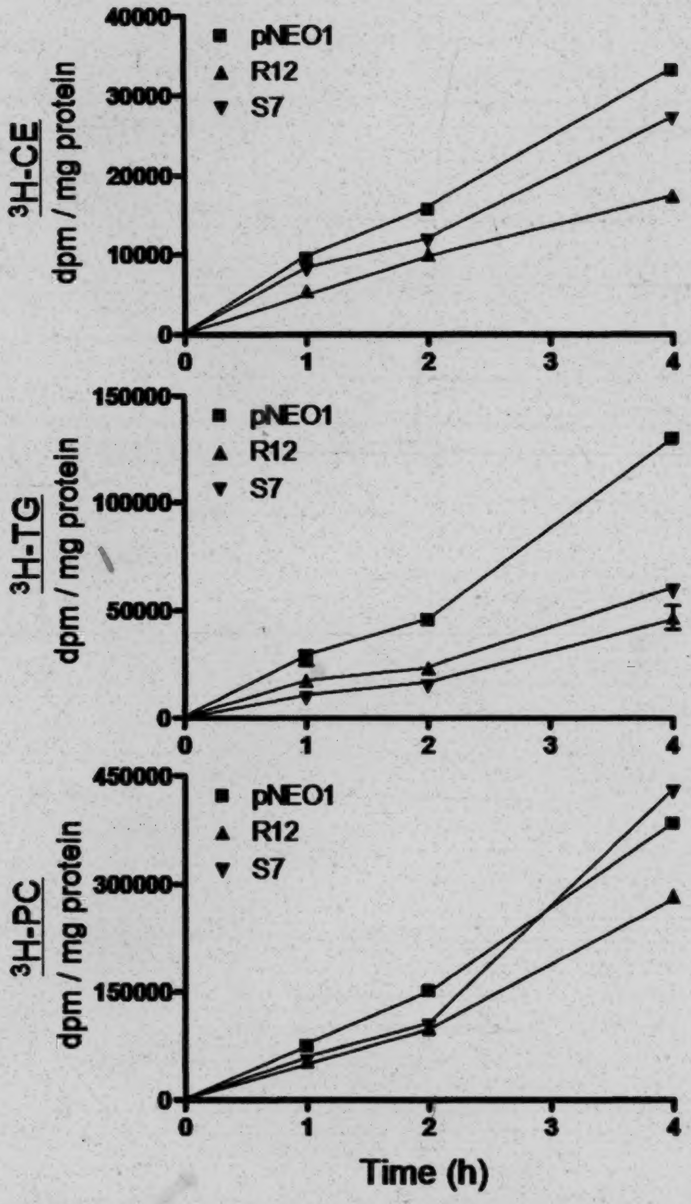

Fig. 3-5: Incorporation of [^{3}H]oleic acid into cellular CE, TG and PC in pNEO1, R12 and S7 cells as a function of time. Values are mean ± SD of triplicate samples at each time point.

of pNEO1 and R12 cells throughout the experiment. This indicates that intracellular HL hydrolyzes cellular lipids.

We performed pulse/chase experiments to study lipid turnover and apoB secretion in our stably transfected McA cells. pNEO1, R12 and S7 cells were incubated with DMEM + 0.4 mM oleic acid/0.5% BSA for 4 h to stimulate lipid synthesis and VLDL secretion (Lehner and Vance, 1999). Cellular TG mass increased from 6.5 µg/mg cell protein in untreated cells to 22 µg/mg cell protein in oleate supplemented pNEO1 cells and from 2 µg/mg cell protein to 12-13 µg/mg cell protein in both HL-R and HL-S cells (Fig. 3-6). Oleate supplementation also increased the mass of glycerophospholipids by 20-30% in all cell lines but had no effect on cholesterol levels (Fig. 3-6). At the end of incubations with oleate (4 h Pulse), although the levels of cellular TG increased 3- to 6-fold with respect to non-supplemented cells, TG mass remained significantly lower in the HL cell lines R12 and S7 compared to the control pNEO1 (Fig. 3-6). R12 cells were also depleted of cellular CE relative to pNEO1 cells after the pulse, whereas S7 cellular CE levels were similar; both HL cell lines had 40-60% of the CE mass found in pNEO1 cells in the untreated and chase conditions, however (Fig. 3-6). The radiolabeled oleate pulse/chase results mirror those of lipid mass analyses (Fig. 3-7).

This suggests that HL hydrolyzes neutral lipids formed de novo. Further incubation of cells in the absence of oleate (16 h Chase) resulted in depletion of 56% of TG in the control pNEO1 cells (Fig. 3-6). The depletion rate of TG in R12 and S7 cells were comparable; this suggests that HL hydrolyzes TG as they are being synthesized in the ER but does not access stored cytosolic TG, because

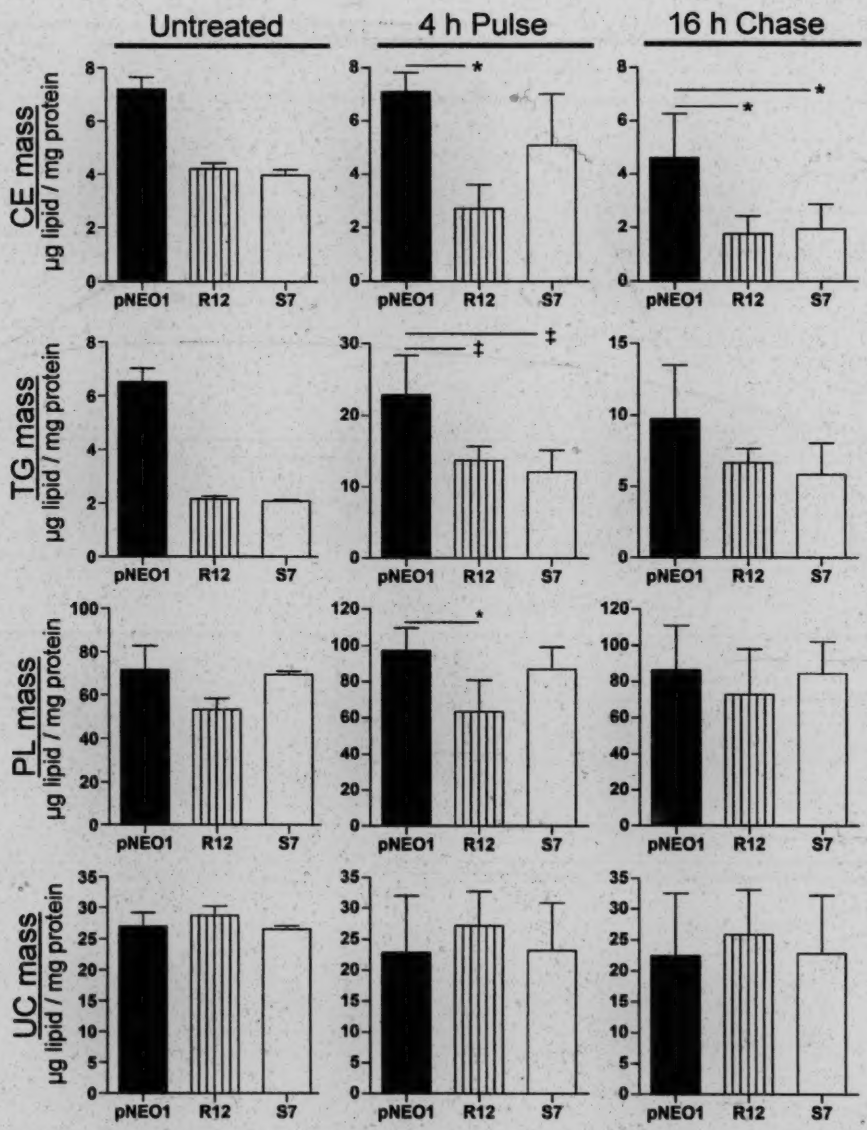

Fig. 3-6: HL depletes R12 and S7 cells of neutral lipid stores. Cellular CE, TG, PL and cholesterol (UC) mass in pNEO1, R12 and S7 cells grown to ~70% confluency (untreated; n=1), after pulse with oleic acid followed by chase in the absence of oleic acid (n=4). Values are mean ± SD for n experiments with triplicate samples. * *P* < 0.05, ‡ *P* < 0.001

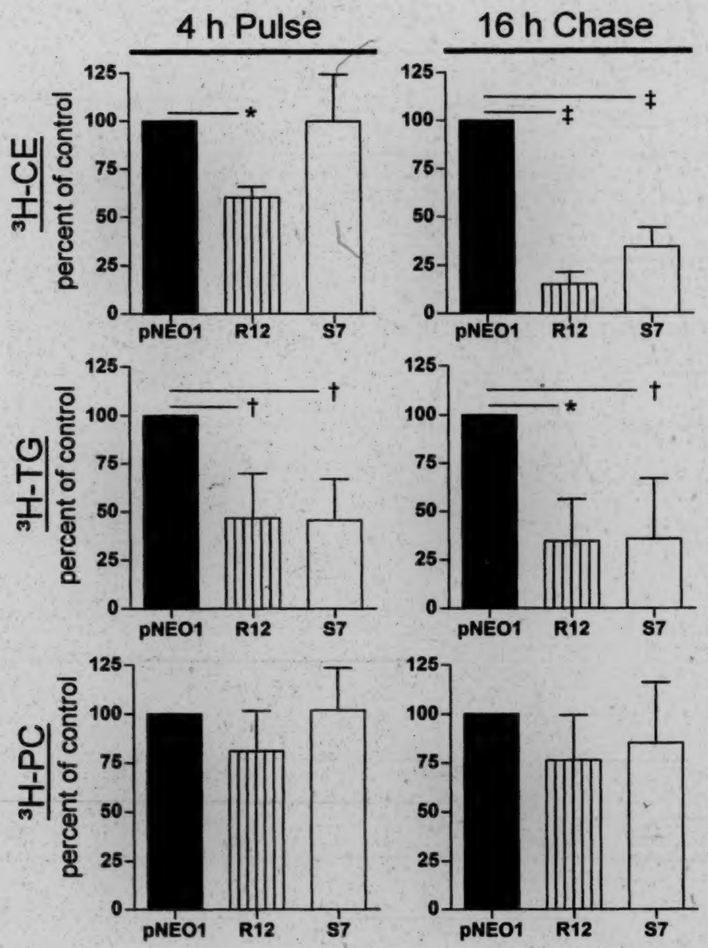

Fig. 3-7: HL depletes R12 and S7 cells of radiolabeled neutral lipid stores. Radioactivity in cellular CE, TG and PC of pNEO1, R12 and S7 cells after radiolabeled pulse with [^{3}H]oleic acid followed by chase in the absence of oleic acid. Values are mean dpm/mg cell protein ± SD for n=3 experiments with triplicate samples, expressed as a percentage of control (pNEO1). * $P < 0.05$, † $P<0.01$, ‡ $P<0.001$

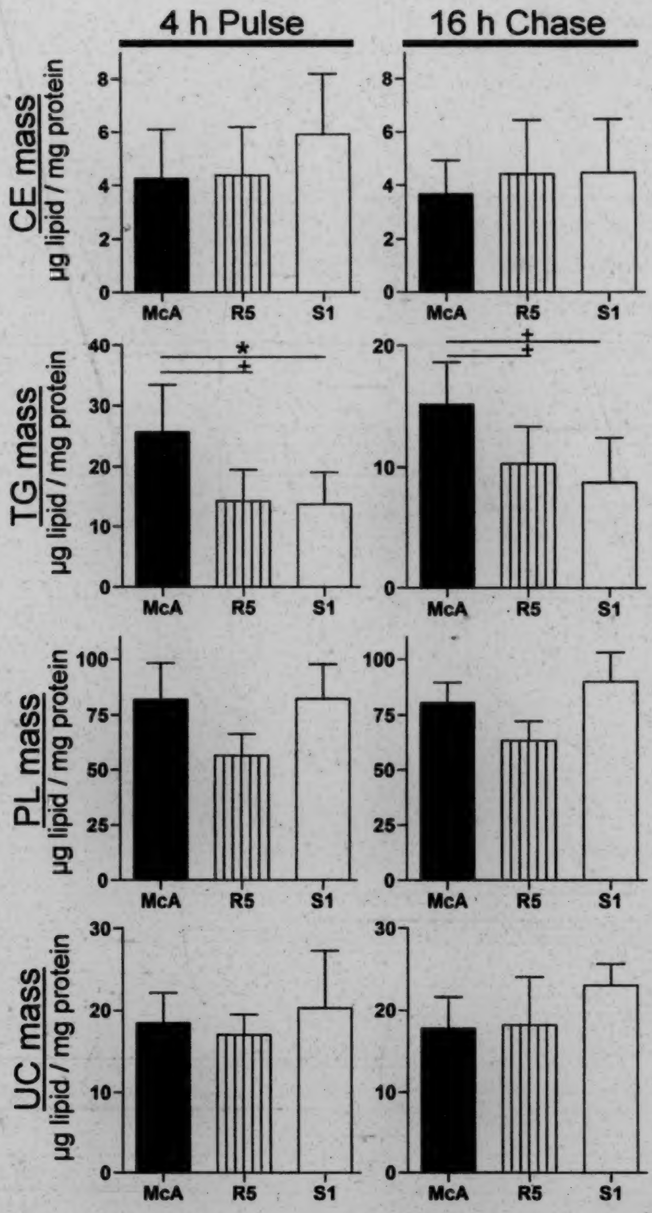

Fig. 3-8: HL depletes R5 and S1 cells of neutral lipid stores. Cellular CE, TG, PL and cholesterol (UC) mass in McA, R5 and S1 cells after pulse with oleic acid followed by chase in the absence of oleic acid. Values are mean ± SD for n=3 experiments with triplicate samples. * $P < 0.05$, + $P < 0.01$

the depletion rate of the preformed lipids appears to be independent of HL expression levels.

In addition, we assessed whether HL depleted neutral lipids in another set of stable cell lines: R5 and S1, expressing HL-R or HL-S respectively (Fig. 3-8). Identical pulse/chase experiments were performed and cells were analyzed for lipid content by GC. The results of these studies were very similar to those obtained with the cell lines R12 and S7. TG was significantly depleted in cells expressing HL after both the pulse and the chase relative to wild-type McA cells. cholesterol and PL masses were statistically similar between the 3 groups (yet HL-R trended towards lower PL mass per protein mass, consistent with results obtained with R12 (Figs. 3-6 and 3-7)). The cellular mass of CE did not differ between the three groups in these experiments, however, which is in opposition to the results presented above.

3.3.3 Intracellular HL Reduces TG Secretion

TG and CE are the major neutral lipid components of VLDL. Because overexpression of the retained or secreted form of HL reduced intracellular neutral lipids, lipid secretion from pNEO1, R12 and S7 cells was analyzed by both GC and radiolabeling. Expression of ER-targeted HL resulted in an 80-90% decrease of TG secretion into the media during both the pulse and the chase (Figs. 3-9 and 3-10). S7 cells expressing secretion-competent HL secreted somewhat less TG mass in oleate supplemented conditions than control cells, although this trend did not achieve statistical significance (Figs. 3-9 and 3-10). Removal of oleic acid during the chase period resulted in S7 cells

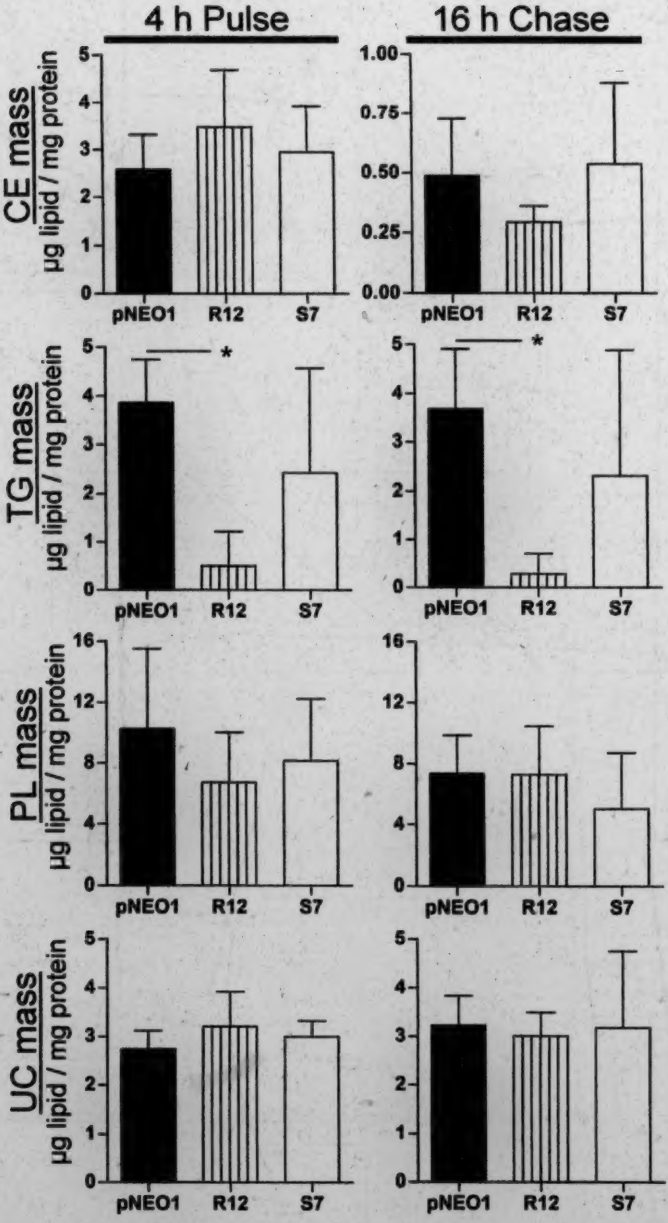

Fig. 3-9: HL cells secrete less TG into the media than control cells. Media CE, TG, PL and cholesterol (UC) mass from pNEO1, R12 and S7 cells after pulse with oleic acid followed by chase in the absence of oleic acid. Values are mean ± SD for n=4 experiments with triplicate samples. * $P < 0.05$

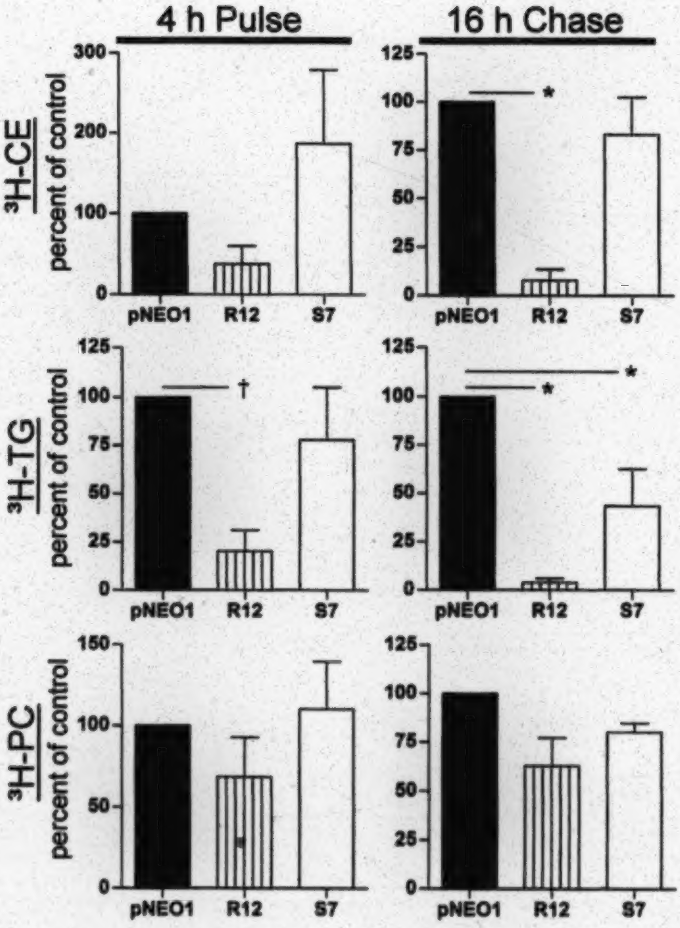

Fig. 3-10: HL cells secrete less radiolabeled TG into the media than control cells. Radioactivity associated with CE, TG and PC in media from pNEO1, R12 and S7 cells after radiolabeled pulse with [^{3}H]oleic acid followed by chase in the absence of oleic acid. Values are mean dpm/mg cell protein ± SD for n=3 experiments with triplicate samples, expressed as a percentage of control (pNEO1). * $P < 0.05$, † $P<0.01$

secreting approximately half the TG of control cells, which reached statistical significance via metabolic labeling (Fig. 3-9 and 3-10). The mass of secreted CE, cholesterol and PL were comparable between pNEO1, R12 and S7 cell lines (Fig. 3-9); the secretion of CE was greatly attenuated in the absence of oleic acid (Fig. 3-9). Therefore, it appears that HL greatly reduces TG secretion via its activity in the microsomal compartment.

3.3.4 Intracellular HL Reduces ApoB100 Secretion

We rationalized that if HL is capable of modulating lipid secretion then it may also affect apoB secretion. ApoB concentrations in pulse and chase media were analyzed after capturing lipoproteins by adsorption to Cab-o-sil (Vance et al., 1984). In the presence of exogenous oleate and active TG synthesis, the secretion of both apoB100 and apoB48 were nearly equivalent between HL cells and control cells (Fig. 3-11A,C). Given that HL-R expression resulted in 80-90% decreased TG secretion in oleate-supplemented conditions compared to control cells (Figs. 3-9 and 3-10), this suggests that both apoB100 and apoB48 were secreted as lipid-poor lipoprotein particles from R12 cells. Upon removal of oleate and cessation of active TG synthesis, apoB100 secretion from R12 cells was abolished and S7 cells secreted 33% less apoB100 than pNEO1 cells (Fig. 3-11B,C). ApoB48 secretion, on the other hand, was identical between the three groups (Fig. 3-11B,C). The aforementioned trends were reproducible in another independent experiment (not shown). These data underscore the fact that apoB48 can be secreted as a very TG-poor, dense lipoprotein particle by McA cells while apoB100 secretion is dependent on the availability of TG. This

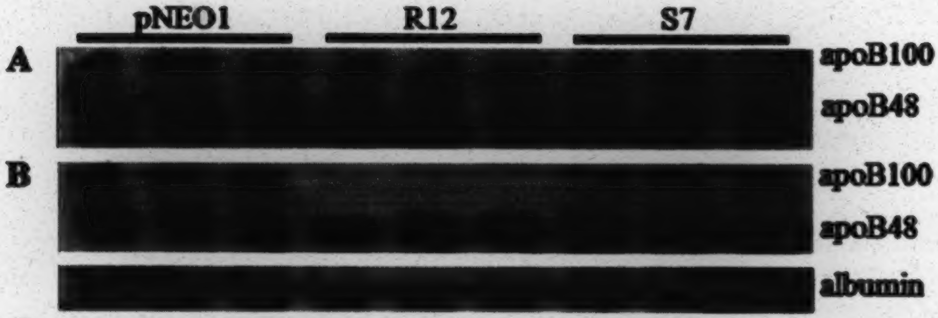

C

	Pulse Blot		Chase Blot	
Media	apoB100	apoB48	apoB100 / albumin	apoB48 / albumin
pNEO1	143 ± 8	180 ± 13	0.91 ± 0.17	0.94 ± 0.03
R12	118 ± 8	156 ± 14	0.06 ± 0.05	1.04 ± 0.03
S7	139 ± 13	167 ± 3	0.60 ± 0.16	0.99 ± 0.14

Fig. 3-11: HL cells secrete less apoB100 into media upon removal of oleate. Western blots of Cab-o-sil treated media from (A) pulse and (B) chase. Each lane is Cab-o-sil treated media from a separate culture dish. (C) Densitometry of Western blots in (A) and (B) in arbitrary units. ApoB is correlated to albumin in the chase, but not in the pulse (since BSA was the carrier for oleic acid in the pulse).

concept has been demonstrated by many groups (Stillemark et al., 2000; Wang et al., 1999; White et al., 1992).

3.3.5 Intracellular HL Does Not Direct Fatty Acids Towards Secretion or Oxidation

The minor TG stores and impaired TG secretion of HL cell lines led us to examine whether HL was directing fatty acids into the oxidative pathway or increasing their secretion. Ectopic expression of HSL in HepG2 cells increased β-oxidation (Pease et al., 1999) and overexpression of human AADA in HepG2 cells increased secretion of fatty acids (Gibbons et al., 2000), suggesting that oxidation or secretion of fatty acids might account for the loss of neutral lipids in HL cells. However, no difference in the amount of radiolabeled [^{3}H]oleic acid between pNEO1, R12 and S7 cells in the chase media could be detected (Fig. 3-12A). Nor was the radioactivity associated with secreted [^{3}H]oleic acid anywhere near the difference between pNEO1 and HL cell TG radioactivity, suggesting that increased secretion was not responsible for the apparent loss of label. Even if radiolabeled fatty acids were hydrolyzed from TG and secreted, they might be taken up again by the cells and not accumulate in the media.

Radioactivity associated with acid soluble products (ASP; ^3H_2O and ^{3}H-ketone bodies) was also assessed (Figs. 3-12B,C) as a crude measurement for fatty acid oxidation. ^{3}H-ASP were nearly equal between the three groups for cell and media fractions in both the pulse and chase. Interestingly, ^{3}H-ASP were far greater in the pulse than in the chase (Figs. 3-12B,C). This is consistent with data from Lankester et al. (1998) who reported a preferential oxidation of

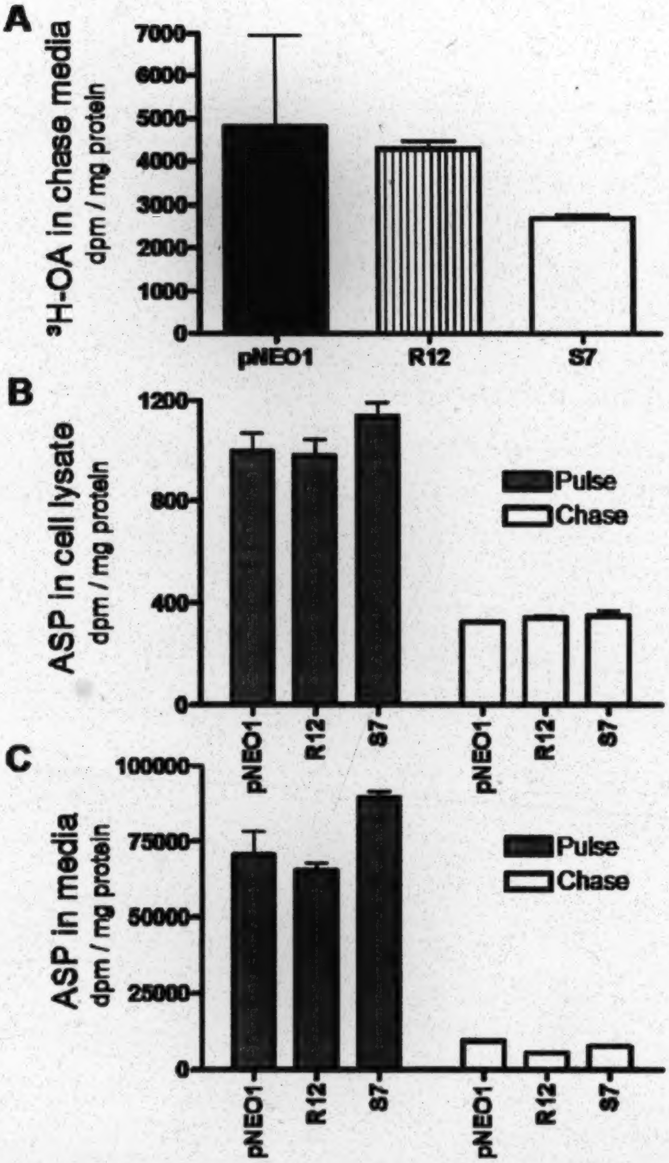

Fig. 3-12: HL cells do not secrete more fatty acids or produce more ^{3}H-acid soluble products (ASP) than control cells. (A) Radioactivity associated with ^{3}H-oleic acid (^{3}H-OA) in chase media after a pulse/chase experiment. ^{3}H-ASP in cell lysates (B) and media (C) after pulse and chase. ^{3}H-oleic acid was isolated from the chloroform phase at pH 3 and ^{3}H-ASP were isolated from the aqueous phase at pH 3. Values are mean ± SD of triplicate samples.

exogenous fatty acids over those derived from stored TG in rat hepatocytes. Still, one would expect to see an increase in ^{3}H-ASP in the chase media from R12 and S7 cells relative to pNEO1 media if HL diverted [^{3}H]oleic acid towards oxidation. Since there is no increase, I conclude that HL does not cause increased oxidation of TG stores.

3.3.6 Extracellular HL Activity is Not Responsible for Reduced Media TG

To assess the contribution of extracellular lipolysis by secreted HL to the observed decreased media TG and apoB levels, we employed P-407 to inhibit extracellular HL activity. Like Triton WR1339, P-407 induces hypertriglyceridemia and hypercholesterolemia in animal models, resulting in atherosclerosis over extended periods (Johnston, 2004; Wasan et al., 2003). P-407 directly inhibits the lipolytic activity of both LpL and HL in rats by greater than 95% for over 24 h (Wasan et al., 2003). P-407 inhibits rat LpL with a K_i=24 µM (Johnston and Palmer, 1993). As LpL and HL are structurally and evolutionarily related (Hide et al., 1992; Kirchgessner et al., 1989), we speculated that a similar concentration of P-407 would inhibit HL activity. We found that 10 µM P-407 was insufficient to inhibit HL activity, but 50 µM P-407 resulted in complete inhibition of HL secreted into the media over a 16 h time course (Fig. 3-13). The cell impermeability, solubility and stability of this compound (Millar et al., 2005) made it an attractive inhibitor for HL in our studies; previous experiments had revealed that 100 µM THL only reduced secreted HL activity by ~50% over a 16 h period (data not shown). 50 µM P-407 was not toxic to S7 cells, as there was no leakage of cytosolic LDH into media

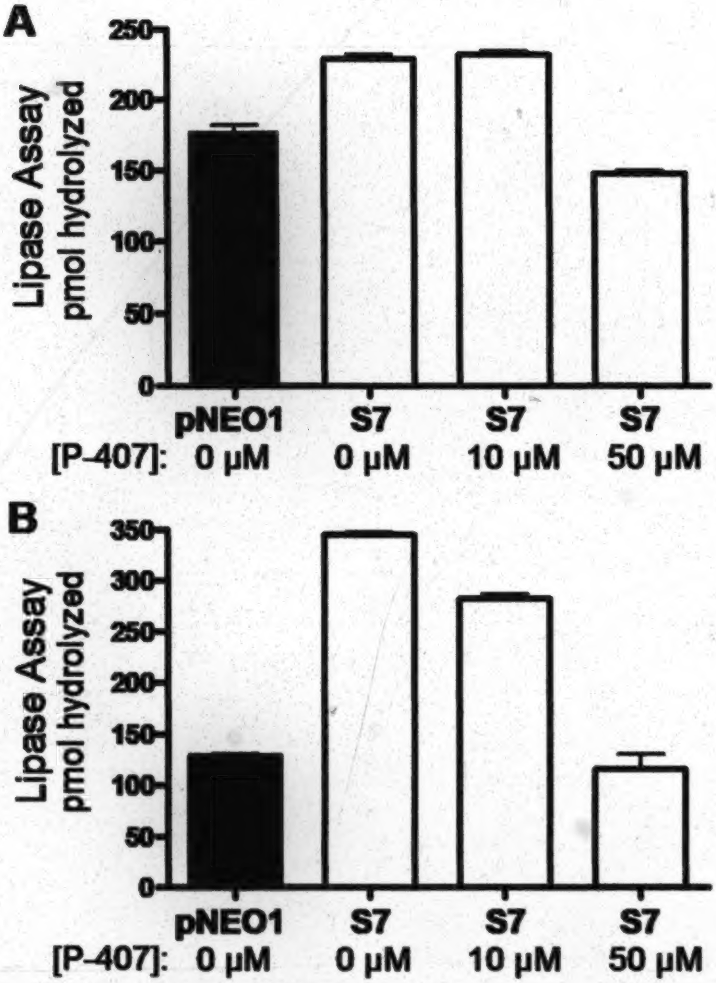

Fig. 3-13: 50 µM P-407 completely inhibits secreted HL activity. Lipase assay measuring the hydrolysis of resorufin ester by cell lysates (A) and media (B) from pNEO1 and S7 cells incubated for 16 h with DMEM and S7 cells incubated for 16 h with DMEM in the presence of 10 µM or 50 µM P-407. Values are mean ± SD of triplicate samples at 40 min into the linear range of the lipase assay.

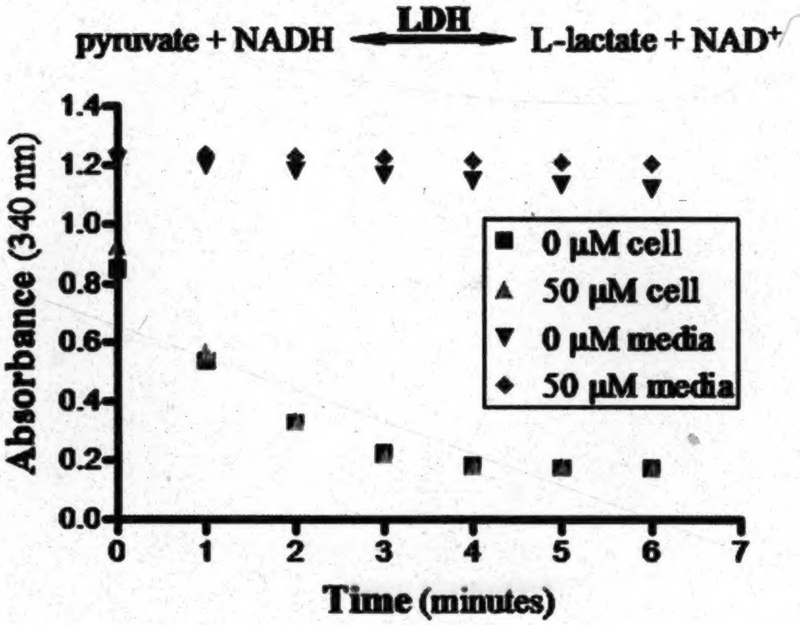

Fig. 3-14: 50 µM P-407 is not toxic to cells during a 16 h incubation. LDH activity assay of cell lysates and media from S7 cells incubated for 16 h with DMEM in the presence or absence of 50 µM P-407. Absorbance at 340 nm measures reduced NADH. Values are means of duplicate samples at each time point.

(Fig. 3-14): LDH activity was entirely in S7 cell lysates after a 16 h incubation regardless of the presence or absence of 50 µM P-407 in media.

Radiolabeled pulse/chase experiments were repeated in the presence or absence of 50 µM P-407 to eliminate the contribution of extracellular lipolysis. Incorporation of radiolabeled oleate into cellular lipids and lipid secretion from the cells were comparable in the same cell lines irrespective of whether the cells were untreated or treated with 50 µM P-407 (Tables 3-1A,B), indicating that extracellular HL activity was not responsible for the observed differences in lipid metabolism between pNEO1 and HL cell lines. These data testify that intracellular HL activity is responsible for decreased secretion of TG from HL-R and HL-S cells, rather than increased extracellular TG lipolysis and fatty acid uptake.

3.3.7 Secreted HL Does Not Expediate Clearance of Secreted Lipoproteins

HL has been implicated in facilitating the clearance of apoB lipoproteins (Dichek et al., 1998; Fan et al., 1994; Homanics et al., 1995; Qiu et al., 1998) and in the selective uptake of HDL-CE (Brundert et al., 2003; Lambert et al., 2000; Lambert et al., 1999; Rinninger et al., 1998). To ascertain that the perceptibly lower levels of TG and apoB100 in media from HL-R and HL-S expressing cells was in fact a genuine result of decreased secretion rather than increased lipoprotein lipolysis or uptake in the presence of HL, we evaluated the ability of the three cell lines to clear exogenous lipoproteins. Two independent experiments yielded similar results (Tables 3-2A,B). The exogenous radiolabeled lipoproteins secreted from wild-type McA cells were readily

A

		Cells - Pulse		Cells - Chase	
Cell Line	^{3}H-lipid	0μM Poloxamer	50μM Poloxamer	0μM Poloxamer	50μM Poloxamer
pNEO1	^{3}H-CE	35.7 ± 9.5	32.9 ± 8.7	16.4 ± 3.2	34.4 ± 2.3
R12		21.8 ± 1.2	19.0 ± 2.3	4.6 ± 0.1	8.2 ± 0.9
S7		48.2 ± 6.6	36.0 ± 5.4	8.8 ± 0.5	12.5 ± 3.4
pNEO1	^{3}H-TG	518.6 ± 76.3	793.6 ± 30.7	148.7 ± 13.8	221.3 ± 12.9
R12		414.4 ± 17.1	536.3 ± 65.5	81.8 ± 7.9	88.1 ± 10.3
S7		383.0 ± 71.5	548.4	105.8 ± 6.6	112.1 ± 26.3
pNEO1	^{3}H-PC	418.3 ± 40.5	551.8 ± 52.8	465.5 ± 10.3	617.1 ± 16.9
R12		464.3 ± 35.3	539.3 ± 70.1	473.8 ± 26.0	572.9 ± 26.1
S7		533.6 ± 37.3	517.1	548.7 ± 11.8	604.5 ± 207.7

B

		Media - Pulse		Media - Chase	
Cell Line	^{3}H-lipid	0μM Poloxamer	50μM Poloxamer	0μM Poloxamer	50μM Poloxamer
pNEO1	^{3}H-CE	0.99 ± 0.21	1.36 ± 0.20	0.90 ± 0.14	1.02 ± 0.14
R12		0.63 ± 0.05	0.75 ± 0.11	0.11 ± 0.01	0.21 ± 0.02
S7		2.89 ± 0.37	2.26 ± 0.40	0.87 ± 0.31	0.59 ± 0.28
pNEO1	^{3}H-TG	10.47 ± 2.86	10.67 ± 5.27	9.02 ± 0.81	10.58 ± 1.43
R12		2.17 ± 0.09	3.11 ± 1.58	0.50 ± 0.03	0.79 ± 0.30
S7		10.31 ± 1.40	6.12 ± 0.65	5.14 ± 1.94	2.42 ± 1.13
pNEO1	^{3}H-PC	3.06 ± 0.19	4.15 ± 0.66	6.51 ± 0.62	20.34 ± 0.82
R12		2.79 ± 0.83	3.49 ± 0.48	3.42 ± 0.42	9.87 ± 1.68
S7		3.94 ± 0.77	4.28 ± 0.61	5.43 ± 1.10	15.73 ± 1.80

Tables 3-1: Reduced TG in media from HL cells is due to intracellular HL activity and not extracellular HL activity. Radiolabeled pulse/chase experiment in the absence or presence of 50 μM P-407 in the pulse and chase media. Values are mean dpm x10^3/mg cell protein ± SD associated with CE, TG and PC in pNEO1, R12 and S7 cells (A) and media (B).

A

	Cell Protein	Cells			Media		
Sample	(mg)	^{3}H-CE	^{3}H-TG	^{3}H-PC	^{3}H-CE	^{3}H-TG	^{3}H-PC
Control	-	-	-	-	322	4960	3314
LpL	-	-	-	-	131	938	3811
pNEO1	1.258	113±15	777±63	3986±994	110±11	1077±67	647±33
R12	1.016	81±10	664±92	4314±1010	126±8	1304±9	784±189
S7	1.396	85±9	635±84	4163±457	142±11	907±88	595±45

B

	Cell Protein	Cells			Media		
Cell Line	(mg)	^{3}H-CE	^{3}H-TG	^{3}H-PC	^{3}H-CE	^{3}H-TG	^{3}H-PC
Control	-	-	-	-	899±45	4088±83	5003±440
LpL	-	-	-	-	142±38	497±98	6235±849
pNEO1	1.032	179±27	1159±50	17267±788	520±30	2356±126	2775±241
R12	1.074	146±6	865±84	17197±4021	568±45	2401±75	2623±80
S7	1.008	140±7	811±34	17496±656	609±14	2030±157	3084±253

Tables 3-2: Reduced TG in media from HL cells is due to intracellular HL activity and not HL-facilitated lipid or lipoprotein uptake. pNEO1, R12 and S7 cells were incubated with exogenous radiolabeled lipoproteins for 16 h and the radioactivity associated with CE, TG and PC in cells and media was determined. Values are mean dpm ± SD from triplicate samples. (A) and (B) are repeat experiments. Note: ~14,000 dpm in (A) and ~43,000 dpm in (B) was in free [^{3}H]oleic acid along with exogenous lipoproteins, which significantly contributed to cellular lipid radioactivity.

hydrolyzed by a bacterial LpL, yet there was no difference in clearance of lipoprotein CE, TG or PC from media between pNEO1, R12 or S7 stable cell lines (Tables 3-2A,B). Consistent with my previous data, [^{3}H]oleic acid (either liberated from the radiolabeled lipoproteins by lipolysis or already pre-existing in the control media) was less abundant in cellular ^{3}H-CE and ^{3}H-TG of HL cells than in pNEO1 cells after the 16 h incubation, whilst ^{3}H-PC levels were equal between the three groups (Tables 3-2A,B). Therefore the observed lowering of chase media apoB100 and TG levels were a result of decreased secretion in the presence of HL, rather than increased metabolism of secreted lipoproteins.

3.3.8 HL-S Overexpression Levels

To determine the extent of mouse HL overexpression in the S7 stable cell line, we compared the secretion of HL activity from pNEO1 and S7 cells with that of wild-type primary hepatocytes obtained from male C57Bl mice. After a 4 h incubation in serum-free DMEM, media was collected and assayed for lipolytic activity towards the artificial TG substrate resorufin ester. Primary mouse hepatocytes secreted 75% more activity than pNEO1 cells and S7 cells secreted 25% more activity than primary mouse hepatocytes (Fig. 3-15). Similar results were found in a second experiment (not shown).

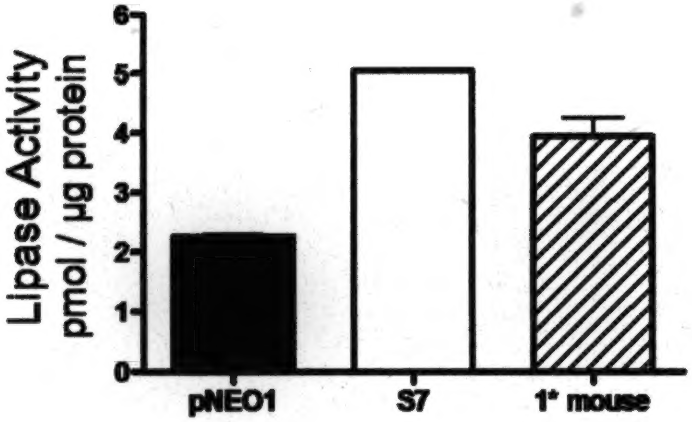

Fig. 3-15: HL activity secreted from S7 cells is only 25% greater than that secreted from primary mouse hepatocytes. pNEO1, S7 and primary mouse hepatocytes were incubated in DMEM for 4 h and the total lipase activity secreted into media was calculated and normalized for total cell protein. Values are mean ± SD of triplicate samples at 20 min into the linear range of the assay.

3.4 Discussion

We set out to investigate whether HL has intracellular lipolytic activity and, if so, if it could mobilize TG for VLDL assembly. To address this issue, a mouse HL cDNA was isolated from a λgt11 mouse cDNA library by PCR. The mouse HL cDNA was modified by PCR using oligonucleotides which introduced sequence for the FLAG-epitope (for protein detection) plus the mammalian ER retrieval signal (HVEL) in one construct (to retain the protein within the cell). Stable expression of the chimeric cDNAs in McA rat hepatoma cell lines allowed us to address these questions. Previously, stable expression of a TGH cDNA in McA cells was shown to be sufficient to enhance VLDL secretion (Lehner and Vance, 1999). Inhibition studies in primary hepatocytes revealed that lipases other than TGH might be involved in the mobilization of TG stores for VLDL secretion (Gilham et al., 2005). We proposed that HL was a likely candidate for mobilizing TG for VLDL secretion based on its transient localization within the ER and its known TG hydrolase activity.

The results presented in this chapter unambiguously reveal that HL exhibits lipolytic activity prior to its secretion. Microsomes isolated from HL expressing McA cells had elevated lipolytic activity towards the TG analogue resorufin ester compared to pNEO1 microsomes (Fig. 3-3B,C). Moreover, cells enriched in HL activity tended to store less neutral lipids and accumulate less neutral lipids than those with lower HL activity (Figs. 3-5 to 3-8). Contrary to our hypothesis, microsomal HL activity did not stimulate VLDL secretion from McA cells as TGH did. Neutral lipid depletion and/or HL mediated TG hydrolysis also markedly depressed both apoB100 and TG secretion into the media. Since every VLDL and LDL particle is associated with a single apoB100 molecule in humans (Elovson et al., 1988), intracellular HL activity leads to decreased VLDL secretion (not just a reduction in VLDL-TG). This is an important finding suggestive of an anti-atherogenic potential for intracellular HL activity since VLDL is the precursor of LDL-a pro-atherogenic lipoprotein (Sniderman et al., 2004).

HL deficiency in humans is most commonly attributed to polymorphisms in the *LIPC* promoter (Isaacs et al., 2004; Santamarina-Fojo et al., 2004; Zambon et al., 1998) which diminish transcriptional efficacy. Less common are mutations in the coding region of the gene (Hegele et al., 1993; Ruel et al., 2005; Tilly-Kiesi et al., 2004) which alter the structural integrity, secretion and catalytic properties of HL. Patients with HL deficiency display elevated total plasma cholesterol and TG concentrations and have a lipoprotein profile characterized by markedly increased TG- and PL-rich lipoprotein remnants and HDL (Deeb et al., 2003).

Similar results have been reported in HL knockout mice (Homanics et al., 1995; Qiu et al., 1998). HL knockout mice have approximately threefold the plasma total cholesterol and twofold total TG as compared to wild-type mice (Qiu et al., 1998). Nearly all of the lipoprotein classes are characterized by enrichment in cholesterol, TG and PL, resulting from absent HL TG hydrolase and phospholipase activities as well as decreased remnant removal. Importantly, both male and female HL knockout mice have nearly double the TG content in VLDL compared to their wild-type counterparts (Qiu et al., 1998). Female mice, but not males, also show a twofold increase in apoB100 and apoB48 in the VLDL fraction compared to controls (Qiu et al., 1998). Since VLDL-TG are the primary substrate for LpL and a secondary substrate for HL in plasma, it seems counterintuitive that plasma HL deficiency results in such an accumulation of VLDL-TG even in the presence of normal levels of LpL. We hypothesize that HL knockout mice may secrete TG-enriched VLDL as a result of decreased intracellular TG lipase activity. This situation is consistent with our results, where we have demonstrated increased intracellular HL activity leading to decreased TG and apoB100 secretion.

Two studies in patients with compound heterozygous mutations in the coding region of *LIPC* also provide clues suggesting the feasibility of this hypothesis (Ruel et al., 2005; Tilly-Kiesi et al., 2004). Both of these studies measured plasma lipid profiles and utilized a primed-constant infusion of deuterated leucine over a 12 h period to investigate the turnover of lipoproteins. In both studies the VLDL apoB100 pool size in HL deficient men were approximately threefold those of normotriglyceridemic men and the total plasma TG levels were also highly elevated. Decreased fractional catabolic rate certainly contributed to accumulation of VLDL apoB100 in HL deficient men from both studies. However, Tilly-Kiesi et al (Tilly-Kiesi et al., 2004) reported a threefold higher hepatic VLDL apoB100 production rate in HL deficient men. By contrast, Ruel et al (Ruel et al., 2005) did not observe any difference in hepatic VLDL apoB100 production rate.

These differences might be attributed to the different nutritional status of the subjects in the two studies: in the former study (Tilly-Kiesi et al., 2004) patients were in the fed state whereas in the latter study (Ruel et al., 2005) patients were in the fasted state. Lower insulin concentrations during the fasted state are associated with increased adipose lipolysis, liberation of fatty acids into the plasma and increased hepatic VLDL secretion; conversely, in the fed state, fatty acids liberated from chylomicrons are largely directed towards adipose tissue storage and oxidation by extrahepatic tissues. Thus the fasted state is analogous to the pulse in our studies (maximum VLDL secretion) whereas the fed state is analogous to the chase (less VLDL secretion). Pulse incubation with fatty acids resulted in active TG synthesis and apoB100 secretion being largely rescued from presecretory degradation regardless of intracellular HL activity. This is consistent with no difference in VLDL apoB100 production rate between HL deficient and control subjects reported by Ruel et al. (Ruel et al., 2005). During the chase, when extracellular supply of fatty acids was removed, apoB100 secretion was sensitive to the presence of intracellular HL activity. Increased HL activity resulted in a sizeable decrease in apoB100 secretion. Therefore, in the fed state, it seems plausible that the absence of HL intracellular activity might result in increased VLDL apoB100 secretion, as is reported by Tilly-Kiesi et al. (Tilly-Kiesi et al., 2004).

Hepatic assembly and secretion of apoB is a potential target of pharmaceutical intervention for reversing atherosclerosis and coronary heart disease. One strategy involves the inhibition of the lipases which mobilize TG for VLDL secretion, such as TGH (Dolinsky et al., 2004b; Gilham et al., 2003; Lehner and Vance, 1999). An additional approach, revealed by this study, could be to stimulate the expression of the HL gene. Since HL facilitates clearance of lipids via the RCT pathway (Dichek et al., 2004; Rinninger et al., 1998), the overall effect of elevated HL levels would presumably contribute to a less atherogenic lipoprotein profile. This concept is supported by premature atherosclerosis in patients with heritable HL deficiency (Hegele et al., 1993).

Many studies have demonstrated that HL is a TG hydrolase and a phospholipase in the circulation. Additionally, HL hydrolyzes ^{3}H-triolein in vitro (Brown et al., 2003). Both our mass analyses and radiolabel turnover studies indicate that HL also hydrolyzes TG in intact McA cells. The depletion of CE in HL cell lines was unexpected though, since a CE hydrolase activity has not been previously reported for this enzyme. We are currently uncertain whether HL elicits intracellular CE hydrolase activity since depletion of CE stores was not consistent between cell lines like TG depletion was. Still, the fact that [^{3}H]oleic acid incorporation into ^{3}H-CE by pNEO1 and S7 cells was similar (Fig. 3-7) and CE mass in S7 cells increased during the pulse (Fig. 3-6), whereas R12 cells had markedly lower CE radiolabel and mass at all time points, indicates that HL may have CE hydrolase activity at elevated concentrations. The TG hydrolase activity of S7 microsomes (150% of pNEO1 microsomes) was not as pronounced as that of R12 microsomes (300% of pNEO1 microsomes) (Fig. 3-3C), yet it was sufficient to reduce TG mass to the same extent during active TG synthesis (Fig. 3-6). I speculate that HL-S activity was also adequate to hydrolyze CE in the absence of active TG synthesis, since the CE stores in S7 cells were depleted compared to pNEO1 cells in the untreated and chase conditions (Fig. 3-6). It is entirely possible that HL has CE hydrolase activity, albeit HL may have lower specificity for CE than for TG and PL.

The role of HL in governing CE levels deserves further investigation. For example, HL knockout mice accumulate CE in hepatic endosomes during clearance of radiolabeled chylomicrons (Qiu et al., 1998). Internalization and degradation of HL is mediated through the LDL receptor-related protein (Kounnas et al., 1995; Verges et al., 2004), which also participates in hepatic removal of remnant lipoproteins (Krapp et al., 1996). This process concentrates HL in endosomal fractions (Verges et al., 2004), a subcellular compartment where HL hydrolyzes TG (Hornick et al., 1992). Thus it is conceivable that CE accumulation in endosomal fractions of HL knockout mice is a result of decreased CE hydrolase activity resulting from HL deficiency.

The phospholipase activity of HL in McA cells was not obvious. The incorporation of [^{3}H]oleic acid into PC and the mass of phospholipids were very comparable between pNEO1 and S7 stable cell lines, suggesting that de novo synthesized PL are either inaccessible substrates for HL or that resulting lysophospholipids are rapidly re-esterified. Retention of HL in the ER, however, produced a slight trend of decreased mass and label in PL (Figs. 3-5 to 3-8), indicative of active phospholipase activity.

A recent report from Dichek et al. (Dichek et al., 2004) demonstrated that transgenic expression of human HL in mice deficient in both mouse HL and the LDL receptor alleviated atherosclerosis in these mice (on a HF/HC diet), but mice expressing a similar level of ciHL developed atherosclerosis to the same extent as control mice. On this diet, active HL greatly reduced the cholesterol content of all serum lipoproteins whereas ciHL only marginally reduced the cholesterol content of IDL and LDL fractions. What I find most interesting about this report (from the perspective of my studies) is that, on a chow diet alone, livers from mice expressing ciHL accumulated large lipid globules throughout the cytoplasm (4-8 μm), whereas lipid staining in control livers was slightly less and lipid droplets in catalytically active HL livers were small (1-2 μm) (Dichek et al., 2004). The authors say: "whereas the small lipid droplets in the livers of HL-expressing mice may reflect normal endogenous synthesis of triglycerides from FFAs derived from fully processed lipoproteins, we speculate that the larger lipid globules in the livers of ciHL-expressing mice reflect accumulation of incompletely processed triglyceride-rich remnant lipoproteins from ciHL-facilitated liver uptake" (Dichek et al., 2004).

Another plausible explanation could be that ciHL facilitates uptake of lipoproteins and therefore causes a greater accumulation of hepatic TG than the control double knockout mice. However, active human HL in this study resulted in an even greater depletion of plasma apoB lipoproteins. In a previous study by the same author (Dichek et al., 1998) active human HL also resulted in hepatic clearance of apoB lipoproteins. In this regard, I would also expect increased steatosis in livers of mice expressing active HL compared to livers from control mice, regardless of whether the clearance was a result of increased TG hydrolysis and fatty acid uptake or via the bridging function of HL. The fact that catalytically active HL mice have less hepatosteatosis and markedly reduced plasma apoB lipoproteins compared to both control and ciHL mice is consistent with my observations. I speculate that the minimal TG storage and plasma apoB lipoproteins in these mice result from intracellular HL activity.

Overexpression studies are often criticised for being unphysiological. The resulting phenotype is said to be an artifact created by overexpression of a protein to levels which would never be found in nature. Yet gene overexpression and/or deletion often provide insight to a protein's biological function that might otherwise go unrecognized. A fine example of this is the study mentioned earlier, where both ciHL and wild-type human HL were shown to mediate the clearance of apoB lipoproteins from mouse plasma (Dichek et al., 1998). Despite the fact that post-heparin human HL activity (~50 fold mouse HL activity) and inactive human HL protein levels (~one third of active human HL) were unphysiological, these studies revealed an important function of HL in clearing lipoprotein remnants via its bridging function. Further studies with HL knockout mice corroborated these studies later that same year (Qiu et al., 1998).

Overexpression and retention of HL-R in the ER of McA cells was admittedly unphysiological. It enhanced the lipolytic activity of microsomes threefold and cell lysates twofold compared to pNEO1 cells (Fig. 3-3B,C). This unnatural lipase concentration concomitantly obliterated TG secretion regardless of exogenous oleate and abolished apoB100 secretion in the absence of exogenous oleate (Figs. 3-9, 3-10 and 3-11B,C). Nonetheless, the retention of HL in the ER did not destroy the secretory pathway in R12 cells, which is evidenced by their unimpaired ability to secrete albumin into media (Fig. 3-11B). These cells were also able to grow and divide normally since they were cultured continuously for months at a time (personal observation). The retention of HL in the ER, however, did serve its purpose: we were able to demonstrate HL is active intracellularly and hydrolyzes cellular lipids.

The overexpression of HL-S, on the other hand, was more reasonable. HL-S only elevated lipolytic activity of cell lysates by 20% and microsomes by 50% relative to pNEO1 cells (Fig. 3-3B,C). Intracellular HL-S did not impair secretion either, since both albumin (Fig. 3-11B) and HL-S (Fig. 3-3A) were both readily secreted from S7 cells. The total activity secreted into the media by S7 cells was merely 25% higher than the total activity secreted by primary mouse hepatocytes (Fig. 3-15). Considering that post-heparin HL activities vary by ~8 fold in the general human population (Deeb et al., 2003), the overexpression of HL in S7 hepatocytes was not overly extreme. Therefore, the results of these studies are most likely not artifacts of overexpression.

Despite similar overall depletion of neutral lipid stores in cell lines expressing HL-R and HL-S (Figs. 3-6 and 3-7), cells synthesizing secretion-competent HL were capable of secreting more TG than cells synthesizing the ER-localized HL (Figs. 3-9 and 3-10). One feasible explanation is that microsomes isolated from HL-R expressing cells contained twofold the lipolytic activity of microsomes isolated from HL-S expressing cells (Fig. 3-3C). The prolonged residence of HL-R in the ER likely diminishes the TG pool available for bulk lipidation of lipid-poor apoB particles (Alexander et al., 1976; Kulinski et al., 2002; Raabe et al., 1999). HL could also potentially hydrolyze TG associated with apoB lipoproteins present in the secretory route, hydrolyze TG as they are formed in the ER by DGAT, or may access all of these TG pools.

Our results show that HL reduces the TG content of apoB lipoproteins before secretion. This was obvious from experiments where the extracellular activity of HL-S was inhibited by P-407 (Tables 3-1). It is also verified by the fact that very little HL-R was secreted and HL-S was readily secreted (Fig. 3-3A), meanwhile media incubated with R12 cells contained less TG than media incubated with S7 cells (Figs. 3-9 and 3-10). Further, the uptake of exogenous lipoproteins was not increased by extracellular mouse HL protein (Tables 3-2). In conclusion, HL hydrolyzes lipids intracellularly and reduces apoB100 and VLDL-TG secretion and does not mobilize lipids for VLDL assembly.

Chapter 4:

Role of Arylacetamide Deacetylase in the Mobilization of Intracellular Lipids and VLDL Assembly

4.1 Introduction

AADA is a 45 kilodalton esterase (Preuss and Svensson, 1996; Probst et al., 1994). It is supposedly targeted to the ER membrane by an uncleaved N-terminal signal peptide sequence which acts as a transmembrane anchor, giving AADA a Type II conformation with the bulk of the protein oriented in the lumenal space (Gibbons et al., 2000; Preuss and Svensson, 1996). This enzyme has limited sequence homology with other lipases or carboxylesterases, although it contains two stretches of approximately 40 amino acids which have considerable homology with the active site of HSL (Trickett et al., 2001). The presence of the GXSXG serine motif indicates that this enzyme might be a lipase. Gibbons et al. (2000) have provided limited information suggesting that AADA is a glycosylated enzyme which mobilizes lipids for VLDL secretion. Still, no lipase activity has been reported for AADA and its role in intracellular lipid metabolism remains obscure.

Since AADA is reported to be a lumenal enzyme with potential for hydrolyzing TG, it could be involved in VLDL assembly. To investigate this possibility, a cDNA encoding a FLAG-tagged mouse AADA was stably expressed in McA cells. Previously, McA cells stably expressing a TGH cDNA were shown to enhance VLDL-TG secretion (Lehner and Vance, 1999). Using similar pulse / chase experiments, McA cells stably expressing AADA were analyzed for cellular lipid turnover as well as apoB and TG secretion. Furthermore, the topology and subcellular distribution of this poorly characterized enzyme was investigated.

4.2 Materials and Methods

4.2.1 Chemicals and Materials

Na_2CO_3, (3-[(3-Cholamidopropyl)dimethylammonio]-1-propane-sulfonate) (CHAPS), *p*-nitrophenylacetate (pNp-acetate), *p*-nitrophenol (pNp-OH), Ponceau S protein stain, endoglycosidase H (Endo H) and glycopeptidase F (PNGase) were from Sigma. Rabbit anti-CNX and rabbit anti-PDI were from Stressgen Biotechnologies. [9,10(n)-^{3}H]oleic acid and [U-^{14}C]glycerol were from Amersham Biosciences.

4.2.2 Screening of Stable McA Cell Lines for Expression of FLAG-tagged AADA

Generation of McA cells stably expressing FLAG-tagged AADA proteins was described in Chapter 2, Sections 2.2, 2.3 and 2.4. Stable cell lines were identified as described in Chapter 3, Section 3.2.2, for HL-R.

4.2.3 Esterase Assay

pNp-acetate is a substrate used to measure esterase activity (Gilham and Lehner, 2005). Hydrolysis of pNp-acetate liberates the chromogenic product pNp-OH whose absorbance is measured at 410 nm. 20 µL (38 µg protein) of pNEO1 and A13 microsomes (prepared as described in Chapter 2, Section 2.10) were assayed in triplicate in clear 96-well microtiter plates. The assay was initiated by adding 200 µL of 0.2 mM pNp-acetate in TBS containing 0.01% TX-100 to microsomes. Absorbance at 405 nm was measured every minute with a spectrophotometer. Hydrolysis of pNp-acetate was calculated from a standard curve generated using free pNp-OH.

4.2.4 4-MUH Lipase Assay

Followed procedure using 4-MUH described in Chapter 2, Section 2.5.1, with 50 µg microsomal protein. Microsomes were prepared as described in Chapter 2, Section 2.10.

4.2.5 Determination of the AADA Membrane Interaction

Microsomes were prepared from McA cells expressing FLAG-tagged AADA (A13 line) as described in Chapter 2, Section 2.10, and 30 µL microsomes (~100 µg microsomal protein) were treated with either 200 µL TBS, 200 µL 0.2 M Na_2CO_3 in ddH_2O, pH 12, or 200 µL 1% CHAPS in TBS. Treatments were mixed gently and incubated on ice for 30 min. Subsequently treatments were centrifuged at 315,000 *g* for 45 min to separate supernatant and pellet fractions. The pellets were resuspended in 200 µL TBS by sonication. 10 µL of supernatant, 10 µL of pellet and 50 µg of total lysate were resolved by SDS-PAGE and visualized by Western blotting.

4.2.6 PNGase Treatments

Vivien Lo (graduate student in Lehner Lab) did the following experiment. Mouse liver and A13 cells were homogenized in 100 mM TrisHCl, pH 8. Bovine fetuin (Spiro, 1960) was also dissolved in this buffer to a final concentration of 1 mg/mL. 100 µL of liver homogenate, cell lysate and fetuin solution were each treated with 10 µL 10% SDS, 10 µL 10% Triton X-100 and 2 µL of 2-mercaptoethanol. Proteins were denatured at 100°C for 5 minutes and were subsequently cooled on ice for 20 minutes. One half of each sample received 2 µL (10U) PNGase F whereas the other half received 2 µL Tris buffer (control). Samples were incubated overnight at 37°C for deglycosylation. Denaturing loading buffer was added, samples were boiled and resolved by SDS-PAGE. AADA and TGH were visualized by Western blotting whereas fetuin was visualized by staining nitrocellulose membranes with Ponceau stain.

4.2.7 Endo H Treatments

Vivien Lo did the following experiment. Mouse liver and A13 cells were homogenized in TBS and 2% Triton X-100. Bovine fetuin (Spiro, 1960) was also dissolved in this buffer to a final concentration of 1 mg/mL. 100 µL of liver homogenate, cell lysate and fetuin solution were combined with 100 µL of 100 mM sodium citrate, pH 5.5. One half of each sample received 10 µL (50 mU) Endo H whereas the other half received 10 µL sodium citrate buffer (control). Samples were incubated overnight at 37°C for deglycosylation. Denaturing loading buffer was added, samples were boiled and resolved by SDS-PAGE. AADA and TGH were visualized by immunoblotting whereas fetuin was visualized by staining nitrocellulose membranes with Ponceau stain.

4.2.8 Incorporation of [^{3}H]Oleic Acid into Radiolabeled Lipids

Followed the same procedure described in Chapter 3, Section 3.2.6 except with pNEO1 and A13 cell lines.

4.2.9 Pulse/Chase Experiments

Experiments were performed using McA and A13 cell lines with a 4 h pulse and 12 h chase, as described in Chapter 2, Section 2.7. Lipid masses were quantified by GC as described in Chapter 2, Section 2.9.

4.2.10 Radiolabel Pulse/Chase Experiments

Experiments were performed using McA and A13 cell lines with a 4 h pulse and 12 h chase, as described in Chapter 2, Section 2.7, except with the addition of 5 μCi [^{3}H]oleic acid and 0.5 μCi [U-^{14}C]glycerol per dish in the pulse. Radiolabel incorporation into lipids was quantified as described in Chapter 2, Section 2.8.

4.2.11 Secretion of ApoB

Experiments were performed exactly as described in Chapter 3, Section 3.2.9, except with media from McA and A13 cell lines.

4.2.12 Protein Electrophoresis and Western Blotting

Electrophoresis and Western blotting were performed as described in Chapter 2, Section 2.11, with these additional incubations: 1:10,000 rabbit anti-CNX primary antibodies followed by 1:10,000 HRP-goat anti-rabbit secondary antibodies and 1:10,000 rabbit anti-PDI primary antibodies followed by 1:10,000 HRP-goat anti-rabbit secondary antibodies. TGH in mouse liver homogenates was detected by 1:50,000 rabbit anti-mouse TGH antiserum (produced in our laboratory) followed by 1:10,000 HRP-goat anti-rabbit secondary antibodies. Fetuin was visualized using Ponceau S protein stain.

4.2.13 Statistical Analyses

Statistical analyses were calculated by paired student's t-test using Prism software. $P<0.05$ were considered statistically significant.

4.3 Results

4.3.1 AADA has Esterase and Lipase Activity

We generated a chimeric cDNA construct encoding the full length mouse AADA with sequence encoding the FLAG epitope immediately before the stop codon. The chimeric cDNA was ligated into the mammalian expression vector pCI-neo. This vector confers neomycin resistance, which facilitated the isolation of stable clones from transfected McA cells. A clone stably expressing FLAG-tagged AADA (Fig. 4-1A), hereafter referred to as A13 (Fig. 4-1B), was further characterized. A13 microsomes hydrolyzed the substrate *p*-nitrophenylacetate whereas pNEO1 microsomes showed limited hydrolysis of this compound (Fig. 4-1C), consistent with previous reports that AADA is an esterase (Preuss and Svensson, 1996; Probst et al., 1994). Furthermore, A13 microsomes had increased hydrolytic activity against the water-insoluble substrate 4-MUH compared to microsomes isolated from pNEO1 cells (Fig. 4-1D). These data suggest that AADA is in fact a lipase, as it hydrolyzes carboxylester bonds of lipid substrates.

4.3.2 AADA is a Glycosylated Lumenal-facing ER Transmembrane Enzyme

The elevated lipase activity associated with A13 microsomal membranes indicated that AADA is targeted to intracellular membrane fractions. To verify that full length mouse FLAG-tagged AADA retains its membrane assotiation, A13 microsomes were subjected to treatments that release peripheral and soluble lumenal proteins or membrane-spanning proteins (Fig. 4-2). The soluble lumenal ER chaperone PDI was released from microsomes through incubations

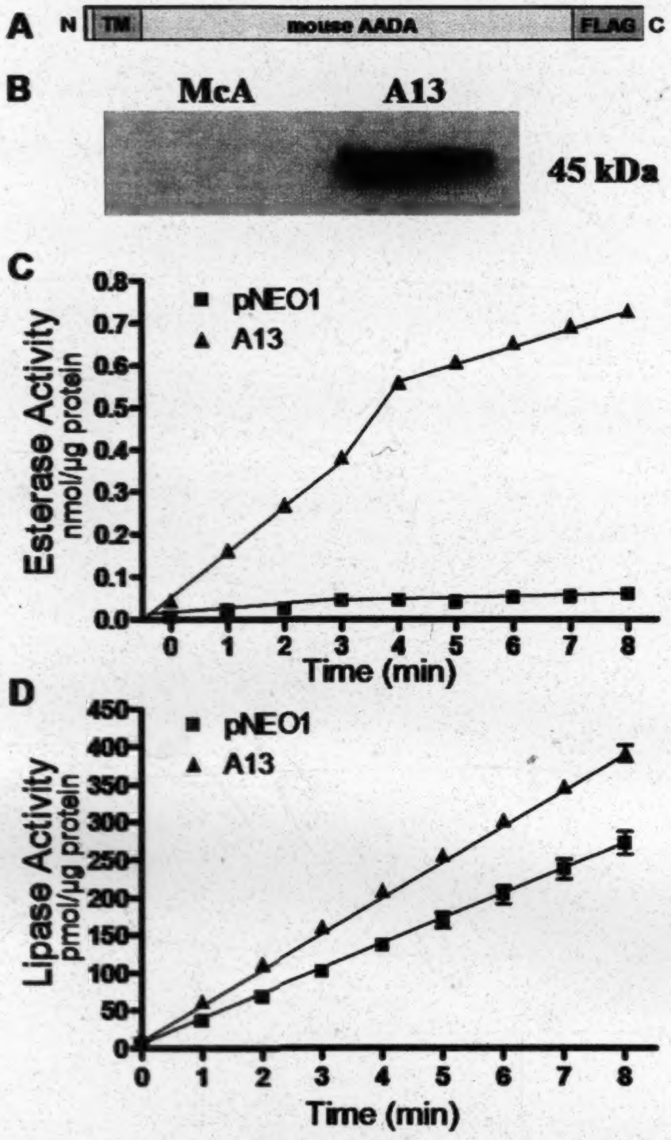

Fig. 4-1: AADA has both esterase and lipase activity. (A) Schematic representation of AADA-FLAG with its N-terminal transmembrane (TM) domain. (B) Western blot of AADA-FLAG in A13 cell lysate. (C) Esterase assay. Hydrolysis of pNp-acetate by pNEO1 and A13 microsomes; values are the mean of duplicate samples at each time point. (D) Lipase assay. Hydrolysis of 4-MUH by pNEO1 and A13 microsomes; values are mean ± SD of triplicate samples at each time point.

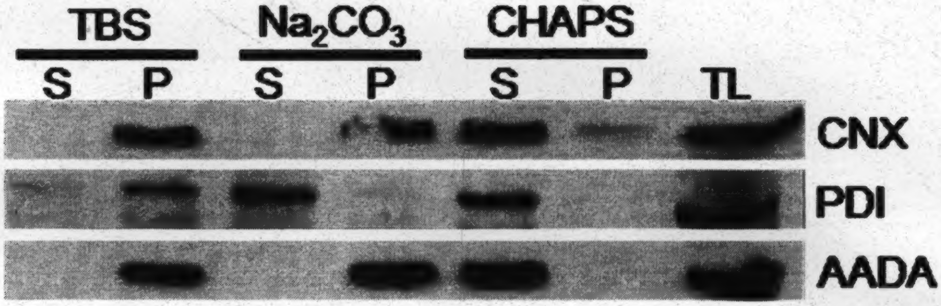
TBS
Na_2CO_3
CHAPS
S
P
S
P
S
P
TL
CNX
PDI
AADA

Fig. 4-2: AADA is a integral microsomal membrane protein. A13 microsomes were isolated and subjected to 3 treatments as described in Section 4.2.5. Western blot of supernatants (S) and pellets (P) after treatments and of untreated total cell lysate (TL) from A13 cells.

with high ionic strength-high pH buffer, while the ER transmembrane protein chaperone CNX only partitioned into the soluble supernatant after treatments with detergent (Fig. 4-2). AADA's solubilization profile is identical to that of CNX: therefore, mouse FLAG-tagged AADA has the property of an intrinsic membrane protein (Fig. 4-2).

We sought to establish the orientation of mouse AADA and its subcellular location. Previously it has been suggested that human AADA is a glycosylated protein based on in vitro translation of AADA on canine pancreatic microsomes (Gibbons et al., 2000). They concluded that human AADA is glycosylated at both Asn78 and Asn282 from the presence of three distinct AADA bands separated by electrophoresis. Using the MAXHOM alignment program in the PredictProtein database (http://www.predictprotein.org), we found that mouse AADA shares 70% identity with human AADA at the amino acid level. Mouse AADA has one potential N-linked glycosylation motif at Asn281, implying that it too might be glycosylated.

To determine if mouse AADA is glycosylated, Vivien Lo performed digestions with PNGase and Endo H. PNGase is a non-specific glycosidase which removes virtually all N-linked oligosaccharides from glycoproteins, whereas Endo H only cleaves oligosaccharides with a high-mannose content. Treatment of A13 cell lysate with PNGase or Endo H resulted in faster electrophoretic mobility of AADA, indicating that deglycosylation took place (Fig. 4-3). Importantly, sensitivity of AADA to Endo H indicates the presence of a high-mannose content and this confirms that the enzyme has not been exposed to Golgi mannosidases. TGH is localized to the ER lumen (Gilham et al., 2005)

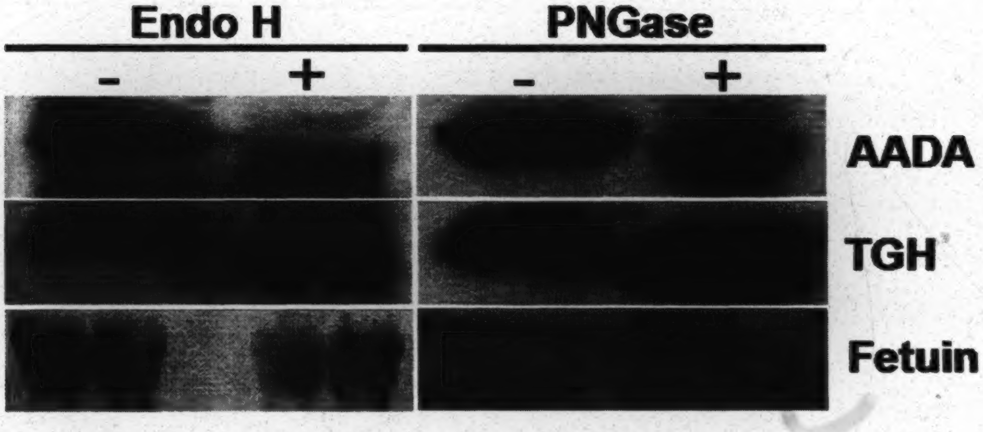

Fig. 4-3: AADA is a glycosylated enzyme which localizes to the ER. This work was performed by Vivien Lo. AADA, TGH and fetuin were treated with Endo H or PNGase as described in Sections 4.2.6 and 4.2.7. AADA and TGH are visualized by Western blotting and fetuin is visualized by staining nitrocellulose with Ponceau S.

and it displayed an identical digestion profile (Fig. 4-3). The secreted glycoprotein fetuin (Spiro, 1960), on the other hand, was not deglycosylated by Endo H, testifying to the selectivity of Endo H for high-mannose glycans only. Glycosylation of mouse AADA at Asn-281 thus confirms a Type II conformation with the bulk of the protein inside the ER lumen.

4.3.3 AADA Hydrolyzes Cellular TG in McA Cells

To assess whether AADA affects intracellular lipid metabolism, we measured the incorporation of [^{3}H]oleic acid into pNEO1 and A13 cellular lipids over a time course of 4 h (Fig. 4-4). The radioactivity associated with ^{3}H-PC was similar between pNEO1 and A13 cells at every time point analyzed, whereas ^{3}H-TG was far lower and ^{3}H-CE levels were increased in A13 cells compared to control cells. These data imply that AADA is capable of TG hydrolysis.

We then set out to establish whether or not AADA mobilizes intracellular lipids for lipoprotein secretion. Radiolabeled and unlabeled pulse/chase experiments were performed with a 4 h pulse in the presence of exogenous oleic acid (and [^{3}H]oleic acid and [^{14}C]glycerol) and a 12 h chase in the absence of exogenous oleic acid, to quantify both cellular lipid radioactivity and lipid mass. Cellular PL mass (90-95 µg/mg cell protein) and cholesterol mass (25 µg/mg cell protein) were identical between wild-type McA and A13 cells after both pulse (Fig. 4-5) and chase (Fig. 4-6) incubations. Additionally, incorporation of [^{3}H]oleic acid into PC during the pulse (A13 518,586 ± 229,096 vs. McA 490,720 ± 236,622 dpm/mg cell protein) was nearly identical between the two cell lines (Fig. 4-5), indicating that fatty acid uptake and PL biosynthesis were not impaired by the

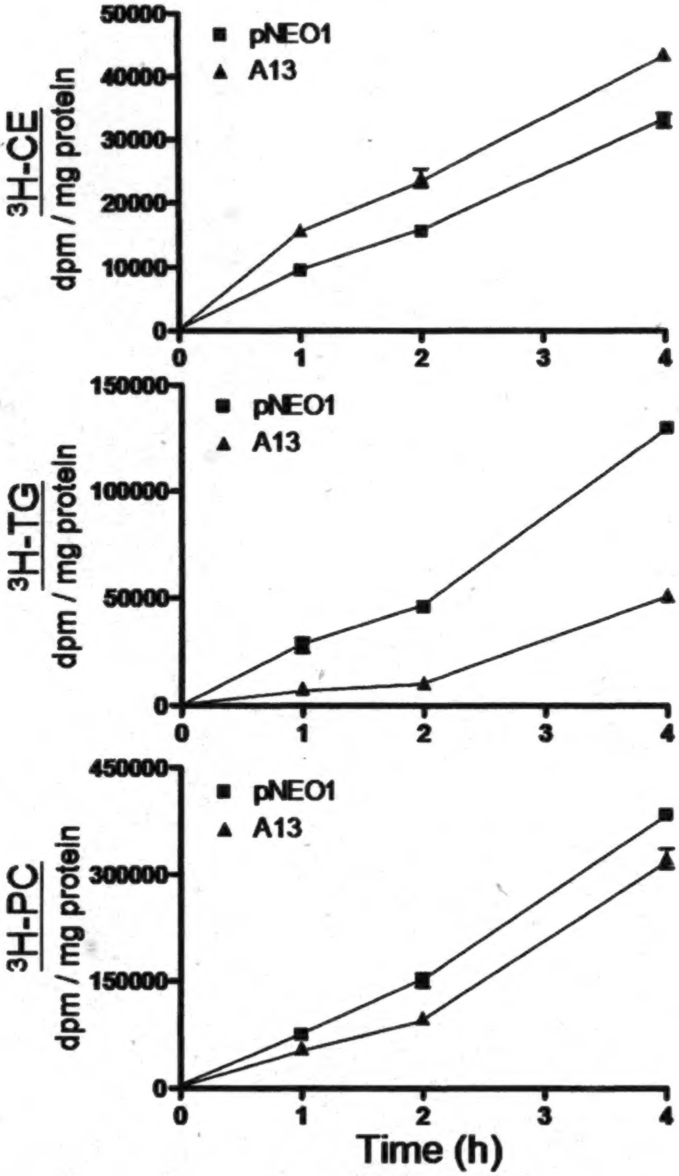

Fig. 4-4: Incorporation of [^{3}H]oleic acid into cellular CE, TG and PC in pNEO1 and A13 cells as a function of time. Values are mean ± SD of triplicate samples.

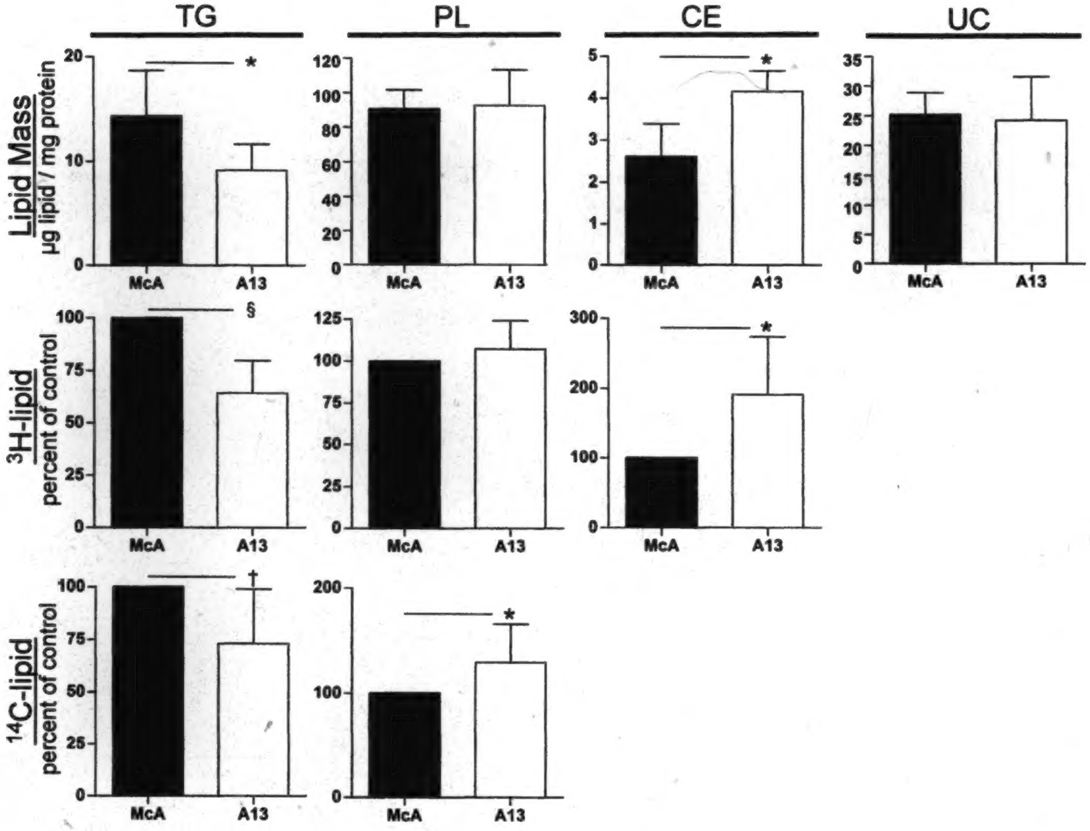

Fig. 4-5: (Pulse) AADA depletes cells of TG. (Top row) Cellular TG, PL, CE and cholesterol (UC) mass in McA and A13 cells after the 4 h pulse with oleic acid; values are mean ± SD for n=4 experiments with triplicate samples. (Middle + bottom rows) Radioactivity in cellular TG, PC and CE of McA and A13 cells after the radiolabeled pulse with [^{3}H]oleic acid and [^{14}C]glycerol; values are mean dpm/mg cell protein ± SD for n=10 experiments with triplicate samples, expressed as a percentage of control (McA). * $P < 0.05$, ‡ $P < 0.001$, § $P < 0.0001$

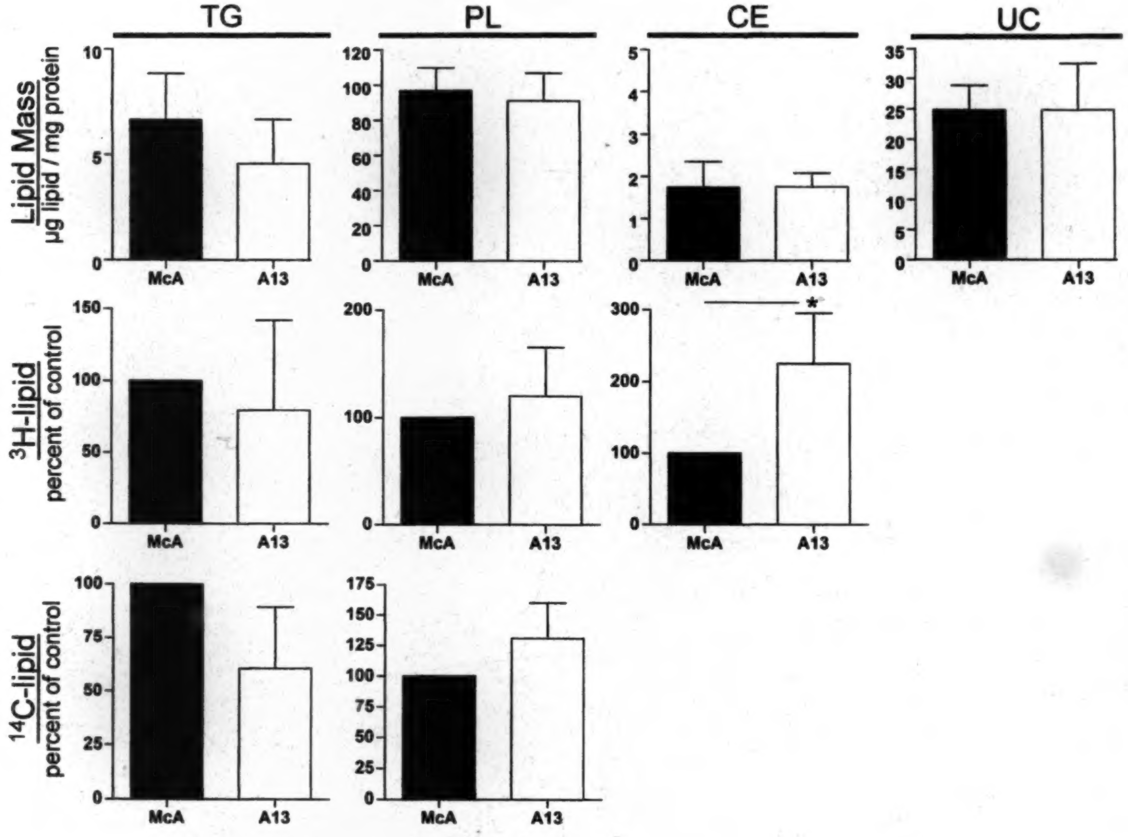

Fig. 4-6: (Chase) AADA depletes cells of TG. (Top row) Cellular TG, PL, CE and cholesterol (UC) mass in McA and A13 cells after the 12 h chase; values are mean ± SD for n=4 experiments with triplicate samples. (Middle + bottom rows) Radioactivity in cellular TG, PC and CE of McA and A13 cells after the chase; values are mean dpm/mg cell protein ± SD for n=4 experiments with triplicate samples, expressed as a percentage of control (McA). * $P < 0.05$

presence of AADA. At the end of the pulse, both the mass and label incorporated into TG were significantly lower (25-35%) in A13 cells than in control McA cells (Fig. 4-5: A13 9.19 ± 2.49 vs. McA 14.32 ± 4.37 μg TG/mg cell protein, A13 482,802 ± 244,962 vs. McA 741,428 ± 351,925 ^{3}H-TG dpm/mg cell protein and A13 49,572 ± 18,776 vs. McA 70,309 ± 24,196 ^{14}C-TG dpm/mg cell protein). Decreased TG levels in AADA-expressing cells were consistent regardless of whether mass, radiolabeled glycerol backbone or radiolabeled acyl chains were measured. A13 cells, on the other hand, incorporated [^{3}H]oleic acid into CE far more efficiently than McA cells (Fig. 4-5: A13 74,280 ± 28,315 vs. McA 48,442 ± 33,850 ^{3}H-CE dpm/mg cell protein), which was also reflected by CE mass (Fig. 4-5; A13 4.16 ± 0.49 vs. McA 2.61 ± 0.77 μg CE/mg cell protein). Notably, although the cellular PL mass and incorporation of oleic acid into PC were similar in control and A13 cells, the utilization of [^{14}C]glycerol for PL biosynthesis was 30% greater in A13 cells than in wild-type McA cells (Fig. 4-5: A13 154,919 ± 96,109 vs. McA 115,186 ± 57,101 ^{14}C-PC dpm/mg cell protein).

Cellular lipid masses and lipid radiolabel data after the chase are presented in Fig. 4-6. The trend of decreased TG mass and label in A13 cells versus McA cells persisted 12 h after the pulse. Although CE mass equilibrated between the two cell lines, the increased incorporation of [^{3}H]oleic acid into CE remained statistically significant. The 30% increased [^{14}C]glycerol incorporation into ^{14}C-PC was also the same. Both McA and A13 cell lines depleted 50% of their cellular TG mass over the 12 h period. This suggests that AADA hydrolyzes TG formed *de novo* during active TG synthesis because A13 cells are depleted of TG at the end of the pulse, yet AADA did not affect the depletion rate of preformed lipids thereafter.

4.3.4 AADA Does Not Increase VLDL Secretion from McA Cells

Because the presence of AADA had profound effects on intracellular lipid metabolism in McA cells, we quantified the secretion of radiolabeled lipids from these cells. Although radiolabeled CE secretion was unchanged between A13 and McA cells, both TG and PC secretion were markedly decreased in AADA-expressing cells (Table 4-I). Approximately 20-30% less TG and PC were secreted by A13 cells compared to control McA cells in the presence of oleic acid (4 h pulse) and 35-55% less in the absence of oleic acid (12 h chase), as quantified by both ^{3}H- and ^{14}C-lipid labeling. ApoB100 secretion was similar between the two cell lines irrespective of exogenous oleate (Fig. 4-7). These data indicate that stable expression of mouse AADA in McA cells is insufficient for the mobilization of TG for VLDL assembly and secretion; instead, its intracellular activity resulted in less TG being secreted with apoB100.

Lipid	^{3}H-Lipid	^{14}C-Lipid
4 h TG	68.4 ± 41.8	63.7 ± 29.6
12 h TG	45.1 ± 49.6	46.5 ± 43.6
4 h PC	71.7 ± 40.1	77.8 ± 12.2 *
12 h PC	43.3 ± 12.1*	62.9 ± 19.3 *
4 h CE	107.0 ± 34.2	/
12 h CE	92.0 ± 51.0	/

A13 Media Lipids (Percent of McA Media Lipids)

Table 4-1: A13 cells secrete less radiolabeled TG and PC than McA cells. Radioactivity in A13 media TG, PC and CE after a 4 h radiolabeled pulse with [^{3}H]oleic acid and [^{14}C]glycerol and after the 12 h chase, expressed as a percentage of radiolabeled lipids secreted by wild-type McA cells. Values are mean percentage ± SD calculated from mean dpm/mg cell protein for n=4 experiments with triplicate samples. * $P < 0.05$

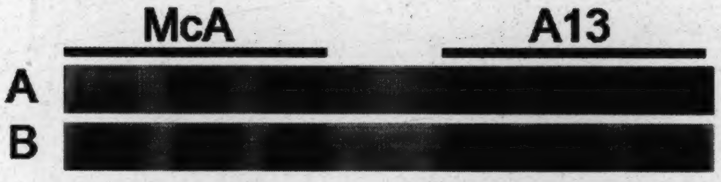

Fig. 4-7: AADA does not alter secretion of apoB100 from McA cells. Western blots of Cab-o-sil treated media from (A) pulse and (B) chase. Each lane is Cab-o-sil treated media from a separate culture dish.

4.4 Discussion

In the present study we have isolated the cDNA for mouse AADA, FLAG-tagged it and expressed the chimeric cDNA in McA rat hepatoma cells to address the issue of whether or not AADA is a true lipase and to establish if it is involved in the mobilization of TG for VLDL secretion. Based on its hydrolytic activity towards the water-insoluble substrate 4-MUH and the depletion of cellular TG in McA cells expressing AADA, we conclude that AADA is indeed a TG lipase. The membrane topology of AADA suggests lumenal orientation of the putative active site residues in close proximity to the inner leaflet of the ER membrane. The ER membrane harbors many enzymes for neutral lipid biosynthesis, including the ACATs (Joyce et al., 2000; Rudel et al., 2001) and the DGATs (Cases et al., 1998; Cases et al., 2001). These enzymes catalyze the penultimate steps in the synthesis of CE and TG, respectively. These lipids constitute the neutral lipid core of VLDL and the availability of these lipids determines the fate of the nascent apoB100 polypeptide (Fisher and Ginsberg, 2002; Kulinski et al., 2002; Wang et al., 1999).

We hypothesized that AADA would hydrolyze the lumenal lipid droplet in a manner similar to TGH (Dolinsky et al., 2004b). Yet our studies show that AADA activity did not augment VLDL secretion from McA cells like TGH (Lehner and Vance, 1999), but rather, reduced both TG and PC secretion (Table 4-1) without significantly altering apoB100 secretion (Fig. 4-7). Therefore, the neutral lipid core of apoB lipoproteins secreted from A13 cells has a higher CE:TG ratio than those from wild-type McA cells. Increased CE synthesis in AADA expressing cells might have rescued apoB from presecretory degradation despite TG depletion. As mentioned in Chapter 1, Section 1.5, several studies have revealed a relationship between active CE synthesis and apoB secretion (Liang et al., 2004; Spady et al., 2000; Zhang et al., 1999).

Although AADA expression in McA cells was insufficient to stimulate TG or apoB secretion, it clearly had a significant effect on lipid metabolism in these cells. Fig. 4-8 is a schematic of my interpretation of the results. I suggest that AADA hydrolyzes TG, liberating fatty acids and DG. Both of these lipids are soluble in the ER membrane and may readily flip across the bilayer (Holthuis and Levine, 2005; Kamp et al., 1995). DG may then become a substrate for CPT (Lim et al., 1986) on the cytosolic face of the ER membrane (Fig. 4-8); this is supported by the preferential incorporation of [^{14}C]glycerol into ^{14}C-PC in the presence of AADA while incorporation of [^{3}H]oleic acid into ^{3}H-PC and total PL mass were indistinguishable between A13 and McA cells (Figs. 4-5 and 4-6). Concomitantly, the liberation of fatty acids from TG in close proximity to the ACATs might create a microenvironment amenable to CE synthesis. Our laboratory has previously shown that at least some fatty acids liberated from TG are incorporated into CE stores in rat hepatocytes: in a pulse/chase experiment, cellular CE more than doubled during the 4 h chase period when the only source of labeled fatty acid was the prelabeled pool of lipids formed in the pulse (Gilham et al., 2003). Stable expression of AADA in McA cells nearly doubled CE synthesis and mass compared to wild-type McA cells (Fig. 4-5). I hypothesize that liberated fatty acids associated with the membrane may be activated by ACSs, whereby they become substrates for ACAT1 or ACAT2

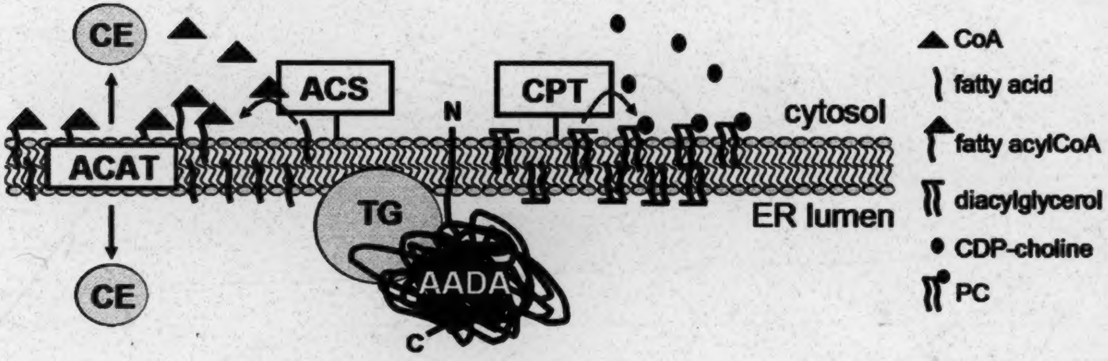
CE
ACS
CPT
N
cytosol
ACAT
TG
AADA
ER lumen
CE
C
▲ CoA
fatty acid
fatty acylCoA
diacylglycerol
● CDP-choline
PC

Fig. 4-8: Schematic depiction of AADA's proposed role in lipid remodeling. AADA hydrolyzes lumenal TG or TG associated with the inner leaflet of the ER membrane. The fatty acid and DG products are able to flip across the bilayer. DG acts as a substrate for CDP-choline:DG cholinephosphotransferase (CPT) which produces PC. Free fatty acids are conjugated to Coenzyme A (CoA) by acylCoA synthetases (ACS). Fatty acylCoA products become a substrate for CE synthesis by the ACAT enzymes. For the sake of simplicity, re-esterification of TG hydrolysis products by the DGAT enzymes has been omitted.

(Fig. 4-8). Additionally, the lipolysis products might be re-esterified to TG in a futile cycle (Fig 1-3).

To date, acylCoA synthetase activities have been identified on the cytoplasmic face of the ER membrane, but not in the ER lumen (Coleman et al., 2002; Lewin et al., 2001). The putative active site serine residue of ACAT1 faces the cytosolic side of the ER membrane while the putative active site serine of ACAT2 is luminal (Joyce et al., 2000). Thus, ACAT1 would have full access to acylCoAs. On the other hand, how ACAT2 acquires its acylCoA substrate is currently unknown. There has been limited evidence for a carnitine acyltransferase activity associated with the ER, suggesting that fatty acids might be imported into the ER lumen in a similar fashion to mitochondrial import via the carnitine palmitoyltransferase (Broadway et al., 2001; Murthy and Pande, 1994). However, recent studies do not support the existence of an acylcarnitine shuttle in the ER (Broadway et al., 2003). It has also been proposed that both ACATs may be able to access acylCoAs associated with the cytosolic leaflet of the ER membrane (Chang et al., 2001). Regardless of ACAT topology and substrate accessibility, increased CE synthesis stimulates hepatic CE secretion (Liang et al., 2004). This could be due to the ability of MTP to transport CE in addition to TG (Atzel and Wetterau, 1993).

In this chapter we have demonstrated that AADA is a glycosylated enzyme that is Endo H sensitive (Fig. 4-3), indicating that it is localized to the ER lumen. Its solubilization profile reveals that AADA is an integral microsomal membrane protein rather than a peripheral or soluble lumenal protein (Fig. 4-2). Proteins with short hydrophobic transmembrane domains (17-20 amino acids) can traverse the ER and cis-Golgi membranes, but not trans-Golgi or plasma membranes (Munro, 1995); this is because the latter membranes are enriched in cholesterol and sphingolipids, which effectively increases bilayer thickness (Holthuis and Levine, 2005). The N-terminal transmembrane segment of AADA is similar to that of 11β-hydroxysteroid dehydrogenase (11β-HSD) and both enzymes are Type II membrane enzymes with the C-terminus projecting into the ER lumen (Mziaut et al., 1999). Mziaut et al. (1999) call this transmembrane domain a lumenal targeting signal (LTS). It is characterized by a short segment of neutral or basic amino acids at the N-terminus, followed by an array of hydrophobic residues (the transmembrane segment) and terminating with acidic residues. Appending the LTS to GFP was enough to target it to the ER lumen (Mziaut et al., 1999). Mutagenesis of the LTS in 11β-HSD caused it to flip to a cytosolic-facing enzyme and abolished its ability to oxidize cortisol (Frick et al., 2004).

The results presented in this chapter support the notion that AADA is a TG lipase and suggest that it may play an important role in lipid remodeling. Mouse AADA did not enhance the secretion of TG from McA cells as human AADA did in HepG2 cells (Gibbons et al., 2000) or rat TGH did in McA cells (Lehner and Vance, 1999). While it appears that AADA hydrolyzes TG within the lumen of the ER, it is presently unclear which TG pool is its substrate. AADA's close proximity to the inner leaflet of the ER membrane might allow it to hydrolyze lipids associated with the bilayer, such as lipid droplets forming contact with the ER membrane or TG solubilized in the membrane. Alternately, it might hydrolyze the apoB-free lumenal lipid droplet (Havel et al., 1973) or apoB-associated lipids. Clearly the physiological role of *AADA in vivo* deserves further investigation.

Chapter 5

Role of Esterase-X and Esterase-22 in Intracellular Lipid Mobilization and VLDL Assembly

5.1 Introduction

Mouse Es-X and Es-22 are potential lipases because they are both 76% identical to mouse TGH at the amino acid level (Fig. 1-5 and (Dolinsky et al., 2004b)). The genes for Es-X, Es-22 and TGH are grouped in a carboxylesterase gene cluster and are believed to have arisen from gene duplication (Dolinsky et al., 2004b). Similar to TGH, these proteins have an ER signal peptide and ER retrieval sequence, indicating that they localize to the ER lumen like TGH (Dolinsky et al., 2004b; Gilham et al., 2005). The GXSXG serine motif-characteristic of lipases and esterases-as well as the glutamate and histidine residues in the active site of TGH have been conserved in Es-X and Es-22 (Fig. 1-5). Divergence in amino acid composition of lid domains between the three carboxylesterases (Fig. 1-5) suggest that they may have different substrate specificities (Wong and Schotz, 2002). Lipase activity has not been reported for Es-X or Es-22, however.

To investigate whether Es-X and Es-22 have lipolytic activity and contribute to VLDL secretion, cDNAs encoding FLAG-tagged mouse Es-X and Es-22 were stably expressed in McA cells. These cells do not express Es-X and have very low level expression of Es-22 compared to primary rat hepatocytes (Fig. 1-6). McA cells stably expressing a TGH cDNA were shown to enhance VLDL-TG secretion (Lehner and Vance, 1999). If these enzymes have the same function as TGH, than they too will stimulate VLDL secretion from McA cells.

5.2 Materials and Methods

5.2.1 Chemicals and Materials

GSKi was provided by collaborators at GlaxoSmithKline (Les Ulice, France). Diethyl-*p*-nitrophenylphosphate (E600) was purchased from Sigma.

5.2.2 Screening of Stable McA Cell Lines for Expression of FLAG-tagged Es-X and Es-22

Generation of McA cells stably expressing FLAG-tagged Es-X and Es-22 proteins was described in Chapter 2, Sections 2.2, 2.3 and 2.4.

5.2.3 Protein Electrophoresis and Western Blotting

Followed the procedure described in Chapter 2, Section 2.11, with 50 µg of cell lysates from wild-type McA, X-8 (FLAG-tagged Es-X), 22-15 (FLAG-tagged Es-22) and 35-5 (FLAG-tagged human TGH, produced by Dr. Dean Gilham in the Lehner laboratory, which is tagged the same as Es-X and Es-22) cell lines.

5.2.4 Resorufin Ester Lipase Assay

Resorufin ester hydrolysis by Es-X and Es-22 was determined as described in Chapter 2, Section 2.5.2, using 100 µg microsomes from pNEO1, X8 or 22-15 cells, prepared as described in Chapter 2, Section 2-10.

5.2.5 4-MUH Lipase Assay and Inhibition by GSKi

Followed the procedure described in Chapter 2, Section 2.5.1. Inhibition profiles of Es-X, Es-22 and TGH were determined using 40 µg cell lysates (McA, X-8, 22-15, 35-5) in the absence of inhibitor or in the presence of 10 μM GSKi or 100 μM E600. Inhibitors were added directly to cell lysates in microtiter dishes to give a final concentration of 10 μM GSKi or 100 μM E600.

5.3 Results

We introduced the FLAG epitope immediately before the ER retrieval signal sequence at the C-terminus (Fig. 5-1A), which occurs naturally in Es-X and Es-22 proteins (Fig. 1-5). McA cells stably transfected with the chimeric cDNAs produced functional enzymes (Fig. 5-1B) which hydrolyzed both 4-MUH (Fig. 5-2) and resorufin ester (Fig. 5-1C). It is interesting that both enzymes have similar hydrolytic activity towards the TG analogue resorufin ester (Fig. 5-1C) whereas Es-X is not nearly as efficient at hydrolyzing 4-MUH as either TGH or Es-22 are (Fig. 5-2).

Since mouse Es-X and Es-22 are structurally similar to TGH, we tested whether GSKi and E600 would inhibit these lipases in addition to TGH. The general esterase inhibitor E600 eliminated the lipolytic activities of wild-type McA, X8, 22-15 and 35-5 cell lysates (Fig. 5-2), confirming that Es-X, Es-22 and TGH are all serine esterases. The TGH-specific GSKi inhibited human TGH activity by 95% in this assay, to the extent that both McA and 35-5 (hTGH) cell lysates had identical residual activity. GSKi also inhibited mouse Es-X and Es-22. 10 μM GSKi inhibited 65% of Es-X activity and 52% of Es-22 activity towards 4-MUH, calculated from the activity difference between treated and untreated cell lysates (Fig. 5-2). It is noteworthy that 10 μM GSKi also reduced the lipase activity of McA lysate by 46% (Fig. 5-2). This might be explained by the low level expression of Es-22 in McA cells (Fig. 1-6), since Es-22 readily hydrolyzes 4-MUH (Fig. 5-2).

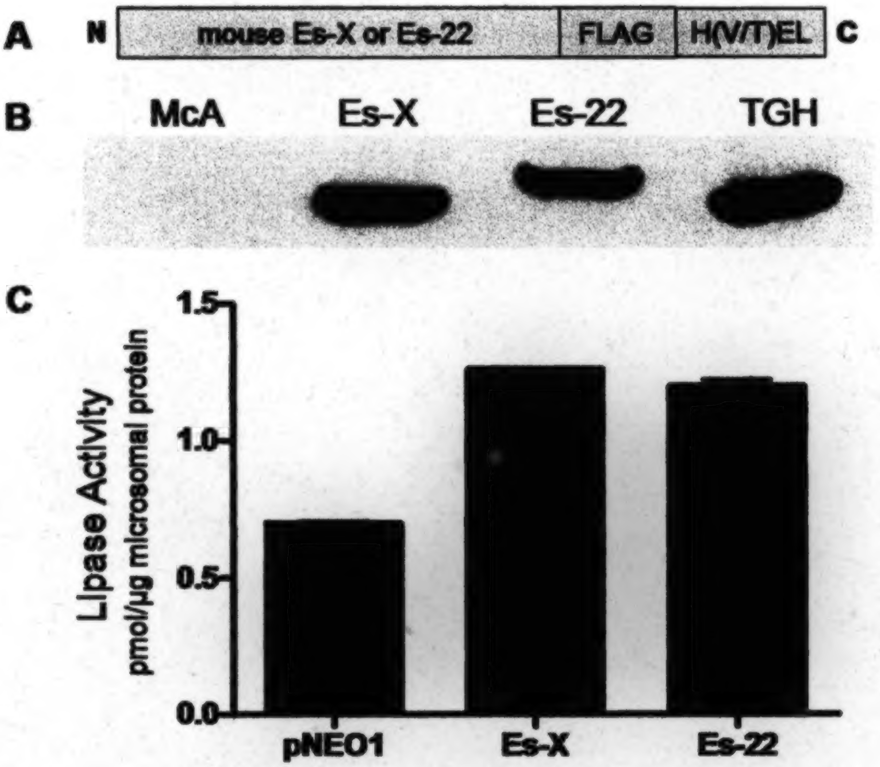

Fig. 5-1: FLAG-tagged Es-X and Es-22 are expressed in McA cells and have lipase activity. (A) Schematic representation of FLAG-tagged Es-X and Es-22 proteins. (B) Western blot of cell lysates from McA cells and McA cells stably transfected with FLAG-tagged mouse Es-X, mouse Es-22 and human TGH. (C) Resorufin ester lipase assay. Values are mean ± SD of triplicate samples at 12 min into the linear range of the assay.

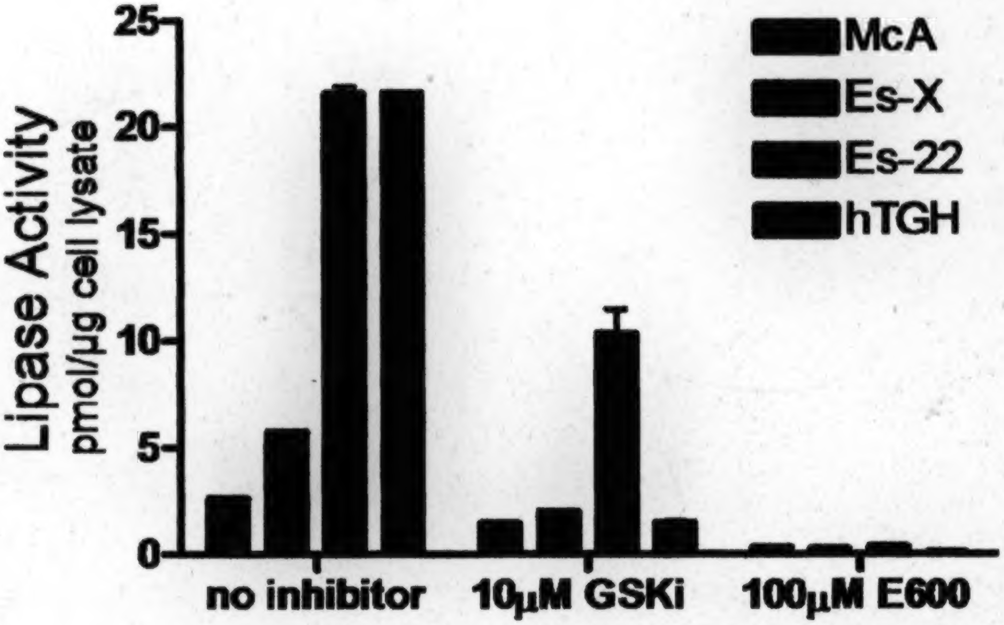

Fig. 5-2: GSKi also inhibits Es-X and Es-22. 4-MUH lipase assay of cell lysates in the absence of inhibitor or in the presence of 10 μM GSKi or 100 μM E600. Values are mean ± SD of triplicate samples at 20 s into the linear range of the assay.

5.4 Discussion

The results presented in this study show that both Es-X and Es-22 have lipolytic activity against the TG analogue resorufin ester, indicating that they might hydrolyze TG *in vivo*. Whether these lipases are involved in lipolysis and re-esterification of TG for VLDL assembly remains to be determined. VLDL secretion is maximum when circulating glucocorticoids are low, which is consistent with glucocorticoid-mediated TGH mRNA instability (Dolinsky et al., 2004a); Es-X and Es-22 mRNA is regulated in a similar fashion to that of TGH, suggesting their involvement in VLDL assembly as well (Dolinsky et al., unpublished observations). It is possible that TGH, Es-X and Es-22 might have overlapping functions since their expression profiles are all very similar. However, the different amino acid composition in lid domains might confer alternate substrate specificity to these enzymes. Consistent with this idea, both TGH and Es-22 hydrolyze 4-MUH very efficiently whereas Es-X hydrolyzes this substrate with lower efficiency (Fig. 5-2). Furthermore, the GSKi did not inhibit Es-X or Es-22 to the same extent as it did TGH (Fig. 5-2), providing evidence that the structural properties of their active sites are not identical.

The role of TGH in VLDL assembly has been demonstrated. Stable transfection of a TGH cDNA in McA cells increased the proportion of TG secreted with VLDL (Lehner and Vance, 1999). The results presented in this chapter, however, show that the TGH-specific inhibitor GSKi inhibits Es-X and Es-22 in addition to TGH, albeit with reduced potency (Fig. 5-2). For this reason, we cannot exclude the possibility that inhibition of primary rat hepatocytes with 10 µM GSKi (Gilham et al., 2003) also inhibited both Es-X and Es-22 activities;

therefore the reduced apoB and TG secretion from GSKi-inhibited hepatocytes might not be fully attributable to absent TGH activity, but also to reduced Es-X and Es-22 activities.

Wild-type McA cells are known to turnover CE for cholesterol efflux to apoAI (Sahoo et al., 2004) and turnover TG (Fig. 4-5 vs. Fig. 4-6). These cells are also capable of VLDL secretion when stimulated with exogenous oleate (Boren et al., 1994; Lehner et al., 1999; Tran et al., 2002), although at a lower rate than VLDL secretion from primary hepatocytes (Lehner et al., 1999). Thus it is possible that Es-22 might contribute to these processes since it is expressed at low levels in McA cells (Fig. 1-6).

In conclusion, both the native and FLAG-tagged cDNAs for Es-X and Es-22 were cloned and the FLAG-tagged cDNAs were stably expressed in McA cells. The role of Es-X and Es-22 in these cell lines is currently under investigation. Clearly these cells are an invaluable tool for the elucidation of Es-X and Es-22 function. The FLAG-tagged proteins are readily isolated on M2 anti-FLAG agarose beads and retain their catalytic activities (not shown). These proteins will be useful for determining antibody and inhibitor specificity for TGH, since TGH is a potential drug target for reducing atherogenic lipoprotein production (Gilham et al., 2003). Furthermore, the cDNAs could be utilized for adenoviral-mediated overexpression of these enzymes in mouse liver to study the *in vivo* function of these lipases.

Chapter 6:

General Discussion and Future Directions

6.1 The Generation of New Research Tools

Both the native and FLAG-tagged cDNAs for mouse HL, AADA, Es-X and Es-22 have been cloned and sequenced to ensure fidelity. The chimeric cDNAs have been transfected into McA cells and stable cell lines with varied levels of expression (as determined by Western blotting and lipase assays) have been isolated. Glycerol stocks of transformed bacteria and cryogenic stocks of stable cell lines will provide an endless supply of plasmids and cells for future research on these enzymes.

6.2 Conclusions from Studies Presented in the Thesis

The objective of the research was to identify hepatic lipases other than TGH which might be involved in VLDL secretion. McA cells stably expressing FLAG-tagged HL-S, HL-R, AADA, Es-X or Es-22 were created in order to study the potential contribution of these enzymes to the TG lipolysis and re-esterification cycle for VLDL secretion. These studies show that AADA, Es-X and Es-22 all possess putative lipase activity since they hydrolyze carboxylester bonds of water-insoluble substrates. Lipase activity has not been reported for any of these enzymes to date (although esterase activity has previously been reported for AADA (Preuss and Svensson, 1996; Probst et al., 1994) and Es-22 (Medda and Swank, 1985)). My research has largely focused on the intracellular role of HL and AADA in McA cells.

Data presented in Chapter 3 show for the first time, that HL hydrolyzes lipids intracellularly. It was previously demonstrated that HL gains lipolytic competence before secretion from primary rat hepatocytes (Verhoeven and

Jansen, 1991; Verhoeven et al., 2000) but there are no published reports addressing hydrolysis of hepatic lipids by HL. The role of HL as a phospholipase and TG hydrolase in the circulation is well established (Zambon et al., 2003). My research demonstrates that HL hydrolyzes TG (and potentially CE) intracellularly, but the products of HL-mediated lipolysis were not diverted into the re-esterification and VLDL assembly pathway. Lumenal HL activity did not increase secretion or oxidation of liberated fatty acids either. Increased HL activity in McA cells resulted in decreased TG and apoB secretion (despite HL-R having the same ER retrieval signal as murine TGH).

Data presented in Chapter 4 reveal that AADA is a Type II ER lumenal lipase. It apparently hydrolyzes TG within the ER lumen, directing a proportion of the liberated fatty acids towards CE synthesis and some of the liberated DG into PC synthesis. ApoB100 secretion from McA cells was not affected by AADA activity, but the composition of secreted lipoproteins was markedly altered: less TG and PC were secreted while CE secretion remained comparable to control McA cells. Therefore AADA does not appear to have the same function as TGH, since its expression in McA cells produced a drastically different phenotype than TGH expression. These results indicate that AADA plays an important role in lipid remodeling rather than VLDL secretion.

Data presented in Chapter 5 demonstrate that Es-X and Es-22 also possess lipolytic activities that can be inhibited to a certain extent (50-65%) by what was previously considered a TGH-specific inhibitor (GSKi). Differences among the lid domains of the three carboxylesterases, GSKi inhibition profiles, and hydrolytic activities towards 4-MUH and resorufin ester indicate that TGH, Es-X and Es-22 have different substrate specificities. However, they might all be capable of TG hydrolysis since cell lysates from Es-X, Es-22 and TGH cell lines all hydrolyzed the TG analogue resorufin ester more rapidly than control cell lysates (not shown).

6.3 Future Directions

The most exciting part of this project, in my mind, has been the discovery that HL reduces neutral lipid stores and reduces the secretion of VLDL-TG and apoB100. Minimizing VLDL secretion without causing hepatic steatosis is a win-win situation. Therefore it is tempting to speculate that increasing HL levels would produce an anti-atherogenic phenotype and alleviate pathologies associated with fatty liver disease (ie. insulin resistance). However, many other factors would have to be taken into consideration: the role of HL in producing small dense LDL, reducing HDL-C levels, mediating remnant removal, facilitating CE selective uptake to the liver in RCT and to the adrenals for steroid production.

One of the most important questions to be addressed is whether the effects of HL on intracellular lipid metabolism in our cell system is a result of overexpression. That is, does HL have this same effect *in vivo*? One might address these issues in HL knockout mice that are available. Liver lipid profiles could be analyzed by gas chromatography and the incorporation of radiolabeled oleic acid into TG stores in hepatocytes could be measured. The secretion of VLDL (apoB, TG, cholesterol) could also be determined in the presence of Triton WR1339 or P-407 (Millar et al., 2005) after a 12 h fast. By extrapolating my studies in McA cells, HL knockout mice would be expected to have increased hepatic TG levels and secrete more VLDL compared with control mice. Similar studies could be performed after adenoviral mediated expression of HL or FLAG-tagged HL cDNAs in mouse liver. In this situation, one would expect to see the opposite results (less TG accummulation and lower VLDL secretion rates).

If HL deficiency caused hepatosteatosis, it would be worthwhile to investigate whether these mice are insulin resistant. Hepatic insulin resistance is characterized by the inability to attenuate hepatic glucose production in the presence of insulin (Lam et al., 2003). An association between cytosolic TG stores and hepatic insulin resistance has been identified (Kusunoki et al., 2002). Therefore increasing intracellular HL activity and diminishing TG stores could potentially restore hepatic insulin sensitivity. Yet it is uncertain whether hepatic insulin resistance is caused by elevated hepatic TG stores or high levels of its metabolites, such as DG or acylCoA (Lam et al., 2003). One mechanism which has been proposed to induce insulin resistance in tissues is the activation of protein kinase C (PKC) isoforms by DG (Itani et al., 2002; Lam et al., 2003; Shulman, 2000): PKC phosphorylates serine/threonine residues on the insulin receptor and insulin receptor substrates, attenuating normal insulin signaling. In this regard, TG lipolysis products might cause hepatic insulin resistance rather than restore insulin sensitivity.

Recent studies in mice devoid of adipose TG lipase (ATGL) support the notion that FFAs and acylCoA derivatives-and not TG *per se*-cause lipotoxicity. Although *Atgl* knockout mice have massive TG accumulation in skeletal muscle and the liver, they have improved insulin sensitivity: in the fed state, the plasma insulin levels of *Atgl* knockout mice were 42% lower than their wild-type counterparts despite similar plasma glucose concentrations (Haemmerle et al., 2006). Another new study shows similar results. Feeding mice a high-fat, choline deficient diet increased hepatic TG accumulation above that seen with a high-fat diet alone, yet it improved their glucose tolerance and decreased plasma insulin levels (Raubenheimer et al., 2006). Therefore, accumulation of TG in the liver may not be the cause of insulin resistance.

Although the studies presented in Chapter 3 or Chapter 4 did not establish if microsomal HL or AADA activity increased intracellular DG or fatty acid concentrations, TG hydrolysis obviously generates these products. DG liberation within the ER lumen might not activate PKC, however, if DG and fatty acids were reused for TG synthesis (in a futile cycle) or for CE or PL synthesis by the lipogenic enzymes associated with the ER membrane. Both oleic acid and oleoylCoA have been shown to stimulate translocation of CT from the cytosol to the microsomal membrane in intact HeLa cells (Cornell and Vance, 1987). CT also bound to microsomes which were pretreated with phospholipase C, resulting in 7-fold increased DG (Cornell and Vance, 1987). The enzymatic product of the CT reaction, CDP-choline, and DG are substrates for CPT and stimulate PC biosynthesis (Lim et al., 1986). Thus much of the liberated DG could potentially be used for PC biosynthesis.

Further, DG in the ER membrane might not be able to allosterically activate PKC isoforms as DG within the plasma membrane does; after all, PKC phosphorylation of the insulin receptor and insulin receptor substrates occurs proximal to the plasma membrane rather than the ER membrane. If this were the case, lipases compartmentalized within the ER lumen might be specialized for hydrolyzing neutral lipid stores in a “safe” environment-one which does not cause insulin resistance. DG and FFA are able to flip between bilayers (Holthuis and Levine, 2005; Kamp et al., 1995) and could be used for subsequent PL and CE synthesis.

The finding that radiolabeled fatty acids from TG stores preformed in a 4 h pulse end up in CE after a 4 h chase (Gilham et al., 2003), indicates that TG hydrolysis products are used by ACAT in rat hepatocytes. Moreover, inhibition with E600 or GSKi in the chase decreased radiolabeled CE stores (Gilham et al., 2003), suggesting that TGH (or possibly Es-X or Es-22) might supply fatty acids as substrates for ACAT. This is consistent with the AADA data, where we found decreased TG stores and increased CE levels. The increased incorporation of [^{14}C]glycerol into ^{14}C-PC was also accompanied by decreased levels of ^{14}C-TG in AADA cells; this suggests that AADA hydrolyzes ^{14}C-TG, liberating ^{14}C-DG which was used for ^{14}C-PC synthesis.

TG hydrolysis products may be a very important source of PC precursors. Choline deficiency in mice fed a high-fat diet increased hepatosteatosis (Raubenheimer et al., 2006). Potentially, decreased substrate utilization (DG, fatty acids) resulting from impaired PC production exacerbated the hepatosteatosis, since choline deficiency in mice does not decrease hepatic apoB or TG secretion (Kulinski et al., 2004). TG catabolites might be recycled back to TG in a futile cycle, since mitochondrial GPAT, AGPAT and DGAT2 mRNA levels are elevated in livers of choline deficient mice compared to those supplemented with choline (Raubenheimer et al., 2006).

It would be important to learn if DG does accumulate in McA cells expressing HL or AADA compared to wild-type McA cells. One might evaluate this via radiolabeling cells with [^{14}C]glycerol in the presence of E600 and exogenous oleate. Inactivating lipase activity would allow both wild-type and lipase expressing McA cells to accumulate similar levels of neutral lipid stores. Collecting cells after a chase period in plain DMEM and analyzing DG levels for radioactive content might reveal if the lipases cause intracellular DG accumulation. To test if DG is soaked up by PC biosynthesis, one might follow ^{14}C-TG and ^{14}C-PC levels at different time points in the pulse. If ^{14}C -TG lipolysis yielded ^{14}C-DG which was used for ^{14}C-PC generation, lipase enriched cells would be expected to accumulate more radioactivity in ^{14}C-PC than lipase-poor cells.

One study suggests that overexpression of HL in the liver might not be a good idea. Tissue specific overexpression of LpL in mouse liver resulted in twofold liver TG accumulation and increased intracellular acylCoA metabolites (Kim et al., 2001). This was associated with decreased glucose tolerance and increased hepatic glucose production (Kim et al., 2001). This suggests that LpL mediates hepatic lipid clearance and results in hepatic insulin resistance. Since HL and LpL share many functions (bridging lipoproteins and TG hydrolysis), it might seem that overexpression of HL would also cause steatosis. However, this study differs with that of Dichek et al. where human HL was overexpressed in LDL receptor / mouse HL double knockout mice (Dichek et al., 2004). HL overexpressing mice had markedly less steatosis than HL deficient mice (Dichek et al., 2004). Why does overexpressing LpL in the liver cause steatosis while overexpressing HL depletes TG stores? My studies show that HL is active intracellularly, whereas LpL may not be.

Very recently, a novel member of the carboxylesterase family with 70% identity to TGH has been reported (Okazaki et al., 2006). It has been named TGH-2 based on its homology, substrate specificity and tissue expression profiles which are very similar to TGH (which these authors have renamed TGH-1). TGH-2 is encoded by M-LK/LOC234564, another gene in the carboxylesterase gene cluster (Dolinsky et al., 2004b). These authors found that TGH-2 hydrolyzes TG in 3T3-L1 adipocytes, increasing the release of fatty acids and glycerol (Okazaki et al., 2006). This implies that TGH-2 plays a role in adipose TG metabolism. It is also highly expressed in mouse liver and intestine, suggesting that it may contribute to lipoprotein secretion.

The characterization of Es-22 and Es-X is currently in progress. I expect that these enzymes will also prove to be TG hydrolases *in vivo*. Whether Es-X or Es-22 stimulate VLDL secretion remains to be determined, however. The stable McA cell lines expressing these enzymes will prove to be paramount in revealing the answer to this question. These enzymes are readily isolated from McA cells using M2 anti-FLAG agarose beads. This will facilitate studies of substrate specificity. In addition to cell models and *in vitro* characterization of the carboxylesterases, the *in vivo* function of Es-X and Es-22 could be studied by ablation of the respective genes. Es-X knockout mice are currently being generated for our laboratory.

Knockout mice are invaluable research tools for elucidating the *in vivo* function of an enzyme. The drawback to this technology is its cost: $40,000 US. A cost-effective approach for studying the *in vivo* function of these hepatic lipases would be to overexpress the cDNAs by adenoviral-mediated gene delivery. Adenoviral transfection efficiently targets hepatocytes (Lefesvre et al., 2003). One might also use a liver-specific promoter, such as the albumin promoter, to drive expression of the cDNAs. The native cDNAs for mouse HL, AADA, Es-X and Es-22 as well as the FLAG-tagged mouse cDNAs are now available in the Lehner laboratory. AADA, Es-X and Es-22 knockout mice or liver-overexpressing mice would establish whether these enzymes do mediate VLDL assembly and secretion. Hepatic VLDL secretion could be measured in the presence of Triton WR1339 or P-407 (Millar et al., 2005) after a 12 h fast. If these enzymes are involved, then overexpression would be expected to increase VLDL secretion whereas gene knockout would stifle VLDL secretion. Adenoviral-mediated restoration of enzyme activity in knockout mice coupled with restoration of VLDL secretion would be the ultimate proof.

In conclusion, neither HL nor AADA contribute to VLDL secretion from McA cells. Es-X and Es-22 are both lipases and their intracellular functions are currently being investigated. Clearly the roles of AADA, Es-X and Es-22 in lipid metabolism demand further investigation.

References

Acton, S., A. Rigotti, K.T. Landschulz, S. Xu, H.H. Hobbs, and M. Krieger. 1996. Identification of scavenger receptor SR-BI as a high density lipoprotein receptor. *Science*. 271:518-20.

Alam, M., S. Ho, D.E. Vance, and R. Lehner. 2002a. Heterologous expression, purification, and characterization of human triacylglycerol hydrolase. *Protein Expr Purif.* 24:33-42.

Alam, M., D.E. Vance, and R. Lehner. 2002b. Structure-function analysis of human triacylglycerol hydrolase by site-directed mutagenesis: identification of the catalytic triad and a glycosylation site. *Biochemistry*. 41:6679-87.

Alexander, C.A., R.L. Hamilton, and R.J. Havel. 1976. Subcellular localization of B apoprotein of plasma lipoproteins in rat liver. *J Cell Biol*. 69:241-63.

Amar, M.J., K.A. Dugi, C.C. Haudenschild, R.D. Shamburek, B. Foger, M. Chase, A. Bensadoun, R.F. Hoyt, Jr., H.B. Brewer, Jr., and S. Santamarina-Fojo. 1998. Hepatic lipase facilitates the selective uptake of cholesteryl esters from remnant lipoproteins in apoE-deficient mice. *J Lipid Res*. 39:2436-42.

Andersen, R.V., H.H. Wittrup, A. Tybjaerg-Hansen, R. Steffensen, P. Schnohr, and B.G. Nordestgaard. 2003. Hepatic lipase mutations,elevated high-density lipoprotein cholesterol, and increased risk of ischemic heart disease: the Copenhagen City Heart Study. *J Am Coll Cardiol*. 41:1972-82.

Atzel, A., and J.R. Wetterau. 1993. Mechanism of microsomal triglyceride transfer protein catalyzed lipid transport. *Biochemistry*. 32:10444-50.

Bamberger, M.J., and M.D. Lane. 1990. Possible role of the Golgi apparatus in the assembly of very low density lipoprotein. *Proc Natl Acad Sci U S A*. 87:2390-4.

Becker-Follmann, J., A. Gaa, E. Bausch, E. Natt, G. Scherer, and O. von Deimling. 1997. High-resolution mapping of a linkage group on mouse chromosome 8 conserved on human chromosome 16Q. *Mamm Genome*. 8:172-7.

Bencharit, S., C.L. Morton, Y. Xue, P.M. Potter, and M.R. Redinbo. 2003. Structural basis of heroin and cocaine metabolism by a promiscuous human drug-processing enzyme. *Nat Struct Biol*. 10:349-56.

Bensadoun, A. 1991. Lipoprotein lipase. *Annu Rev Nutr*. 11:217-37.

Ben-Zeev, O., and M.H. Doolittle. 2004. Maturation of hepatic lipase. Formation of functional enzyme in the endoplasmic reticulum is the rate-limiting step in its secretion. *J Biol Chem*. 279:6171-81.

Boden, G., and G.I. Shulman. 2002. Free fatty acids in obesity and type 2 diabetes: defining their role in the development of insulin resistance and beta-cell dysfunction. *Eur J Clin Invest*. 32 Suppl 3:14-23.

Boren, J., S. Rustaeus, and S.O. Olofsson. 1994. Studies on the assembly of apolipoprotein B-100- and B-48-containing very low density lipoproteins in McA-RH7777 cells. *J Biol Chem*. 269:25879-88.

Breedveld, B., K. Schoonderwoerd, A.J. Verhoeven, R. Willemsen, and H. Jansen. 1997. Hepatic lipase is localized at the parenchymal cell microvilli in rat liver. *Biochem J*. 321 (Pt 2):425-30.

Broadway, N.M., R.J. Pease, G. Birdsey, M. Shayeghi, N.A. Turner, and E. David Saggerson. 2003. The liver isoform of carnitine palmitoyltransferase 1 is not targeted to the endoplasmic reticulum. *Biochem J*. 370:223-31.

Broadway, N.M., R.J. Pease, G. Birdsey, N.A. Turner, M. Shayeghi, and E.D. Saggerson. 2001. Microsomal malonyl-CoA-sensitive carnitine acyltransferase. *Biochem Soc Trans*. 29:267-71.

Brown, G., J.J. Albers, L.D. Fisher, S.M. Schaefer, J.T. Lin, C. Kaplan, X.Q. Zhao, B.D. Bisson, V.F. Fitzpatrick, and H.T. Dodge. 1990. Regression of coronary artery disease as a result of intensive lipid-lowering therapy in men with high levels of apolipoprotein B. *N Engl J Med*. 323:1289-98.

Brown, M.S., and J.L. Goldstein. 1983. Lipoprotein metabolism in the macrophage: implications for cholesterol deposition in atherosclerosis. *Annu Rev Biochem*. 52:223-61.

Brown, R.J., J.R. Schultz, K.W. Ko, J.S. Hill, T.A. Ramsamy, A.L. White, D.L. Sparks, and Z. Yao. 2003. The amino acid sequences of the carboxyl termini of human and mouse hepatic lipase influence cell surface association. *J Lipid Res*. 44:1306-14.

Brugger, D., H. Schuster, and N. Zollner. 1996. Familial hypercholesterolemia and familial defective apolipoprotein B-100: comparison of the phenotypic expression In 116 cases. *Eur J Med Res*. 1:383-6.

Brundert, M., J. Heeren, H. Greten, and F. Rinninger. 2003. Hepatic lipase mediates an increase in selective uptake of HDL-associated cholesteryl esters by cells in culture independent from SR-BI. *J Lipid Res*. 44:1020-32.

Buhman, K.F., M. Accad, and R.V. Farese. 2000a. Mammalian acyl-CoA:cholesterol acyltransferases. *Biochim Biophys Acta*. 1529:142-54.

Buhman, K.K., M. Accad, S. Novak, R.S. Choi, J.S. Wong, R.L. Hamilton, S. Turley, and R.V. Farese, Jr. 2000b. Resistance to diet-induced hypercholesterolemia and gallstone formation in ACAT2-deficient mice. *Nat Med*. 6:1341-7.

Cardozo, C., X. Wu, M. Pan, H. Wang, and E.A. Fisher. 2002. The inhibition of microsomal triglyceride transfer protein activity in rat hepatoma cells promotes proteasomal and nonproteasomal degradation of apoprotein b100. *Biochemistry*. 41:10105-14.

Cases, S., S.J. Smith, Y.W. Zheng, H.M. Myers, S.R. Lear, E. Sande, S. Novak, C. Collins, C.B. Welch, A.J. Lusis, S.K. Erickson, and R.V. Farese, Jr. 1998. Identification of a gene encoding an acyl CoA:diacylglycerol acyltransferase, a key enzyme in triacylglycerol synthesis. *Proc Natl Acad Sci U S A*. 95:13018-23.

Cases, S., S.J. Stone, P. Zhou, E. Yen, B. Tow, K.D. Lardizabal, T. Voelker, and R.V. Farese, Jr. 2001. Cloning of DGAT2, a second mammalian diacylglycerol acyltransferase, and related family members. *J Biol Chem*. 276:38870-6.

Castelli, W.P., R.J. Garrison, P.W. Wilson, R.D. Abbott, S. Kalousdian, and W.B. Kannel. 1986. Incidence of coronary heart disease and lipoprotein cholesterol levels. The Framingham Study. *Jama*. 256:2835-8.

Chang, S., and J. Borensztajn. 1993. Hepatic lipase function and the accumulation of beta-very-low-density lipoproteins in the plasma of cholesterol-fed rabbits. *Biochem J*. 293 (Pt 3):745-50.

Chang, T.Y., C.C. Chang, X. Lu, and S. Lin. 2001. Catalysis of ACAT may be completed within the plane of the membrane: a working hypothesis. *J Lipid Res*. 42:1933-8.

Chen, S.H., G. Habib, C.Y. Yang, Z.W. Gu, B.R. Lee, S.A. Weng, S.R. Silberman, S.J. Cai, J.P. Deslypere, M. Rosseneu, and et al. 1987. Apolipoprotein B-48 is the product of a messenger RNA with an organ-specific in-frame stop codon. *Science*. 238:363-6.

Choi, S.Y., K. Hirata, T. Ishida, T. Quertermous, and A.D. Cooper. 2002. Endothelial lipase: a new lipase on the block. *J Lipid Res*. 43:1763-9.

Chubet, R.G., and B.L. Brizzard. 1996. Vectors for expression and secretion of FLAG epitope-tagged proteins in mammalian cells. *Biotechniques*. 20:136-41.

Coleman, R.A., E.B. Haynes, T.M. Sand, and R.A. Davis. 1988. Developmental coordinate expression of triacylglycerol and small molecular weight apoB synthesis and secretion by rat hepatocytes. *J Lipid Res*. 29:33-42.

Coleman, R.A., and D.P. Lee. 2004. Enzymes of triacylglycerol synthesis and their regulation. *Prog Lipid Res*. 43:134-76.

Coleman, R.A., T.M. Lewin, C.G. Van Horn, and M.R. Gonzalez-Baro. 2002. Do long-chain acyl-CoA synthetases regulate fatty acid entry into synthetic versus degradative pathways? *J Nutr*. 132:2123-6.

Cornell, R., and D.E. Vance. 1987. Translocation of CTP: phosphocholine cytidylyltransferase from cytosol to membranes in HeLa cells: stimulation by fatty acid, fatty alcohol, mono- and diacylglycerol. *Biochim Biophys Acta*. 919:26-36.

Curtiss, L.K., D.T. Valenta, N.J. Hime, and K.A. Rye. 2006. What is so special about apolipoprotein AI in reverse cholesterol transport? *Arterioscler Thromb Vasc Biol*. 26:12-9.

Deeb, S.S., A. Zambon, M.C. Carr, A.F. Ayyobi, and J.D. Brunzell. 2003. Hepatic lipase and dyslipidemia: interactions among genetic variants, obesity, gender, and diet. *J Lipid Res*. 44:1279-86.

Dichek, H.L., W. Brecht, J. Fan, Z.S. Ji, S.P. McCormick, H. Akeefe, L. Conzo, D.A. Sanan, K.H. Weisgraber, S.G. Young, J.M. Taylor, and R.W. Mahley. 1998. Overexpression of hepatic lipase in transgenic mice decreases apolipoprotein B-containing and high density lipoproteins. Evidence that hepatic lipase acts as a ligand for lipoprotein uptake. *J Biol Chem*. 273:1896-903.

Dichek, H.L., K. Qian, and N. Agrawal. 2004. Divergent effects of the catalytic and bridging functions of hepatic lipase on atherosclerosis. *Arterioscler Thromb Vasc Biol*. 24:1696-702.

Dolinsky, V.W., D.N. Douglas, R. Lehner, and D.E. Vance. 2004a. Regulation of the enzymes of hepatic microsomal triacylglycerol lipolysis and re-esterification by the glucocorticoid dexamethasone. *Biochem J*. 378:967-74.

Dolinsky, V.W., D. Gilham, M. Alam, D.E. Vance, and R. Lehner. 2004b. Triacylglycerol hydrolase: role in intracellular lipid metabolism. *Cell Mol Life Sci*. 61:1633-51.

Dolinsky, V.W., S. Sipione, R. Lehner, and D.E. Vance. 2001. The cloning and expression of a murine triacylglycerol hydrolase cDNA and the structure of its corresponding gene. *Biochim Biophys Acta*. 1532:162-72.

Doolittle, M.H., H. Wong, R.C. Davis, and M.C. Schotz. 1987. Synthesis of hepatic lipase in liver and extrahepatic tissues. *J Lipid Res*. 28:1326-34.

Ellinghaus, P., U. Seedorf, and G. Assmann. 1998. Cloning and sequencing of a novel murine liver carboxylesterase cDNA. *Biochim Biophys Acta*. 1397:175-9.

Elovson, J., J.E. Chatterton, G.T. Bell, V.N. Schumaker, M.A. Reuben, D.L. Puppione, J.R. Reeve, Jr., and N.L. Young. 1988. Plasma very low density lipoproteins contain a single molecule of apolipoprotein B. *J Lipid Res*. 29:1461-73.

Fan, J., J. Wang, A. Bensadoun, S.J. Lauer, Q. Dang, R.W. Mahley, and J.M. Taylor. 1994. Overexpression of hepatic lipase in transgenic rabbits leads to a marked reduction of plasma high density lipoproteins and intermediate density lipoproteins. *Proc Natl Acad Sci U S A*. 91:8724-8.

Farese, R.V. 2001. Insulin-sensitive phospholipid signaling systems and glucose transport. Update II. *Exp Biol Med (Maywood)*. 226:283-95.

Fielding, C.J., and P.E. Fielding. 2001. Cellular cholesterol efflux. *Biochim Biophys Acta*. 1533:175-89.

Fisher, E.A., and H.N. Ginsberg. 2002. Complexity in the secretory pathway: the assembly and secretion of apolipoprotein B-containing lipoproteins. *J Biol Chem*. 277:17377-80.

Fisher, E.A., M. Pan, X. Chen, X. Wu, H. Wang, H. Jamil, J.D. Sparks, and K.J. Williams. 2001. The triple threat to nascent apolipoprotein B. Evidence for multiple, distinct degradative pathways. *J Biol Chem*. 276:27855-63.

Fleming, C.D., S. Bencharit, C.C. Edwards, J.L. Hyatt, L. Tsurkan, F. Bai, C. Fraga, C.L. Morton, E.L. Howard-Williams, P.M. Potter, and M.R. Redinbo. 2005. Structural insights into drug processing by human carboxylesterase 1: tamoxifen, mevastatin, and inhibition by benzil. *J Mol Biol*. 352:165-77.

Folch, J., M. Lees, and G.H. Sloane Stanley. 1957. A simple method for the isolation and purification of total lipides from animal tissues. *J Biol Chem*. 226:497-509.

Fredenrich, A., and P. Bayer. 2003. Reverse cholesterol transport, high density lipoproteins and HDL cholesterol: recent data. *Diabetes Metab*. 29:201-5.

Frick, C., A.G. Atanasov, P. Arnold, J. Ozols, and A. Odermatt. 2004. Appropriate function of 11beta-hydroxysteroid dehydrogenase type 1 in the endoplasmic reticulum lumen is dependent on its N-terminal region sharing similar topological determinants with 50-kDa esterase. *J Biol Chem*. 279:31131-8.

Fuchs, M., A. Hafer, C. Munch, F. Kannenberg, S. Teichmann, J. Scheibner, E.F. Stange, and U. Seedorf. 2001. Disruption of the sterol carrier protein 2 gene in mice impairs biliary lipid and hepatic cholesterol metabolism. *J Biol Chem*. 276:48058-65.

Ganesh, S.K., C.M. Nass, and R.S. Blumenthal. 2003. Anti-atherosclerotic effects of statins: lessons from prevention trials. *J Cardiovasc Risk*. 10:155-9.

Gibbons, G.F., S.M. Bartlett, C.E. Sparks, and J.D. Sparks. 1992. Extracellular fatty acids are not utilized directly for the synthesis of very-low-density lipoprotein in primary cultures of rat hepatocytes. *Biochem J*. 287 (Pt 3):749-53.

Gibbons, G.F., A.M. Brown, D. Wiggins, and R. Pease. 2002. The roles of insulin and fatty acids in the regulation of hepatic very-low-density lipoprotein assembly. *J R Soc Med*. 95 Suppl 42:23-32.

Gibbons, G.F., K. Islam, and R.J. Pease. 2000. Mobilisation of triacylglycerol stores. *Biochim Biophys Acta*. 1483:37-57.

Gibbons, G.F., R. Khurana, A. Odwell, and M.C. Seelaender. 1994. Lipid balance in HepG2 cells: active synthesis and impaired mobilization. *J Lipid Res*. 35:1801-8.

Gibbons, G.F., D. Wiggins, A.M. Brown, and A.M. Hebbachi. 2004. Synthesis and function of hepatic very-low-density lipoprotein. *Biochem Soc Trans*. 32:59-64.

Gilham, D., M. Alam, W. Gao, D.E. Vance, and R. Lehner. 2005. Triacylglycerol hydrolase is localized to the endoplasmic reticulum by an unusual retrieval sequence where it participates in VLDL assembly without utilizing VLDL lipids as substrates. *Mol Biol Cell*. 16:984-96.

Gilham, D., S. Ho, M. Rasouli, P. Martres, D.E. Vance, and R. Lehner. 2003. Inhibitors of hepatic microsomal triacylglycerol hydrolase decrease very low density lipoprotein secretion. *Faseb J*. 17:1685-7.

Gilham, D., and R. Lehner. 2005. Techniques to measure lipase and esterase activity in vitro. *Methods*. 36:139-47.

Goldstein, J.L., S.K. Basu, and M.S. Brown. 1983. Receptor-mediated endocytosis of low-density lipoprotein in cultured cells. *Methods Enzymol*. 98:241-60.

Gonzalez-Navarro, H., Z. Nong, L. Freeman, A. Bensadoun, K. Peterson, and S. Santamarina-Fojo. 2002. Identification of mouse and human macrophages as a site of synthesis of hepatic lipase. *J Lipid Res*. 43:671-5.

Grundy, S.M. 1990. Cholesterol and atherosclerosis: diagnosis and treatment. J.B. Lippincott Company, Philadelphia, PA.

Gusarova, V., J.L. Brodsky, and E.A. Fisher. 2003. Apolipoprotein B100 exit from the endoplasmic reticulum (ER) is COPII-dependent, and its lipidation to very low density lipoprotein occurs post-ER. *J Biol Chem*. 278:48051-8.

Gwynne, J.T., and J.F. Strauss, 3rd. 1982. The role of lipoproteins in steroidogenesis and cholesterol metabolism in steroidogenic glands. *Endocr Rev*. 3:299-329.

Haemmerle, G., A. Lass, R. Zimmermann, G. Gorkiewicz, C. Meyer, J. Rozman, G. Heldmaier, R. Maier, C. Theussl, S. Eder, D. Kratky, E.F. Wagner, M. Klingenspor, G. Hoefler, and R. Zechner. 2006. Defective lipolysis and altered energy metabolism in mice lacking adipose triglyceride lipase. *Science*. 312:734-7.

Han, G.S., W.I. Wu, and G.M. Carman. 2006. The Saccharomyces cerevisiae Lipin homolog is a Mg2+-dependent phosphatidate phosphatase enzyme. *J Biol Chem.* 281:9210-8.

Havel, R.J., J.P. Kane, and M.L. Kashyap. 1973. Interchange of apolipoproteins between chylomicrons and high density lipoproteins during alimentary lipemia in man. *J Clin Invest.* 52:32-8.

Hegele, R.A., J.A. Little, C. Vezina, G.F. Maguire, L. Tu, T.S. Wolever, D.J. Jenkins, and P.W. Connelly. 1993. Hepatic lipase deficiency. Clinical, biochemical, and molecular genetic characteristics. *Arterioscler Thromb.* 13:720-8.

Hegele, R.A., C. Vezina, S. Moorjani, P.J. Lupien, C. Gagne, L.D. Brun, J.A. Little, and P.W. Connelly. 1991. A hepatic lipase gene mutation associated with heritable lipolytic deficiency. *J Clin Endocrinol Metab.* 72:730-2.

Hide, W.A., L. Chan, and W.H. Li. 1992. Structure and evolution of the lipase superfamily. *J Lipid Res.* 33:167-78.

Holthuis, J.C., and T.P. Levine. 2005. Lipid traffic: floppy drives and a superhighway. *Nat Rev Mol Cell Biol.* 6:209-20.

Homanics, G.E., H.V. de Silva, J. Osada, S.H. Zhang, H. Wong, J. Borensztajn, and N. Maeda. 1995. Mild dyslipidemia in mice following targeted inactivation of the hepatic lipase gene. *J Biol Chem.* 270:2974-80.

Hornick, C.A., C. Thouron, J.G. DeLamatre, and J. Huang. 1992. Triacylglycerol hydrolysis in isolated hepatic endosomes. *J Biol Chem.* 267:3396-401.

Isaacs, A., F.A. Sayed-Tabatabaei, O.T. Njajou, J.C. Witteman, and C.M. van Duijn. 2004. The -514 C->T hepatic lipase promoter region polymorphism and plasma lipids: a meta-analysis. *J Clin Endocrinol Metab.* 89:3858-63.

Itani, S.I., N.B. Ruderman, F. Schmieder, and G. Boden. 2002. Lipid-induced insulin resistance in human muscle is associated with changes in diacylglycerol, protein kinase C, and IkappaB-alpha. *Diabetes.* 51:2005-11.

Jacobs, R.L., C. Devlin, I. Tabas, and D.E. Vance. 2004. Targeted deletion of hepatic CTP:phosphocholine cytidylyltransferase alpha in mice decreases plasma high density and very low density lipoproteins. *J Biol Chem.* 279:47402-10.

Jansen, H., A.J. Verhoeven, and E.J. Sijbrands. 2002. Hepatic lipase: a pro- or anti-atherogenic protein? *J Lipid Res.* 43:1352-62.

Ji, Z.S., S.J. Lauer, S. Fazio, A. Bensadoun, J.M. Taylor, and R.W. Mahley. 1994. Enhanced binding and uptake of remnant lipoproteins by hepatic lipase-secreting hepatoma cells in culture. *J Biol Chem*. 269:13429-36.

Jiang, X.C., C. Bruce, J. Mar, M. Lin, Y. Ji, O.L. Francone, and A.R. Tall. 1999. Targeted mutation of plasma phospholipid transfer protein gene markedly reduces high-density lipoprotein levels. *J Clin Invest*. 103:907-14.

Jiang, X.C., S. Qin, C. Qiao, K. Kawano, M. Lin, A. Skold, X. Xiao, and A.R. Tall. 2001. Apolipoprotein B secretion and atherosclerosis are decreased in mice with phospholipid-transfer protein deficiency. *Nat Med*. 7:847-52.

Johnston, T.P. 2004. The P-407-induced murine model of dose-controlled hyperlipidemia and atherosclerosis: a review of findings to date. *J Cardiovasc Pharmacol*. 43:595-606.

Johnston, T.P., and W.K. Palmer. 1993. Mechanism of poloxamer 407-induced hypertriglyceridemia in the rat. *Biochem Pharmacol*. 46:1037-42.

Joyce, C.W., G.S. Shelness, M.A. Davis, R.G. Lee, K. Skinner, R.A. Anderson, and L.L. Rudel. 2000. ACAT1 and ACAT2 membrane topology segregates a serine residue essential for activity to opposite sides of the endoplasmic reticulum membrane. *Mol Biol Cell*. 11:3675-87.

Kamp, F., D. Zakim, F. Zhang, N. Noy, and J.A. Hamilton. 1995. Fatty acid flip-flop in phospholipid bilayers is extremely fast. *Biochemistry*. 34:11928-37.

Kanicky, J.R., and D.O. Shah. 2002. Effect of degree, type, and position of unsaturation on the pKa of long-chain fatty acids. *J Colloid Interface Sci*. 256:201-7.

Kennedy, E.P. 1956. The biological synthesis of phospholipids. *Can J Biochem Physiol*. 34:334-48.

Kennedy, M.A., G.C. Barrera, K. Nakamura, A. Baldan, P. Tarr, M.C. Fishbein, J. Frank, O.L. Francone, and P.A. Edwards. 2005. ABCG1 has a critical role in mediating cholesterol efflux to HDL and preventing cellular lipid accumulation. *Cell Metab*. 1:121-31.

Kim, J.K., J.J. Fillmore, Y. Chen, C. Yu, I.K. Moore, M. Pypaert, E.P. Lutz, Y. Kako, W. Velez-Carrasco, I.J. Goldberg, J.L. Breslow, and G.I. Shulman. 2001. Tissue-specific overexpression of lipoprotein lipase causes tissue-specific insulin resistance. *Proc Natl Acad Sci U S A*. 98:7522-7.

Kim, J.K., O. Gavrilova, Y. Chen, M.L. Reitman, and G.I. Shulman. 2000. Mechanism of insulin resistance in A-ZIP/F-1 fatless mice. *J Biol Chem*. 275:8456-60.

Kirchgessner, T.G., J.C. Chuat, C. Heinzmann, J. Etienne, S. Guilhot, K. Svenson, D. Ameis, C. Pilon, L. d'Auriol, A. Andalibi, and et al. 1989. Organization of the human lipoprotein lipase gene and evolution of the lipase gene family. *Proc Natl Acad Sci U S A*. 86:9647-51.

Kounnas, M.Z., D.A. Chappell, H. Wong, W.S. Argraves, and D.K. Strickland. 1995. The cellular internalization and degradation of hepatic lipase is mediated by low density lipoprotein receptor-related protein and requires cell surface proteoglycans. *J Biol Chem*. 270:9307-12.

Krapp, A., S. Ahle, S. Kersting, Y. Hua, K. Kneser, M. Nielsen, J. Gliemann, and U. Beisiegel. 1996. Hepatic lipase mediates the uptake of chylomicrons and beta-VLDL into cells via the LDL receptor-related protein (LRP). *J Lipid Res*. 37:926-36.

Krauss, R.M. 1995. Dense low density lipoproteins and coronary artery disease. *Am J Cardiol*. 75:53B-57B.

Kulinski, A., S. Rustaeus, and J.E. Vance. 2002. Microsomal triacylglycerol transfer protein is required for lumenal accretion of triacylglycerol not associated with ApoB, as well as for ApoB lipidation. *J Biol Chem*. 277:31516-25.

Kulinski, A., D.E. Vance, and J.E. Vance. 2004. A choline-deficient diet in mice inhibits neither the CDP-choline pathway for phosphatidylcholine synthesis in hepatocytes nor apolipoprotein B secretion. *J Biol Chem*. 279:23916-24.

Kusunoki, M., K. Tsutsumi, T. Hara, H. Ogawa, T. Nakamura, T. Miyata, F. Sakakibara, Y. Fukuzawa, T. Suga, S. Kakumu, and Y. Nakaya. 2002. Correlation between lipid and glycogen contents in liver and insulin resistance in high-fat-fed rats treated with the lipoprotein lipase activator NO-1886. *Metabolism*. 51:792-5.

Lam, T.K., A. Carpentier, G.F. Lewis, G. van de Werve, I.G. Fantus, and A. Giacca. 2003. Mechanisms of the free fatty acid-induced increase in hepatic glucose production. *Am J Physiol Endocrinol Metab*. 284:E863-73.

Lambert, G., M.J. Amar, P. Martin, J. Fruchart-Najib, B. Foger, R.D. Shamburek, H.B. Brewer, Jr., and S. Santamarina-Fojo. 2000. Hepatic lipase deficiency decreases the selective uptake of HDL-cholesteryl esters in vivo. *J Lipid Res*. 41:667-72.

Lambert, G., M.B. Chase, K. Dugi, A. Bensadoun, H.B. Brewer, Jr., and S. Santamarina-Fojo. 1999. Hepatic lipase promotes the selective uptake of high density lipoprotein-cholesteryl esters via the scavenger receptor B1. *J Lipid Res*. 40:1294-303.

Lankester, D.L., A.M. Brown, and V.A. Zammit. 1998. Use of cytosolic triacylglycerol hydrolysis products and of exogenous fatty acid for the synthesis of triacylglycerol secreted by cultured rat hepatocytes. *J Lipid Res*. 39:1889-95.

Lefesvre, P., J. Attema, A. Lemckert, M. Havenga, and D. van Bekkum. 2003. Genetic heterogeneity in response to adenovirus gene therapy. *BMC Mol Biol*. 4:4.

Lehner, R., Z. Cui, and D.E. Vance. 1999. Subcellullar localization, developmental expression and characterization of a liver triacylglycerol hydrolase. *Biochem J*. 338 (Pt 3):761-8.

Lehner, R., and A. Kuksis. 1993. Triacylglycerol synthesis by an sn-1,2(2,3)-diacylglycerol transacylase from rat intestinal microsomes. *J Biol Chem*. 268:8781-6.

Lehner, R., and A. Kuksis. 1996. Biosynthesis of triacylglycerols. *Prog Lipid Res*. 35:169-201.

Lehner, R., and D.E. Vance. 1999. Cloning and expression of a cDNA encoding a hepatic microsomal lipase that mobilizes stored triacylglycerol. *Biochem J*. 343 Pt 1:1-10.

Lehner, R., and R. Verger. 1997. Purification and characterization of a porcine liver microsomal triacylglycerol hydrolase. *Biochemistry*. 36:1861-8.

Lewin, T.M., J.H. Kim, D.A. Granger, J.E. Vance, and R.A. Coleman. 2001. Acyl-CoA synthetase isoforms 1, 4, and 5 are present in different subcellular membranes in rat liver and can be inhibited independently. *J Biol Chem*. 276:24674-9.

Li, Z., L.B. Agellon, T.M. Allen, M. Umeda, L. Jewell, A. Mason, and D.E. Vance. 2006. The ratio of phosphatidylcholine to phosphatidylethanolamine influences membrane integrity and steatohepatitis. *Cell Metab*. 3:321-31.

Liang, J.J., P. Oelkers, C. Guo, P.C. Chu, J.L. Dixon, H.N. Ginsberg, and S.L. Sturley. 2004. Overexpression of human diacylglycerol acyltransferase 1, acyl-coa:cholesterol acyltransferase 1, or acyl-CoA:cholesterol acyltransferase 2 stimulates secretion of apolipoprotein B-containing lipoproteins in McA-RH7777 cells. *J Biol Chem*. 279:44938-44.

Lim, P., R. Cornell, and D.E. Vance. 1986. The supply of both CDP-choline and diacylglycerol can regulate the rate of phosphatidylcholine synthesis in HeLa cells. *Biochem Cell Biol*. 64:692-8.

Lusis, A.J. 2000. Atherosclerosis. *Nature*. 407:233-41.

Mahley, R.W., T.L. Innerarity, S.C. Rall, Jr., and K.H. Weisgraber. 1984. Plasma lipoproteins: apolipoprotein structure and function. *J Lipid Res*. 25:1277-94.

Medda, S., and R.T. Swank. 1985. Egasyn, a protein which determines the subcellular distribution of beta-glucuronidase, has esterase activity. *J Biol Chem*. 260:15802-8.

Meiner, V.L., S. Cases, H.M. Myers, E.R. Sande, S. Bellosta, M. Schambelan, R.E. Pitas, J. McGuire, J. Herz, and R.V. Farese, Jr. 1996. Disruption of the acyl-CoA:cholesterol acyltransferase gene in mice: evidence suggesting multiple cholesterol esterification enzymes in mammals. *Proc Natl Acad Sci U S A*. 93:14041-6.

Michael, M.D., R.N. Kulkarni, C. Postic, S.F. Previs, G.I. Shulman, M.A. Magnuson, and C.R. Kahn. 2000. Loss of insulin signaling in hepatocytes leads to severe insulin resistance and progressive hepatic dysfunction. *Mol Cell*. 6:87-97.

Millar, J.S., D.A. Cromley, M.G. McCoy, D.J. Rader, and J.T. Billheimer. 2005. Determining hepatic triglyceride production in mice: comparison of poloxamer 407 with Triton WR-1339. *J Lipid Res*. 46:2023-8.

Munro, S. 1995. A comparison of the transmembrane domains of Golgi and plasma membrane proteins. *Biochem Soc Trans*. 23:527-30.

Muoio, D.M., K. Seefeld, L.A. Witters, and R.A. Coleman. 1999. AMP-activated kinase reciprocally regulates triacylglycerol synthesis and fatty acid oxidation in liver and muscle: evidence that sn-glycerol-3-phosphate acyltransferase is a novel target. *Biochem J*. 338 (Pt 3):783-91.

Murphy, D.J., and J. Vance. 1999. Mechanisms of lipid-body formation. *Trends Biochem Sci*. 24:109-15.

Murthy, M.S., and S.V. Pande. 1994. Malonyl-CoA-sensitive and -insensitive carnitine palmitoyltransferase activities of microsomes are due to different proteins. *J Biol Chem*. 269:18283-6.

Mziaut, H., G. Korza, A.R. Hand, C. Gerard, and J. Ozols. 1999. Targeting proteins to the lumen of endoplasmic reticulum using N-terminal domains of 11beta-hydroxysteroid dehydrogenase and the 50-kDa esterase. *J Biol Chem*. 274:14122-9.

Noga, A.A., and D.E. Vance. 2003. A gender-specific role for phosphatidylethanolamine N-methyltransferase-derived phosphatidylcholine in the regulation of plasma high density and very low density lipoproteins in mice. *J Biol Chem*. 278:21851-9.

Okazaki, H., M. Igarashi, M. Nishi, M. Tajima, M. Sekiya, S. Okazaki, N. Yahagi, K. Ohashi, K. Tsukamoto, M. Amemiya-Kudo, T. Matsuzaka, H. Shimano, N. Yamada, J. Aoki, R. Morikawa, Y. Takanezawa, H. Arai, R. Nagai, T. Kadowaki, J. Osuga, and S. Ishibashi. 2006. Identification of a novel member of the carboxylesterase family that hydrolyzes triacylglycerol: a potential role in adipocyte lipolysis. *Diabetes*. 55:2091-7.

Oram, J.F. 2000. Tangier disease and ABCA1. *Biochim Biophys Acta*. 1529:321-30.

Ovnic, M., R.T. Swank, C. Fletcher, L. Zhen, E.K. Novak, H. Baumann, N. Heintz, and R.E. Ganschow. 1991. Characterization and functional expression of a cDNA encoding egasyn (esterase-22): the endoplasmic reticulum-targeting protein of beta-glucuronidase. *Genomics*. 11:956-67.

Pease, R.J., D. Wiggins, E.D. Saggerson, J. Tree, and G.F. Gibbons. 1999. Metabolic characteristics of a human hepatoma cell line stably transfected with hormone-sensitive lipase. *Biochem J*. 341 (Pt 2):453-60.

Peterfy, M., J. Phan, P. Xu, and K. Reue. 2001. Lipodystrophy in the fld mouse results from mutation of a new gene encoding a nuclear protein, lipin. *Nat Genet*. 27:121-4.

Peterson, J., G. Bengtsson-Olivecrona, and T. Olivecrona. 1986. Mouse preheparin plasma contains high levels of hepatic lipase with low affinity for heparin. *Biochim Biophys Acta*. 878:65-70.

Phan, J., M. Peterfy, and K. Reue. 2004. Lipin expression preceding peroxisome proliferator-activated receptor-gamma is critical for adipogenesis in vivo and in vitro. *J Biol Chem*. 279:29558-64.

Pi-Sunyer, F.X. 1998. Executive summary of the clinical guidelines on the identification, evaluation, and treatment of overweight and obesity in adults. *Arch Intern Med*. 158:1855-67.

Preuss, C.V., and C.K. Svensson. 1996. Arylacetamide deacetylase activity towards monoacetyldapsone. Species comparison, factors that influence activity, and comparison with 2-acetylaminofluorene and p-nitrophenyl acetate hydrolysis. *Biochem Pharmacol*. 51:1661-8.

Probst, M.R., M. Beer, D. Beer, P. Jeno, U.A. Meyer, and R. Gasser. 1994. Human liver arylacetamide deacetylase. Molecular cloning of a novel esterase involved in the metabolic activation of arylamine carcinogens with high sequence similarity to hormone-sensitive lipase. *J Biol Chem*. 269:21650-6.

Pullinger, C.R., J.D. North, B.B. Teng, V.A. Rifici, A.E. Ronhild de Brito, and J. Scott. 1989. The apolipoprotein B gene is constitutively expressed in HepG2 cells: regulation of secretion by oleic acid, albumin, and insulin, and measurement of the mRNA half-life. *J Lipid Res*. 30:1065-77.

Qiu, S., N. Bergeron, L. Kotite, R.M. Krauss, A. Bensadoun, and R.J. Havel. 1998. Metabolism of lipoproteins containing apolipoprotein B in hepatic lipase-deficient mice. *J Lipid Res*. 39:1661-8.

Raabe, M., M.M. Veniant, M.A. Sullivan, C.H. Zlot, J. Bjorkegren, L.B. Nielsen, J.S. Wong, R.L. Hamilton, and S.G. Young. 1999. Analysis of the role of microsomal triglyceride transfer protein in the liver of tissue-specific knockout mice. *J Clin Invest*. 103:1287-98.

Ramsamy, T.A., J. Boucher, R.J. Brown, Z. Yao, and D.L. Sparks. 2003. HDL regulates the displacement of hepatic lipase from cell surface proteoglycans and the hydrolysis of VLDL triacylglycerol. *J Lipid Res*. 44:733-41.

Rashid, S., D.K. Trinh, K.D. Uffelman, J.S. Cohn, D.J. Rader, and G.F. Lewis. 2003. Expression of human hepatic lipase in the rabbit model preferentially enhances the clearance of triglyceride-enriched versus native high-density lipoprotein apolipoprotein A-I. *Circulation*. 107:3066-72.

Raubenheimer, P.J., M.J. Nyirenda, and B.R. Walker. 2006. A Choline-Deficient Diet Exacerbates Fatty Liver but Attenuates Insulin Resistance and Glucose Intolerance in Mice Fed a High-Fat Diet. *Diabetes*. 55:2015-2020.

Refsum, H., P.M. Ueland, O. Nygard, and S.E. Vollset. 1998. Homocysteine and cardiovascular disease. *Annu Rev Med*. 49:31-62.

Reue, K., P. Xu, X.P. Wang, and B.G. Slavin. 2000. Adipose tissue deficiency, glucose intolerance, and increased atherosclerosis result from mutation in the mouse fatty liver dystrophy (fld) gene. *J Lipid Res*. 41:1067-76.

Rinninger, F., W.A. Mann, T. Kaiser, S. Ahle, N. Meyer, and H. Greten. 1998. Hepatic lipase mediates an increase in selective uptake of high-density lipoprotein-associated cholesteryl esters by human Hep 3B hepatoma cells in culture. *Atherosclerosis*. 141:273-85.

Ross, R. 1999. Atherosclerosis--an inflammatory disease. *N Engl J Med*. 340:115-26.

Rudel, L.L., R.G. Lee, and T.L. Cockman. 2001. Acyl coenzyme A: cholesterol acyltransferase types 1 and 2: structure and function in atherosclerosis. *Curr Opin Lipidol*. 12:121-7.

Ruel, I.L., P. Couture, J.S. Cohn, and B. Lamarche. 2005. Plasma metabolism of apoB-containing lipoproteins in patients with hepatic lipase deficiency. *Atherosclerosis*. 180:355-66.

Ruel, I.L., P. Couture, C. Gagne, Y. Deshaies, J. Simard, R.A. Hegele, and B. Lamarche. 2003. Characterization of a novel mutation causing hepatic lipase deficiency among French Canadians. *J Lipid Res*. 44:1508-14.

Rusinol, A., H. Verkade, and J.E. Vance. 1993. Assembly of rat hepatic very low density lipoproteins in the endoplasmic reticulum. *J Biol Chem*. 268:3555-62.

Rustaeus, S., K. Lindberg, P. Stillemark, C. Claesson, L. Asp, T. Larsson, J. Boren, and S.O. Olofsson. 1999. Assembly of very low density lipoprotein: a two-step process of apolipoprotein B core lipidation. *J Nutr*. 129:463S-466S.

Rustaeus, S., P. Stillemark, K. Lindberg, D. Gordon, and S.O. Olofsson. 1998. The microsomal triglyceride transfer protein catalyzes the post-translational assembly of apolipoprotein B-100 very low density lipoprotein in McA-RH7777 cells. *J Biol Chem*. 273:5196-203.

Sahoo, D., T.C. Trischuk, T. Chan, V.A. Drover, S. Ho, G. Chimini, L.B. Agellon, R. Agnihotri, G.A. Francis, and R. Lehner. 2004. ABCA1-dependent lipid efflux to apolipoprotein A-I mediates HDL particle formation and decreases VLDL secretion from murine hepatocytes. *J Lipid Res*. 45:1122-31.

Sambrook, J., E.F. Fritsch, and T. Maniatis. 1989. Molecular cloning: a laboratory manual. Cold Spring Harbor Laboratory, Cold Spring Harbor, N.Y.

Sanan, D.A., J. Fan, A. Bensadoun, and J.M. Taylor. 1997. Hepatic lipase is abundant on both hepatocyte and endothelial cell surfaces in the liver. *J Lipid Res*. 38:1002-13.

Santamarina-Fojo, S., H. Gonzalez-Navarro, L. Freeman, E. Wagner, and Z. Nong. 2004. Hepatic lipase, lipoprotein metabolism, and atherogenesis. *Arterioscler Thromb Vasc Biol*. 24:1750-4.

Shafi, S., S.E. Brady, A. Bensadoun, and R.J. Havel. 1994. Role of hepatic lipase in the uptake and processing of chylomicron remnants in rat liver. *J Lipid Res*. 35:709-20.

Shulman, G.I. 2000. Cellular mechanisms of insulin resistance. *J Clin Invest*. 106:171-6.

Sniderman, A., K. Williams, S. Haffner, and N. Sattar. 2004. Insights from apoB: from better diagnosis & therapy to the Medusa Hypothesis. *Atheroscler Suppl*. 5:19-24.

Spady, D.K., M.N. Willard, and R.S. Meidell. 2000. Role of acyl-coenzyme A:cholesterol acyltransferase-1 in the control of hepatic very low density lipoprotein secretion and low density lipoprotein receptor expression in the mouse and hamster. *J Biol Chem*. 275:27005-12.

Spiro, R.G. 1960. Studies on fetuin, a glycoprotein of fetal serum. I. Isolation, chemical composition, and physiochemical properties. *J Biol Chem*. 235:2860-9.

Stillemark, P., J. Boren, M. Andersson, T. Larsson, S. Rustaeus, K.A. Karlsson, and S.O. Olofsson. 2000. The assembly and secretion of apolipoprotein B-48-containing very low density lipoproteins in McA-RH7777 cells. *J Biol Chem*. 275:10506-13.

Tilly-Kiesi, M., E.J. Schaefer, P. Knudsen, F.K. Welty, G.G. Dolnikowski, M.R. Taskinen, and A.H. Lichtenstein. 2004. Lipoprotein metabolism in subjects with hepatic lipase deficiency. *Metabolism*. 53:520-5.

Tran, K., G. Thorne-Tjomsland, C.J. DeLong, Z. Cui, J. Shan, L. Burton, J.C. Jamieson, and Z. Yao. 2002. Intracellular assembly of very low density lipoproteins containing apolipoprotein B100 in rat hepatoma McA-RH7777 cells. *J Biol Chem*. 277:31187-200.

Trickett, J.I., D.D. Patel, B.L. Knight, E.D. Saggerson, G.F. Gibbons, and R.J. Pease. 2001. Characterization of the rodent genes for arylacetamide deacetylase, a putative microsomal lipase, and evidence for transcriptional regulation. *J Biol Chem*. 276:39522-32.

Uchida, T., and S. Yamashita. 1992. Molecular cloning, characterization, and expression in Escherichia coli of a cDNA encoding mammalian choline kinase. *J Biol Chem*. 267:10156-62.

Unger, R.H., Y.T. Zhou, and L. Orci. 1999. Regulation of fatty acid homeostasis in cells: novel role of leptin. *Proc Natl Acad Sci U S A*. 96:2327-32.

Vance, D.E. 1990. Boehringer Mannheim Award lecture. Phosphatidylcholine metabolism: masochistic enzymology, metabolic regulation, and lipoprotein assembly. *Biochem Cell Biol*. 68:1151-65.

Vance, D.E., and N.D. Ridgway. 1988. The methylation of phosphatidylethanolamine. *Prog Lipid Res*. 27:61-79.

Vance, D.E., D.B. Weinstein, and D. Steinberg. 1984. Isolation and analysis of lipoproteins secreted by rat liver hepatocytes. *Biochim Biophys Acta*. 792:39-47.

Vance, J.E., and D.E. Vance. 1985. The role of phosphatidylcholine biosynthesis in the secretion of lipoproteins from hepatocytes. *Can J Biochem Cell Biol*. 63:870-81.

Verges, M., A. Bensadoun, J. Herz, J.D. Belcher, and R.J. Havel. 2004. Endocytosis of hepatic lipase and lipoprotein lipase into rat liver hepatocytes in vivo is mediated by the low density lipoprotein receptor-related protein. *J Biol Chem*. 279:9030-6.

Verhoeven, A.J., and H. Jansen. 1991. Secretion-coupled increase in the catalytic activity of rat hepatic lipase. *Biochim Biophys Acta*. 1086:49-56.

Verhoeven, A.J., B.P. Neve, and H. Jansen. 1999. Secretion and apparent activation of human hepatic lipase requires proper oligosaccharide processing in the endoplasmic reticulum. *Biochem J.* 337 (Pt 1):133-40.

Verhoeven, A.J., B.P. Neve, and H. Jansen. 2000. Intracellular activation of rat hepatic lipase requires transport to the Golgi compartment and is associated with a decrease in sedimentation velocity. *J Biol Chem.* 275:9332-9.

Voet, D., Voet, J.G. and C.W. Pratt. 1999. Fundamentals of Biochemistry. John Wiley and Sons, New York.

Walkey, C.J., L. Yu, L.B. Agellon, and D.E. Vance. 1998. Biochemical and evolutionary significance of phospholipid methylation. *J Biol Chem.* 273:27043-6.

Wang, N., W. Weng, J.L. Breslow, and A.R. Tall. 1996. Scavenger receptor BI (SR-BI) is up-regulated in adrenal gland in apolipoprotein A-I and hepatic lipase knock-out mice as a response to depletion of cholesterol stores. In vivo evidence that SR-BI is a functional high density lipoprotein receptor under feedback control. *J Biol Chem.* 271:21001-4.

Wang, Y., K. Tran, and Z. Yao. 1999. The activity of microsomal triglyceride transfer protein is essential for accumulation of triglyceride within microsomes in McA-RH7777 cells. A unified model for the assembly of very low density lipoproteins. *J Biol Chem.* 274:27793-800.

Wasan, K.M., R. Subramanian, M. Kwong, I.J. Goldberg, T. Wright, and T.P. Johnston. 2003. Poloxamer 407-mediated alterations in the activities of enzymes regulating lipid metabolism in rats. *J Pharm Pharm Sci.* 6:189-97.

Wetterau, J.R., L.P. Aggerbeck, M.E. Bouma, C. Eisenberg, A. Munck, M. Hermier, J. Schmitz, G. Gay, D.J. Rader, and R.E. Gregg. 1992. Absence of microsomal triglyceride transfer protein in individuals with abetalipoproteinemia. *Science.* 258:999-1001.

White, A.L., D.L. Graham, J. LeGros, R.J. Pease, and J. Scott. 1992. Oleate-mediated stimulation of apolipoprotein B secretion from rat hepatoma cells. A function of the ability of apolipoprotein B to direct lipoprotein assembly and escape presecretory degradation. *J Biol Chem.* 267:15657-64.

Wiggins, D., and G.F. Gibbons. 1992. The lipolysis/esterification cycle of hepatic triacylglycerol. Its role in the secretion of very-low-density lipoprotein and its response to hormones and sulphonylureas. *Biochem J.* 284 (Pt 2):457-62.

Wolins, N.E., B.K. Quaynor, J.R. Skinner, M.J. Schoenfish, A. Tzekov, and P.E. Bickel. 2005. S3-12, Adipophilin, and TIP47 package lipid in adipocytes. *J Biol Chem.* 280:19146-55.

Wong, H., and M.C. Schotz. 2002. The lipase gene family. *J Lipid Res*. 43:993-9.

Wu, X., A. Shang, H. Jiang, and H.N. Ginsberg. 1996. Low rates of apoB secretion from HepG2 cells result from reduced delivery of newly synthesized triglyceride to a "secretion-coupled" pool. *J Lipid Res*. 37:1198-206.

Yamaguchi, J., M.V. Gamble, D. Conlon, J.S. Liang, and H.N. Ginsberg. 2003. The conversion of apoB100 low density lipoprotein/high density lipoprotein particles to apoB100 very low density lipoproteins in response to oleic acid occurs in the endoplasmic reticulum and not in the Golgi in McA RH7777 cells. *J Biol Chem*. 278:42643-51.

Yang, L.Y., A. Kuksis, J.J. Myher, and G. Steiner. 1995. Origin of triacylglycerol moiety of plasma very low density lipoproteins in the rat: structural studies. *J Lipid Res*. 36:125-36.

Yang, L.Y., A. Kuksis, J.J. Myher, and G. Steiner. 1996. Contribution of de novo fatty acid synthesis to very low density lipoprotein triacylglycerols: evidence from mass isotopomer distribution analysis of fatty acids synthesized from [2H6]ethanol. *J Lipid Res*. 37:262-74.

Yao, Z., and R.S. McLeod. 1994. Synthesis and secretion of hepatic apolipoprotein B-containing lipoproteins. *Biochim Biophys Acta*. 1212:152-66.

Yao, Z.M., and D.E. Vance. 1988. The active synthesis of phosphatidylcholine is required for very low density lipoprotein secretion from rat hepatocytes. *J Biol Chem*. 263:2998-3004.

Zambon, A., M.A. Austin, B.G. Brown, J.E. Hokanson, and J.D. Brunzell. 1993. Effect of hepatic lipase on LDL in normal men and those with coronary artery disease. *Arterioscler Thromb*. 13:147-53.

Zambon, A., S. Bertocco, N. Vitturi, V. Polentarutti, D. Vianello, and G. Crepaldi. 2003. Relevance of hepatic lipase to the metabolism of triacylglycerol-rich lipoproteins. *Biochem Soc Trans*. 31:1070-4.

Zambon, A., S.S. Deeb, J.E. Hokanson, B.G. Brown, and J.D. Brunzell. 1998. Common variants in the promoter of the hepatic lipase gene are associated with lower levels of hepatic lipase activity, buoyant LDL, and higher HDL2 cholesterol. *Arterioscler Thromb Vasc Biol*. 18:1723-9.

Zhang, Z., K. Cianflone, and A.D. Sniderman. 1999. Role of cholesterol ester mass in regulation of secretion of ApoB100 lipoprotein particles by hamster hepatocytes and effects of statins on that relationship. *Arterioscler Thromb Vasc Biol*. 19:743-52.